Transfer and Development Length of Debonded 15.2 mm (0.6 in)

Prestressing Strand in AASHTO Type I Girder Specimens


By


John William Grove, BSArchE, BSCE


Thesis


Presented to the Faculty of the Graduate School of
The University of Texas at Austin
in Partial Fulfillment
of the Requirements
for the Degree of


Master of Science in Engineering


The University of Texas at Austin

August 1998

# Transfer and Development Length of Debonded 15.2 mm (0.6 in) Prestressing Strand in AASHTO Type I Girder Specimens

Approved by
Supervising Committee:

Ned H. Burns

Michael E. Kreger

# Dedication

To my family

# Acknowledgements

July 1998

# Abstract

## Transfer and Development Length of Debonded 15.2 mm (0.6 in) Prestressing Strand in AASHTO Type I Girder Specimens

John William Grove, M.S.E.

The University of Texas at Austin, 1998

Supervisor: Ned H. Burns

The use of 15.2 mm (0.6 in) diameter prestressing strand in pretension concrete specimens has become necessary to fully precompress the tension region of specimens using high performance/high strength concrete. Current code requirements for transfer and development length are based on laboratory testing of specimens with prestressing strands of a smaller diameter. Subsequently, the Federal Highway Administration has placed restrictions on the use of 15.2 mm strands until further laboratory testing can determine if the current code requirements are adequate for their use.

This study investigated the transfer and development lengths of 15.2 mm prestressing strand in AASHTO Type I beam specimens with a composite deck slab. Each specimen in this study contained strands that had a bright surface condition. In addition, 60% to 75% of the total number of strands in each specimen were debonded. Three concrete strengths were specified for the specimens, so that the effect of concrete strength on the transfer and development lengths could be investigated. The change of the transfer length over time was also investigated.

The results of the transfer and development length testing are presented in this thesis. These results are compared with current AASHTO and ACI code requirements, as well as with equations that have been developed by previous researchers. Conclusions and recommendations on the use of the current code requirements are also discussed.

# Table of Contents

ix

# List of Tables

# List of Figures

# CHAPTER ONE

## Introduction

### 1.1    PROJECT BACKGROUND

Prestressed concrete is a widely used material for highway bridges in much of the United States. Prestressed concrete members are a combination of concrete and steel, in which the steel is used to precompress the tensile zone of the concrete. This is beneficial because it helps to counteract the poor tensile capacity of the concrete. With the recent introduction of higher strength concrete, higher prestressing forces may be applied to increase member capacity, which may result in increased span lengths and/or beam spacings.

Prestressed concrete construction is divided into two categories: pretensioned and post-tensioned. Pretensioned concrete has the prestressing strands tensioned prior to the concrete being placed around them, while post-tensioned concrete has the strands tensioned after the concrete has been cast. Unlike prestressed post-tensioned concrete, which uses mechanical anchorage devices to transfer the full prestress force instantaneously at the beam ends, prestressed pretensioned concrete members require sufficient bond of the prestressing steel to the concrete to fully transfer the prestress force over a finite length.

At this time, the use of 12.7 mm (0.5 in) prestressing strands configured with a grid spacing of 50.8 mm (2.0 in) is the most common practice in the fabrication of prestressed pretensioned concrete members. However, this configuration cannot generate enough prestressing force to fully precompress the tensile zone of high strength concrete girders[1]. A larger area of steel must be used to produce the higher prestressing forces that are desired for use with high strength concrete. This can be accomplished in one of two ways: increase the number of strands that are used by decreasing the strand grid spacing or use strands with a larger cross-sectional area with the same grid spacing. It is more economical to use strands with a larger area, which has led to the introduction of 15.2 mm (0.6 in) prestressing strands in the construction of pretensioned members. This strand size is already commonly used in post-tensioned members.

After unfavorable bond capacity was reflected in the results of laboratory tests[2] using 15.2 mm (0.6 in) diameter prestressing strands, the Federal Highway Administration (FHWA) issued a moratorium[3] on October 26, 1988 disallowing the use of these strands. In addition, the required development length for fully bonded strands of all lesser diameters was increased to 1.6

1

times the current AASHTO requirement[4] and an additional 2.0 times this increased length for debonded strands. Following numerous experimental studies, the FHWA issued a memorandum[5] on May 8, 1996 that reinstated the use of 15.2 mm (0.6 in) prestressing strands, but continued to require the increased development lengths proposed in the 1988 memorandum for all strand diameters pending further research results.

Concern over the possibility of significant increases in the required design transfer and development lengths was accompanied by another important concern; namely the strand spacing that was being used. The AASHTO and ACI codes currently require four times the strand diameter as a minimum center-to-center spacing. The spacing for 15.2 mm (0.6 in) strand using the code requirements is 60.8 mm (2.4 in) center-to-center, but a 50.8 mm (2.0 in) grid spacing is being used. This study involved the testing of pretensioned prestressed concrete members with 15.2 mm (0.6 in) diameter strands in a grid pattern of 50.8 mm (2.0 in) on center to address these concerns.

## 1.2    OBJECTIVES OF THE RESEARCH PROGRAM

The Texas Department of Transportation (TxDOT) and the Federal Highway Administration (FHWA) funded a research study entitled *Development Length of 15-mm (0.6-inch) Diameter Prestressing Strand at 50-mm (2-inch) Grid Spacing in Standard I-Shaped Pretensioned Concrete Beams*. The test program consists of 36 beams containing a combination of four variables. These variables are beam concrete strength, number/percentage of debonded strands, strand surface condition and horizontal web reinforcement.

The primary purpose of the research project is to investigate the bond performance of 15.2 mm (0.6 in) diameter prestressing strands at 50.2 mm (2.0 in) spacing in fully bonded and partially debonded pretensioned specimens. In addition, the results of these tests will be used to evaluate current transfer and development length equations. These tests will also increase the database of experimental data for members with debonded strands. Furthermore, the benefit to member performance from the inclusion of horizontal web reinforcement in pretensioned anchorage zones will be investigated to a very limited degree in these tests.

## 1.    OBJECTIVE OF THIS STUDY

This thesis covers the third segment of the larger study, described above, investigating the transfer and development length of 15.2 mm (0.6 in) diameter prestressing strands. This

particular study will focus on the investigation of the transfer and development length of all specimens in this project containing at least 60% debonded prestressing strands with a bright surface condition. Presentation and discussion of fabrication processes, as well as test procedures and results, will be included. In addition, strand pull-out testing will be investigated and the results presented. Finally, the use of horizontal web reinforcement to control crack width in the transfer zone and to reduce strand slip will be examined.

# CHAPTER TWO

## Definitions and Related Research

### 2.1    INTRODUCTION

To better explain the results presented in this thesis, it is necessary to introduce a few important definitions and some prior research that is relevant to this study. This chapter will introduce the nature of bond and discuss its importance. Transfer and development lengths will be defined, and current AASHTO and ACI code requirements for each will be investigated. Finally, a review of related research will be presented, and the results of the studies will be discussed.

### 2.2    BOND CHARACTERISTICS OF PRETENSIONED CONCRETE

Many variables make it difficult to quantify the bond stresses[9] in pretensioned concrete. Cracking of the concrete, strand slip and untwisting of strand in the transfer region after release of the prestressing force are just a few of the more important variables. However, the most important variable is the friction between the strand and concrete.

As the prestressing strand is released at transfer, the strand will expand. This exerts a normal force on the concrete and introduces the friction component. This force is not easily determined, because of the variability of surface conditions of the strand and concrete.

#### 2.2.1    Elements of Bond

Although the bond stresses are difficult to quantify, a good estimation can be predicted using a qualitative model[10]. This model is based on the contributions of three distinctive elements of bond. They are Hoyer's effect, mechanical interlocking, and adhesion. Each of these elements is described further in the following sections.

4

### 2.2.1.1  Hoyer's Effect

The cross-sectional area of prestressing strand decreases when tensioned axially due to the Poisson effect. Concrete is cast around the prestressing strand while the strand is under tension and has a reduced cross-section. Hoyer's Effect[11] is the wedge action that is developed between the strand and the concrete when the strand is released and the cross-section tries to return to its original size. This wedging action exerts a normal force between the strand and the concrete, which activates a friction force. The friction force is responsible for anchoring the strand. Figure 2.1 shows the wedge action of Hoyer's effect.
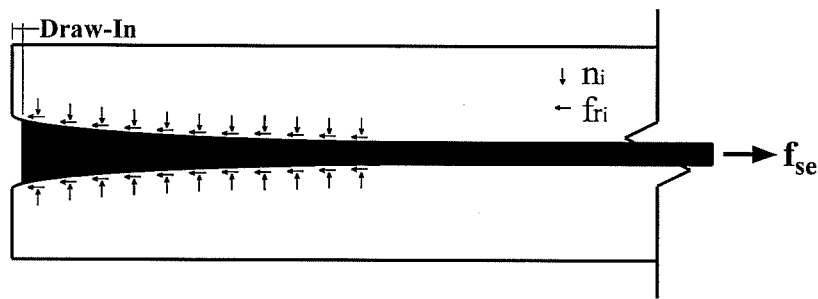


**Figure 2.1:  Wedge Action of Hoyer's Effect**

The contribution of Hoyer's effect is typically seen exclusively in the transfer zone. This is because there is very little change in the strand stress outside the transfer zone after release of the prestressing force. This results in a minimal increase in the strand diameter, and furthermore minimal induced normal force.

During loading of the pretensioned specimen, the stress in the strand increases and the diameter decreases. Increases in strand stress occur adjacent to crack locations, where the strand must carry all of the tensile force that had been shared with the concrete. Therefore, cracks in the transfer zone will significantly reduce the contribution of Hoyer's effect to the bond.

### 2.2.1.2  Mechanical Interlocking

When concrete is cast around seven-wire strand, it forms a sleeve around the strand. If the strand is restrained from twisting, the strand will bear against the ridges of concrete that form in the interstices of the strand, similar to the bond of mild steel rebar. This mechanism is called mechanical interlocking[10]. Mechanical interlocking is a function of the normal force and

5

coefficient of friction between the concrete and steel, and the pitch angle of the outer wires of the strand.

Mechanical interlocking is the largest contributor to flexural bond, especially in cracked sections. It is important to remember that for mechanical interlocking to be effective, twisting of the strand must be restrained. Therefore, mechanical interlocking is dependent on Hoyer's effect in the transfer zone to anchor the strand and prevent twist.

### 2.2.1.3 Adhesion

Adhesion[10] is a chemical bond that acts like glue to anchor the strand to the concrete. This glue has a rigid-brittle failure mechanism. As soon as any slip in the strand is introduced, adhesion is broken between the strand and concrete, and there is no further contribution to bond from adhesion.

Adhesion contributes solely to flexural bond before cracking of the concrete. Adhesion has no contribution to transfer bond or bond at cracked sections. This is a result of the strand slip that occurs in the transfer zone when the prestressing force is released, and in the vicinity of cracks in the concrete. It can be seen that the contribution of adhesion to bond is negligible.

### 2.2.2    Importance of Bond

Without bond of the prestressing strand to the concrete, pretensioned prestressed concrete would not be possible. Bond is necessary to anchor the strands and transfer the prestressing force to the concrete.

It has been observed[2,9] that there are two important types of bond stresses in pretensioned concrete: transfer bond stresses and flexural bond stresses. Transfer bond stresses are activated at release of the prestressing force. Flexural bond stresses are activated when applied loads cause an increase in steel stress due to bending.

### 2.2.2.1  Transfer Bond Stress

The transfer bond stresses anchor the prestressing strand to the concrete after release of the prestressing force. Transfer bond stresses are responsible for increasing the stress in the prestressing strand from zero at the free end to the effective prestressing force, $f_{se}$, at the end of the transfer zone. Hoyer's effect is the main contributor to the development of transfer bond stresses. Mechanical interlocking begins to contribute near the end of the transfer zone, where the twist of

6

the strand becomes restrained due to Hoyer's effect. The assumed contribution of Hoyer's effect and mechanical interlocking through the transfer zone can be seen in Figure 2.2.
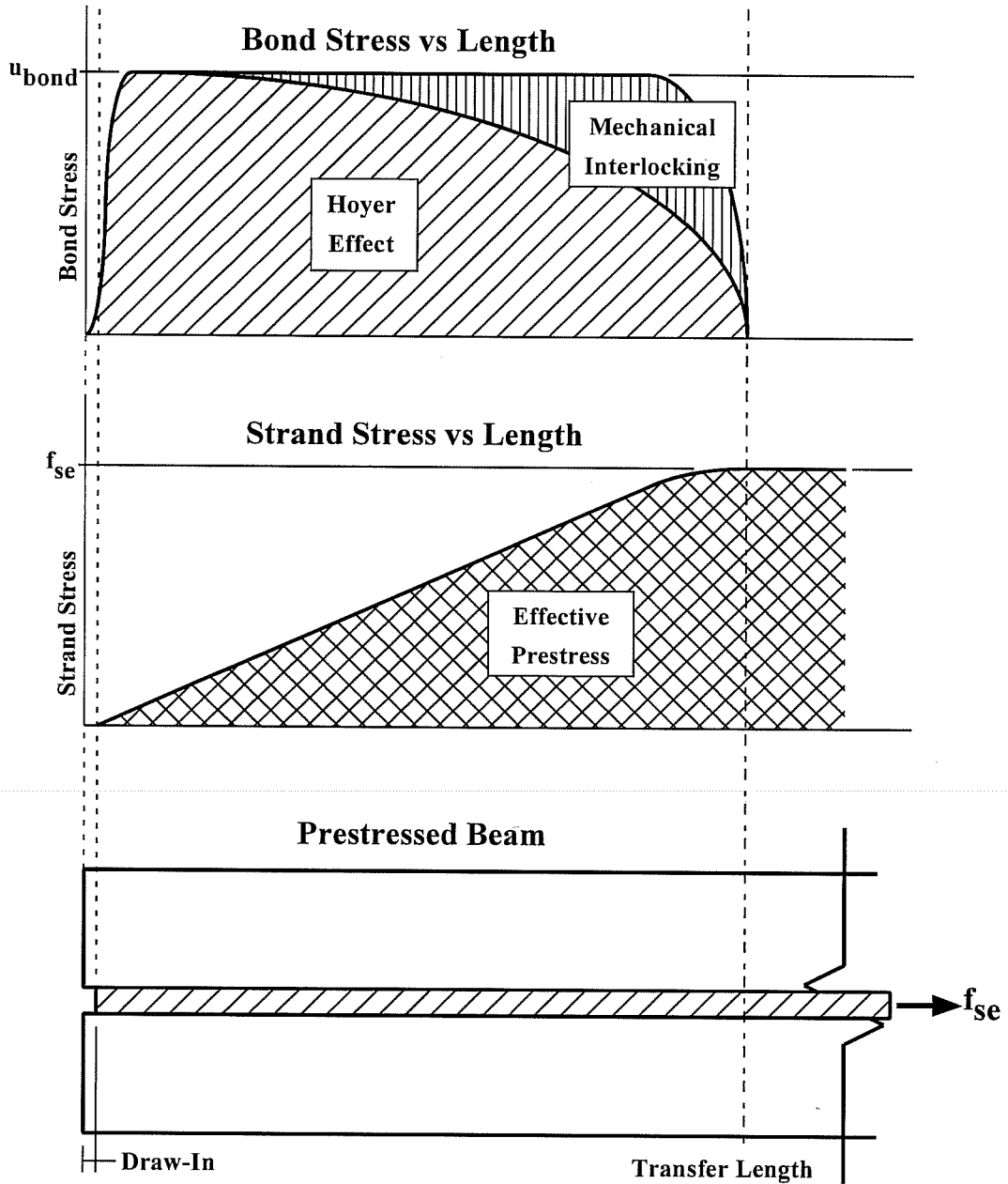


**Figure 2.2: Distribution of Transfer Bond Stresses**

From the integration of the bond stress over a finite surface length, the stress change in the prestressing steel can be determined. The steel stress is known to increase approximately linearly through the transfer zone for prestressing strand, which means that the bond stress must be nearly constant through the transfer zone. Figure 2.2 shows the steel stress along the length of the transfer zone.

Previous work by Janney[9] determined the steel stress distribution for prestressing wire through the transfer zone. From this, the bond stress profile in the transfer zone can also be determined. Because of its smooth surface, the wire does not have the contribution from mechanical interlocking. Hoyer's effect is the sole contributor to the transfer bond stress for smooth wire.

It is assumed that the contribution from Hoyer's effect is the same for prestressing strand as it is for wire. Since the transfer bond stress is known to be fairly constant and adhesion does not contribute, the contribution due to mechanical interlocking can also be determined.

### 2.2.2.2 Flexural Bond Stress

Flexural bond stresses are responsible for developing the additional tensile stresses in the prestressing strand that are induced by cracks in the concrete due to applied loads. Flexural bond stresses are responsible for the increase of steel stress from the effective prestressing force, $f_{se}$, to the ultimate prestressing force, $f_{ps}$.

Before the concrete is cracked, the increase of steel stress in the strand due to applied loads is very small. However, the strand must account for the loss of tensile stress that was present in the concrete at the time when cracking occurs. The steel stress in the strand adjacent to the crack increases rapidly and results in very high bond stresses.

Mechanical interlocking is the main contributor to flexural bond stresses. After cracking, adhesion is eliminated due to strand slip at the crack. The reduction of the strand cross-section due to additional tensile forces due to applied loads eliminates any contribution due to Hoyer's effect.

### 2.2.2.3 Interaction of Transfer and Flexural Bond

There is little interaction between transfer and flexural bond. Even during bond failure flexural bond stresses barely overlap the transfer bond stresses. This is because of the fact that as the flexural bond stresses overlap the transfer bond stresses, the additional stresses begin to reduce

the cross-section of the strand, which results in reduced anchorage strength. Therefore, any interaction between the transfer and flexural bond would lead to bond failure.

## 2.3    TRANSFER AND DEVELOPMENT LENGTH

This section introduces the definitions of transfer and development length as well as other related terms. Also, the importance of transfer and development length will be discussed, and the current code requirements for each will be introduced.

### 2.3.1    Definitions

#### 2.3.1.1    *Transfer Length*

The transfer bond length, or transfer length, is quite simply the bonded strand length required to develop the full effective prestress, $f_{se}$, in the strand, as shown in Figure 2.3. The transfer length begins from the point of first bond, where there is no stress in the strand, and extends to the point were the stress in the strand becomes constant. This constant stress is the effective prestress.
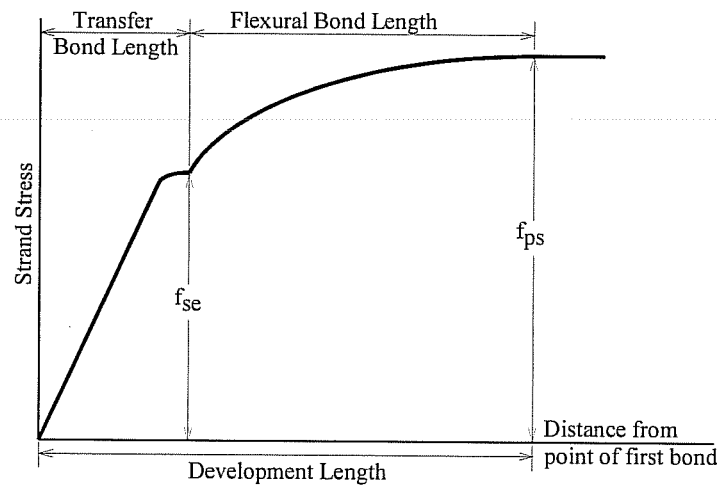


Figure 2.3: Distribution of Steel Stress

The point of first bond can occur at the beam end for fully bonded strands or the end of the debonding sleeve for debonded strands. Therefore, in beams with a mix of fully bonded and debonded strands there will be more than one transfer length.

### 2.3.1.2 Flexural Bond Length

The flexural bond length is the length that is required to develop the strand stress from the effective prestress, $f_{se}$, to the ultimate stress, $f_{ps}$. This length begins at the end of the transfer length and extends to the point where the ultimate prestress is capable of being achieved, as seen in Figure 2.3. The flexural bond length is defined similarly for fully bonded and debonded strands.

### 2.3.1.3 Development Length

The development length, $L_d$, is the combination of the transfer length and the flexural bond length. Development length is the total bond length required to allow the strand to achieve the ultimate prestress. The required development length to achieve ultimate prestress in all strands is always the development length from the transfer region that is farthest from the beam end.

### 2.3.1.4 Embedment Length

Embedment length, $L_e$, is the length of bonded strand from the point of first bond to the critical section. The critical section is the point where the steel stresses are maximum, typically the point of maximum moment. It is important that the embedment length be greater than the development length to avoid bond failure.

## 2.4     RELATED RESEARCH

### 2.4.1     Kaar and Magura, 1965

Kaar and Magura[12] studied flexural behavior and shear capacity of pretensioned specimens with debonded strands. The test specimens used in the study were half scale AASHTO Type III beams with twelve 9.5 mm (0.375 in) prestressing strands. The flexural behavior study consisted of three specimens: one control beam with fully bonded draped strands, one "partially"

debonded specimen with four debonded strands, and one "fully" debonded specimen with six debonded strands. The shear capacity study consisted of two specimens: one control beam with fully bonded draped strands, one "partially" debonded specimen with four debonded strands.

Of the four debonded strands in the "partially" debonded specimens, two strands were debonded a length of 711 mm (28 in) and two additional strands were debonded 1930 mm (76 in). The "fully" debonded specimens contained six debonded strands; two strands were debonded a length of 1194 mm (47 in), two strands were debonded 2108 mm (83 in), and the last two strands were debonded 3327 mm (131 in). The tested embedment length of the specimens was equal to 2.5 times the calculated development length for the fully bonded specimens, 2.0 times the calculated development length for the "partially" debonded specimens, and 1.0 times the calculated development length for the "fully" debonded specimens.

During the flexural testing, each specimen was subjected to five million cycles of the design live load and then loaded statically to failure. All three beams performed well throughout the cyclic loading, with no strand end slip observed. Behavior of the specimens during the static loading was similar until flexural cracks formed, which was when slip of the debonded strands was observed. The fully bonded specimens failed in flexure by rupturing of the prestressing strands, with no strand end slip observed. The "partially" debonded specimens also failed in flexure by rupturing of the prestressing strands, but in this case very small strand end slips were observed. The "fully" debonded specimens suffered a bond failure of the debonded prestressing strands as evidenced by the large slips observed at failure.

The effect of strand debonding on the shear capacity was tested by increasing the spacing of the vertical shear reinforcement to 50% greater than the AASHTO code requirement. The specimens were subjected to static loading to failure. The fully bonded specimen failed in horizontal shear at the intersection of the web and bottom flange. The "partially" debonded specimen failed in flexure by rupturing of the prestressing strands.

It was observed that the "fully" debonded specimens with an embedment length of 1.0 times the required development length did not perform favorably. However, "partially" debonded specimens with an embedment length of 2.0 times the required development length performed as well or better than fully bonded specimens. The current AASHTO and ACI code provisions requiring an embedment of 2.0 times the calculated fully bonded development length are based on these results.

11

## 2.4.2    Dane and Bruce, 1975

Dane and Bruce[13] performed flexural tests on nine pretensioned specimens. Six of the specimens were half scale AASHTO Type III beams with twelve 9.5 mm (0.375 in) diameter prestressing strands and the remaining three were full scale AASHTO Type II beams with twenty-two 11.1 mm (0.4375 in) diameter prestressing strands. Of the six half scale Type III specimens, two were control specimens with draped strands, and four specimens contained two strands that were debonded for a length of 2959 mm (116.5 in). Two of the four debonded specimens contained anchor plates, which were attached to the debonded strands to aid strand anchorage. The three full scale Type II beams consisted of one control beam with draped strands and two beams with four strands debonded for a length of 3658 mm (144 in) without anchor plates.

In the testing of the half scale Type III specimens, the embedment length was 2.2 times the calculated development length for the fully bonded specimens and for the debonded specimens it was equal to the calculated transfer length which was 0.34 times the calculated development length. The embedment lengths used for the full scale Type II specimens were 3.3 times the calculated development length for the fully bonded specimens and 1.0 times the calculated development length for the debonded specimens.

All beams were loaded statically to failure. All beams failed by crushing of the concrete in compression. Significant strand end slips ranging from 22.4 to 43.2 mm (0.88 to 1.70 in) were observed in all of the debonded specimens. However, all specimens reached nominal capacity. It was assumed that the small percentage (17%) of debonded strands allowed the specimens to achieve nominal capacity despite the presence of large strand end slips.

## 2.4.3    Rabbat, Kaar, Russell, and Bruce, 1979

Rabbat et al[14] performed development length testing on six full scale Type II AASHTO specimens with twenty-two 11.1 mm (0.4375 in) diameter prestressing strands. The intent of the study was to investigate the response of specimens designed for zero tensile stress at service load compared with those designed for a maximum tensile stress of $0.5\sqrt{f_c'}$ MPa ($6\sqrt{f_c'}$ psi) at service load. The testing procedure consisted of fatigue loading of five million cycles at full dead plus live load, followed by static loading to failure.

Of the three specimens designed for a maximum tensile stress of $0.5\sqrt{f_c'}$ MPa ($6\sqrt{f_c'}$ psi) at service load, one specimen was fully bonded with draped strands, and two specimens had four debonded strands. The debonded specimens had different debonded lengths. The first specimen had two strands debonded for 3505 mm (138 in) and two for 5029 mm (198 in), and the second specimen had two strands debonded for 1829 mm (72 in) and two for 3353 mm (132 in). The embedment length corresponding to each of these specimens was 4.0 times the calculated development length for the fully bonded specimen, 1.0 times the calculated development length for the specimen debonded 5029 mm (198 in), and 2.0 times the calculated development length for the specimen debonded 3353 mm (132 in).

The three specimens that were designed to have zero tensile stress at service load were identical to the specimens discussed previously, except the 3353 mm (132 in) debonded specimen was replaced with a second 5029 mm (198 in) specimen.

The three specimens designed for a maximum tensile stress of $0.5\sqrt{f_c'}$ MPa ($6\sqrt{f_c'}$ psi) at service load all failed due to strand fatigue after approximately 3.5 million cycles of load. Very small strand end slips were observed with the debonded specimens, however the differences were insignificant to the final failure mode. It is important to note that debonding of the prestressing strands did not have an adverse affect on the performance of the specimens, as can be seen by the similar response of the fully bonded specimens.

## 2.4.4    Russell and Burns, 1993

Russell and Burns[10] investigated the transfer and development lengths for pretensioned concrete specimens with a number of variables. These variables included: size and shape of the specimen cross-section, prestressing strand diameter, number of strands, bonded and debonded strands, and the presence of confining reinforcement.

This investigation identified the effect that each variable has on the transfer length. Longer transfer lengths were measured for 15.2 mm (0.6 in) diameter strands than for 12.7 mm (0.5 in) diameter strands. It was also observed that fully bonded strands tended to have a longer transfer length than debonded strands. The smaller specimens with rectangular cross-sections had longer transfer lengths than the larger AASHTO and Texas Type C specimens.

Russell and Burns reported that during development length testing of specimens with debonded strands, bond failure did not occur in any specimen when cracking in the transfer zone

was not present. However, flexural cracking in the transfer zone caused slip of the debonded strands and led to bond failure. In addition, web shear cracking in the transfer zone resulted in sudden collapse of the specimen.

## 2.5 CURRENT CODE REQUIREMENTS AND SUGGESTED EQUATIONS

In this Section, current code requirements for transfer and development length will be introduced. In addition, suggested equations for transfer and development length that were developed from previous research will be presented.

### 2.5.1 Current Code Requirements

Current code requirements for transfer and development length have been established by the American Association of State Highway Transportation Officials (AASHTO) and the American Concrete Institute (ACI). The codes that were referenced for these equations were the *ACI Building Code*[8] (ACI 318-95M and 318-95), *the AASHTO Standard Specification for Highway Bridges*[5] (1996), and the traditional English and S.I. editions of the *AASHTO LRFD Bridge Design Specifications*[6] (1994). These code requirements are introduced in the following sections.

#### 2.5.1.1 Transfer Length

Table 2.1 lists the AASHTO and ACI code recommended equations for transfer length. In each case, the prestress for strand shall increase linearly from zero, at the point of first bond, to its maximum value over the calculated transfer length.

**Table 2.1: AASHTO and ACI Code Transfer Length Equations**

| Code | Section | | S.I. | English |
|---|---|---|---|---|
| ACI | Code | 11.4.3 | $50d_b$ | $50d_b$ |
| | | 11.4.4 | $50d_b$ | $50d_b$ |
| | Commentary | R12.9 | $(1/3 * f_{se})(d_b/7)$ | $(1/3 * f_{se})d_b$ |
| AASHTO | Standard | 9.20.2.4 | N/A | $50d_b$ |
| | LRFD | 5.8.2.3 | $60d_b$ | $60d_b$ |

14

### 2.5.1.2 Development Length

Table 2.1 lists the AASHTO and ACI code recommended equations for development length. In each case, the development length is measured from the point of first bond.

**Table 2.2: AASHTO and ACI Code Development Length Equations**

| Code | Section | | | S.I. | English |
|------|---------|---|---|------|---------|
| ACI | Code | 12.9.1 | fully bonded | $(f_{ps}-2/3f_{se})(d_b/7)$ | $(f_{ps}-2/3f_{se})d_b$ |
| | | 12.9.3 | debonded w/o tension | $(f_{ps}-2/3f_{se})(d_b/7)$ | $(f_{ps}-2/3f_{se})d_b$ |
| | | | debonded w/ tension | 2.0x fully bonded | 2.0x fully bonded |
| AASHTO | Standard | 9.28.1 | fully bonded | N/A | $(f_{ps}-2/3f_{se})d_b$ |
| | | 9.28.3 | debonded w/o tension | N/A | $(f_{ps}-2/3f_{se})d_b$ |
| | | | debonded w/ tension | N/A | 2.0x fully bonded |
| | LRFD | 5.11.4.1 | fully bonded | $(f_{ps}-2/3f_{se})(d_b/7)$ | $(f_{ps}-2/3f_{se})d_b$ |
| | | 5.11.4.2 | debonded w/o tension | $(f_{ps}-2/3f_{se})(d_b/7)$ | $(f_{ps}-2/3f_{se})d_b$ |
| | | | debonded w/ tension | 2.0x fully bonded | 2.0x fully bonded |

Note: The indicator "debonded w/o tension" refers to debonded strand in specimens designed for no tension in the concrete during service loads.

The indicator "debonded w/ tension" refers to debonded strand in specimens designed for tension in the concrete during service loads.

## 2.5.2    Suggested Transfer and Development Length Equations

Previous studies have suggested equations for predicting the transfer and development length of pretensioned prestressed concrete specimens. A partial list of these equations is presented in Table 2.3. The results of the transfer and development length testing of this study will be compared to the predicted lengths from selected equations in Table 2.3 during the discussion of the test results, to determine the adequacy of the equations.

15

**Table 2.3: Suggested Equations for Transfer and Development Length**

| Author | Year | Transfer Length | Development Length |
|---|---|---|---|
| ACI 318[8]/ AASHTO Standard[5] | 1963 | $= \dfrac{f_{se}}{3} d_b$<br><br>$\approx 50 d_b$ | $= L_t + (f_{ps} - f_{se}) d_b$<br><br>$= (f_{ps} - \dfrac{2}{3} f_{se}) d_b$ |
| AASHTO LRFD[6] | 1994 | $= 60 d_b$ | $= (f_{ps} - \dfrac{2}{3} f_{se}) d_b$ |
| Martin[15] & Scott[(1)] | 1976 | $= 80 d_b$ | $f_{ps} \leq \dfrac{L_e}{80 d_b} \left( \dfrac{135}{\sqrt[6]{d_b}} + 31 \right) \quad L_e \leq 80 d_b$ |
| Zia[16] & Mostafa | 1977 | $= 1.5 \dfrac{f_{si}}{f'_{ci}} d_b - 4.6$ | $= L_t + 1.25 (f_{pu} - f_{se}) d_b$ |
| Cousins[3], Johnston & Zia[(2)] | 1990 | $= \dfrac{U'_t \sqrt{f'_{ci}}}{2B} + \dfrac{f_{se} A_{ps}}{\pi d_b U'_t \sqrt{f'_{ci}}}$ | $= L_t + (f_{ps} - f_{se}) \left( \dfrac{\frac{A_{ps}}{\pi d_b}}{U'_d \sqrt{f'_c}} \right)$ |
| Russell[10] & Burns[(3)] | 1993 | $= \dfrac{f_{se}}{2} d_b$ | $M_{cr} > L_t V_u \qquad\qquad\qquad \text{Fully Bonded}$<br><br>$\dfrac{L_b + L_t}{\text{Span}} \leq \dfrac{1}{2} \left( 1 - \sqrt{1 - \dfrac{M_{cr}}{M_u}} \right) \text{ Debonded}$ |
| Mitchell[17], Cook, Khan & Tham | 1993 | $= \dfrac{f_{si} d_b}{3} \sqrt{\dfrac{3}{f'_{ci}}}$ | $= L_t + (f_{ps} - f_{se}) d_b \sqrt{\dfrac{4.5}{f'_c}}$ |
| Burdette[18], Deatherage & Chew | 1994 | $= \dfrac{f_{si}}{3} d_b$ | $= L_t + 1.50 (f_{ps} - f_{se}) d_b$ |
| Buckner[19] (FHWA)[(4)] | 1994 | $= \dfrac{1250 f_{si} d_b}{E_c}$<br><br>$\approx \dfrac{f_{si}}{3} d_b$ | $= L_t + \lambda (f_{ps} - f_{se}) d_b$<br><br>$\lambda = (0.6 + 40 \varepsilon_{ps}) \text{ or } \left( 0.72 + 0.102 \dfrac{\beta_1}{\omega_p} \right)$<br><br>$(1.0 \leq \lambda \leq 2.0)$ |

Notes: Because not all equations have an S.I. equivalent, all equations are in English units.

Some notation was changed to provide consistency between equations.

Units of stress are ksi, except Cousins et al, which use units of psi

(1) Development length equations limit $f_{ps}$ as a function of $L_e$.

(2) B=300psi on average, $U'_t$ and $U'_d$ are coefficients based on strand surface condition.

(3) Development length criteria based on preventing cracks in the transfer zone.

(4) Development length equation based on minimum strand strain at failure

16

# CHAPTER THREE

## Test Specimens

## 3.1    DESIGNATION

Test specimens are identified by a four-character alphanumeric name.  Each character represents a different variable characteristic of the specimen.  The variables that are identified are the concrete compressive strength, the number of debonded strands, the strand surface condition and the development length test sequence number.  The variables are identified in Table 3.1.

**Table 3.1:  Beam Identification Variables**

| Order | Variable | Character | Description |
|---|---|---|---|
| 1 | Concrete Compressive Strength | L | Normal Strength Concrete (34 - 48 MPa [5000 - 7000 psi]) |
| | | M | Medium Strength Concrete (66 - 79 MPa [9500 - 11500 psi]) |
| | | H | High Strength Concrete (90 - 103 MPa [13000 - 15000 psi]) |
| 2 | Number of Debonded Strands | 0 | Fully Bonded (0 Debonded Strands) |
| | | 4 | 50% of Total Strands Debonded |
| | | 6 | 60% of Total Strands Debonded |
| | | 9 | 75% of Total Strands Debonded |
| 3 | Surface Condition | B | Bright Strand Surface Condition |
| | | R | Rusted Strand Surface Condition |
| 4 | Development Test Number | 1, 2, 3 | Do Not Contain H-bar Web Reinforcement |
| | | 4 | Contain H-bar Web Reinforcement |

For example, M9B-4 would identify the fourth development test, which includes horizontal web reinforcement (H-bar), for a beam with medium strength concrete and bright strands in which nine strands are debonded (75% debonding).

## 3.2    SPECIMEN DESIGN

AASHTO Type I prestressed I-girders were used in construction of the test specimens for this study. A composite concrete slab was added to each girder to simulate actual bridge members in Texas and throughout the United States. Figures 3.1 and 3.2 show the typical cross-sections that were used for the specimens. All specimens were identical in cross-section except that the low concrete strength beam specimens (L6B) contained four strands in the bottom row, whereas the medium and high strength concrete beam specimens (M9B and H9B) contained six strands. It was necessary to remove the additional two strands from the L6B specimens to meet the maximum allowable compressive stress requirement in the bottom concrete fibers of the midspan section of the beam at release.

A suitable slab width and thickness had to be determined in designing the composite test specimens for this study. The final design of the cross-section was achieved through an iterative process.  The design had to comply with a requirement that was established by the project sponsors: the prestressing strands in the bottom row had to reach an ultimate strain of 0.035 at flexural failure of the composite test beam.

To determine the final cross-section dimensions, strain compatibility[20,21] was used. Assuming a concrete strength of 38 MPa (5500 psi) and a slab thickness of 165 mm (6.5 in), equilibrium equations were developed for several strand configurations. It was also assumed that the prestress jacking force in the Grade 1860 (Grade 270) strand was 1400 MPa (202.5 ksi) and the slab reinforcement had a negligible contribution to the ultimate strength. While satisfying equilibrium, the neutral axis depth, c, and slab width, b, were varied until a suitable slab width was calculated.  A slab width of approximately 1500 mm (60 in) was calculated, and the strand arrangements shown in Figures 3.1 and 3.2 were determined.

With the cross-sectional properties set, the strand configurations and debond lengths could be determined.  The number of strands that were required was greatly affected by the strain requirement of 0.035.  The specimen had to be under-reinforced to keep the neutral axis high enough in the composite section to meet this requirement.  Top and bottom concrete fiber stresses had to be checked at the critical section points for different strand layouts.  The number of strands required was governed by tension in the top concrete fibers at the debond points during release. Compression in the bottom concrete fibers was also critical for the L-series (low concrete strength) specimens.

18
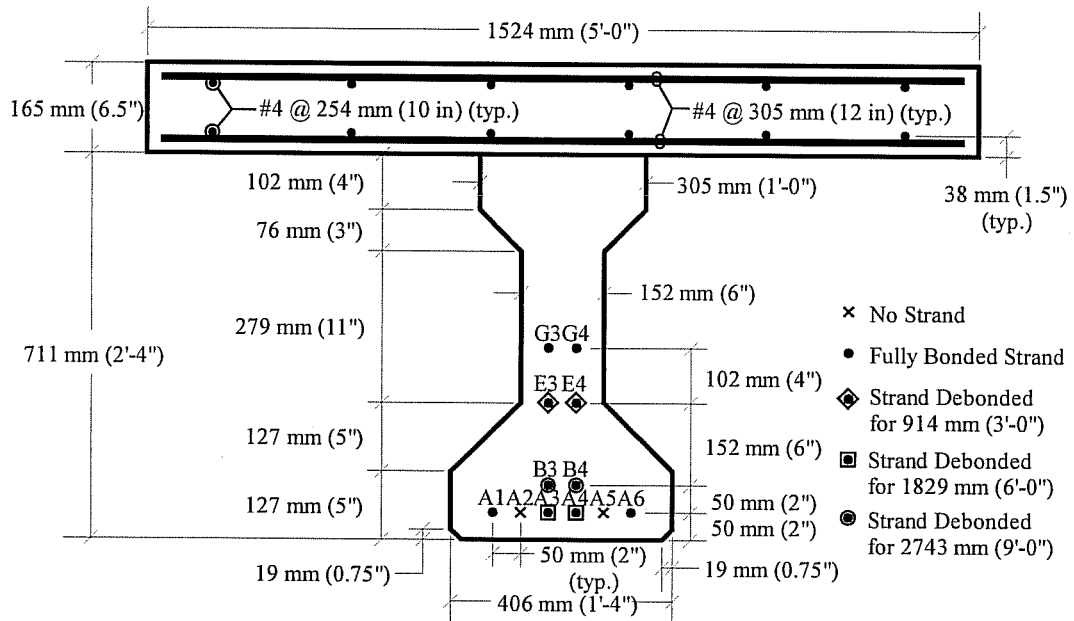
**Figure 3.1: Typical Cross-Section for L6B Series**
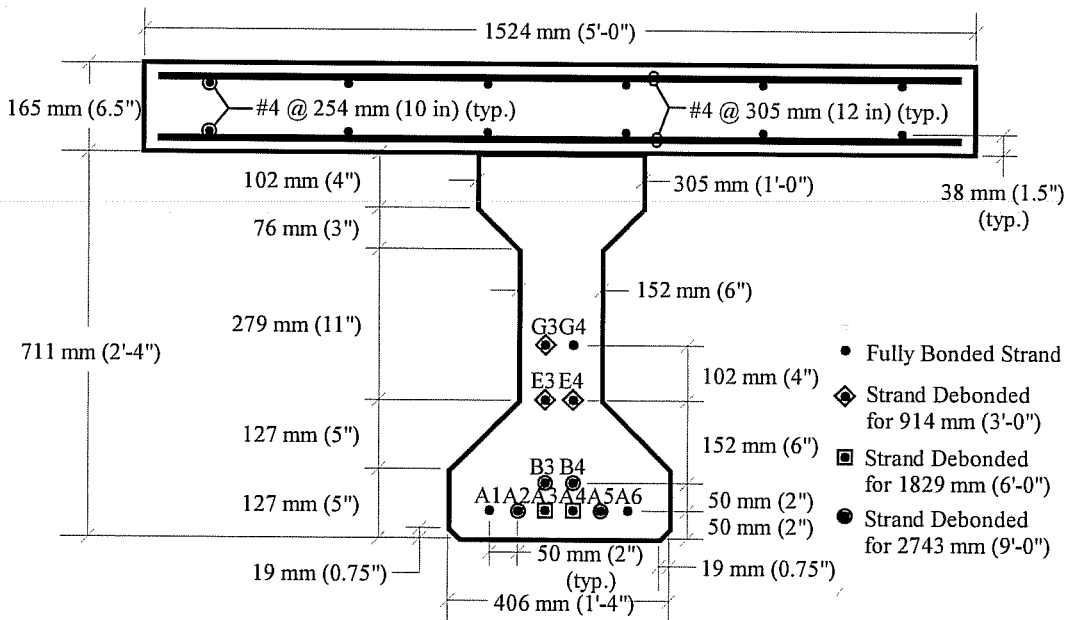


**Figure 3.2: Typical Cross-Section for M9B and H9B Series**

19

For this study, it was ensured that enough strands were present to be able to debond the required percentage in a symmetric pattern. After the correct total number of strands was determined, a debonding length scheme was determined. Allowable stresses were determined at the ends of each debond region and a sufficient number of strands were debonded to conform to these stresses. The total number of prestressing strands and the number and percentage of debonded strands required for each beam series is shown in Table 3.2.

**Table 3.2: Distribution of Debonded Prestressing Strands**

| Beam Series | Total Strands | Number of Strands per Debond Length | | | | Percent Debonded of Total |
|---|---|---|---|---|---|---|
| | | Fully Bonded | 914 mm (36 in) | 1829 mm (72 in) | 2743 mm (108 in) | |
| L6B | 10 | 4 | 2 | 2 | 2 | 60% |
| M9B | 12 | 3 | 4 | 2 | 3 | 75% |
| H9B | 12 | 3 | 4 | 2 | 3 | 75% |

Mild reinforcement was used in both the beam and the slab. Beam steel was configured according to typical TxDOT I-beam details (Appendix D). Slab steel was proportioned approximately from a standard TxDOT design for a slab typically placed on larger girders (Texas Type C). The spacing of Grade 420 #13 (Grade 60 #4) bars is shown for each direction in Figures 3.1 and 3.2.

Shear reinforcement was determined in accordance with ACI requirements[8]. Sufficient reinforcement was used to prevent a shear failure for the loading that produced maximum shear. All of the beams had the same stirrup spacing with Grade 420 #13 (Grade 60 #4) bars at 102 mm (4 in) over the initial 1372 mm (54 in) of each beam end and a spacing of 152 mm (6 in) in between. The shear reinforcement stirrups were exposed 144 mm (4.5 in) through the top of the beam to ensure composite action between the beam and deck slab.

Additional vertical reinforcement was required in the anchorage zone per TxDOT design standards. Grade 420 #16 (Grade 60 #5) bars were spaced at 102 mm (4 in) over the first 813 mm (32 in) of the beam on each end. The reinforcement is required to confine the concrete in the anchorage zone and help control longitudinal end-splitting cracks due to the transfer of the prestressing force.

## 3.3 MATERIAL PROPERTIES

### 3.3.1 Concrete

Two batch plants produced all of the concrete for the test specimens. All of the beams were cast at the Texas Concrete Company in Victoria, Texas. Three different mix designs were used to achieve the required normal, medium and high concrete strengths (Appendix B). The concrete for the deck slabs was supplied by Capital Aggregates of Austin, Texas (Appendix B). The specified concrete strengths for the beams and slab are listed in Table 3.3.

**Table 3.3: Specified Concrete Strengths for Beams and Deck Slab**

| Specimen | | Required Release Strength, $f'_{ci}$ | Required 28 Day Strength, $f'_c$ |
|---|---|---|---|
| Beams | L6B | 28 MPa (4000 psi) | 34-48 MPa (5000-7000 psi) |
| | M9B | 48 MPa (7000 psi) | 66-80 MPa (9500-11,500 psi) |
| | H9B | 66 MPa (9000 psi) | 90-103 MPa (13,000-15,000 psi) |
| Deck Slab | | N/A | 41 MPa (6000 psi) |

Concrete strengths were monitored throughout the test program. Concrete compressive strength[22] and modulus of elasticity[23] were checked on several days. Typically, compression and modulus tests were performed on all concrete specimens at an age of 3 and 28 days, as well as on days of development length testing. Additional compression tests were performed at 7 and 14 days. In addition, beam concrete was tested at prestress transfer (1 day), high strength concrete was tested at an age of 56 days, and slab concrete was tested at 2 days to ensure adequate strength for removal of shores. The concrete strength and modulus of elasticity versus time curves are presented in Appendix C. Average values for 28-day compressive strength, $f'_c$, and modulus of elasticity, $E_c$, for beam and deck slab concrete for each beam series is presented in Table 3.4 and 3.5.

**Table 3.4: Average 28-Day Beam Compressive Strength and Modulus of Elasticity**

| Series | Average $f'_c$ | Average $E_c$ |
|---|---|---|
| L6B | 49.2 MPa (7140 psi) | 38.5 GPa (5550 ksi) |
| M9B | 80.8 MPa (11710 psi) | 48.5 GPa (7000 ksi) |
| H9B | 88.8 MPa (12880 psi) | 49.0 GPa (7150 ksi) |

21

**Table 3.5: Average 28-Day Deck Slab Compressive Strength and Modulus of Elasticity**

| Series | Average f'$_c$ | Average E$_c$ |
|--------|----------------|---------------|
| L6B | 41.0 MPa (5950 psi) | 35.5 GPa (5150 ksi) |
| M9B | 43.4 MPa (6300 psi) | 34.5 GPa (5050 ksi) |
| H9B | 41.9 MPa (6080 psi) | 35.5 GPa (5150 ksi) |

## 3.3.2    Steel

Each test specimen contained a combination of prestressing steel (strand) and mild steel (rebar). The prestressing steel used in all beams was produced by Shinko Wire America, Inc., and was shipped directly to Texas Concrete Company. The prestressing steel was 15.2 mm (0.6 in) diameter, Grade 270, low-relaxation, seven-wire strand. It had a cross-sectional area, A$_{ps}$, of 140 mm$^2$ (0.217 in$^2$) and a modulus of elasticity, E$_{ps}$, of 196 GPa (28,500 ksi). The mild steel was placed in both the beam and the slab. In all cases it was Grade 60 rebar. Various bar sizes were used in the beams for stirrups, confining steel, horizontal reinforcement and H-bars. Slab reinforcement consisted exclusively of #4 rebar.

## 3.4    FABRICATION OF BEAMS

The beams were fabricated at Texas Concrete Company in Victoria, Texas. The fabrication process usually was completed in a period of two days. On the first day, the prestressing strands were placed and jacked to the required force and the mild steel rebar cage was constructed. On the second day, internal instrumentation was inserted prior to the placement of the forms and concrete.

Two identical (except for the presence of H-bars) beams were cast for each test series. It was beneficial to cast both beams at the same time to save time and avoid variability in beam material properties. The two beams were cast on the same prestressing bed. Prestressing strands were run along the entire length of the prestressing bed. End forms were placed 16.46 m (54 ft) apart for each beam. The prestressing strand was then jacked to 1400 MPa (202.5 ksi). After all of the strands were stressed, the reinforcing cage was constructed. The cage consisted of the shear reinforcement and confining steel tied to the already stressed strands. In addition, at one end of one beam in each pair a horizontal H-bar was added. The H-bar was a Grade 420 # 13 (Grade 60 #4) rebar that was bent into a hairpin with a spacing of 57 mm (2.25 in). The bar was located 279 mm (11 in) from the bottom of the beam and extended 4064 mm (160 in) into the end of the beam.

A shop drawing of the mild steel cage reinforcement is located in Appendix D. Figures 3.3 to 3.5 show the procedure described above.

After all of the gages were in place, the prestressing bed was cleaned and oiled. Care was taken to avoid contaminating the strands with the form oil. At this time, the side forms were brought into place and secured to ensure proper geometry and to contain the concrete. The concrete was then placed, and each beam was covered with blankets during curing. This process is shown in Figures 3.6 to 3.9.
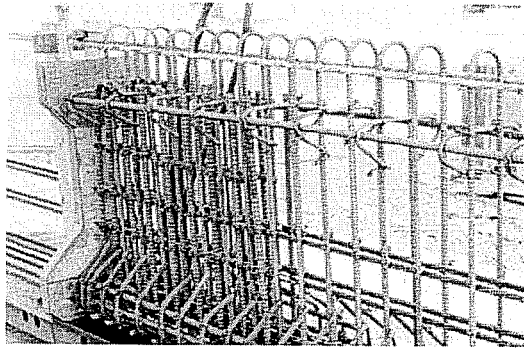


**Figure 3.3: Endforms in Place**
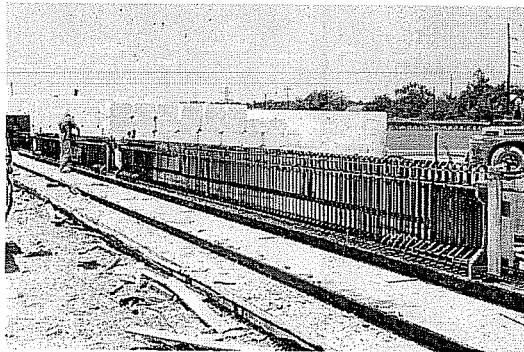


**Figure 3.4: Mild Steel Reinforcing Cage**
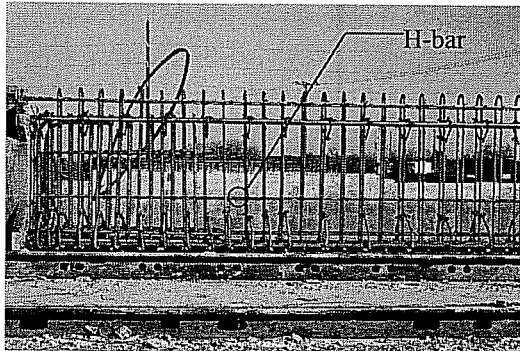
**Figure 3.5: Horizontal Web Reinforcement, H-bar**
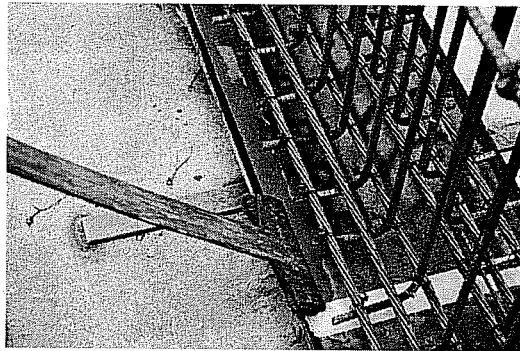


**Figure 3.6: Oiling of the Prestressing Bed**
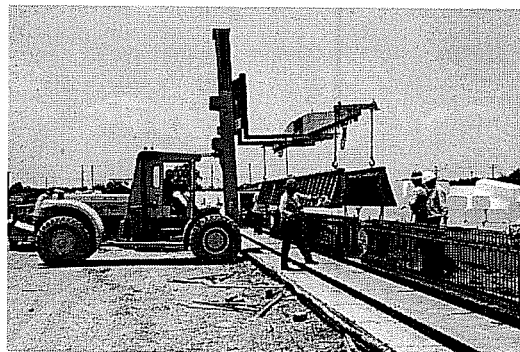


**Figure 3.7: Placement of the Side Forms**
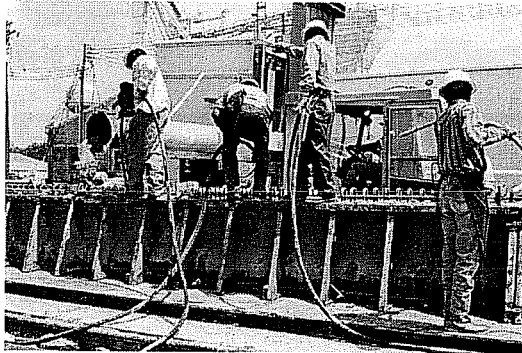
**Figure 3.8: Placement of Concrete**
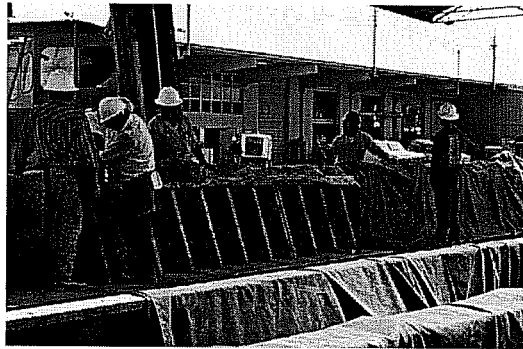


**Figure 3.9: Beams with Curing Blankets**

At the same time that the beams were being cast, concrete test cylinders were prepared and were covered along with the beam during curing. Also, a pull-out test block was prepared using the same prestressing strand and concrete that was used in the beams. Dimensions and properties of the test block are described in Section 6.2.

Concrete cylinders were tested the following day to ensure that the concrete had reached the required release strength. After all of the instrumentation was placed for transfer length testing and the initial readings were taken (see Chapter 4), the release strength was checked. If the strength was adequate, the prestressing force was released from the strands. Release of prestress was performed by flame cutting the strands, as shown in Figure 3.10. Flame cutting was performed because it replicates the most severe release condition.

**Figure 3.10: Release of Prestress by Flame-Cutting**

Two methods of release were used: three-point and single-point. Three-point release involved the same strand being cut at three places simultaneously. The three points where the cuts took place were located at both ends of the prestressing bed and in the space where strands were exposed between the two beams. Three-point release should distribute the release impulse evenly to all ends of the beams. This type of release was used for the normal strength specimens.

Single-point release involved a single cut of each strand at a point between the two beams. This results in two release end conditions, the live end and the dead end. The live end was the beam end adjacent to where the flame cutting took place. The dead end had no strands cut until all of the prestressing force had been transferred. Single-point release was performed to investigate the difference between the sudden strand release at the live end of the beam with the more gradual strand release at the dead end. This type of release was used with the medium and high strength beams.

## 3.5 PLACEMENT OF CONCRETE DECK

The beams were shipped in pairs to the Phil M. Ferguson Structural Engineering Laboratory of the University of Texas at Austin where composite concrete slabs were cast prior to testing. The beam slabs were cast one at a time due to space limitations. Plywood forms were erected and the two layers of slab reinforcement were placed. The reinforcement consisted of Grade 420 #13 (Grade 60 #4) rebar at 250 mm (10 in) spacing in the longitudinal direction and at 300 mm (12 in) spacing in the transverse direction. The beams were designed assuming shored slab construction. Therefore, self-supporting forms were used and the beam was shored prior to placement of concrete. Figures 3.11 through 3.13 show this process.

26
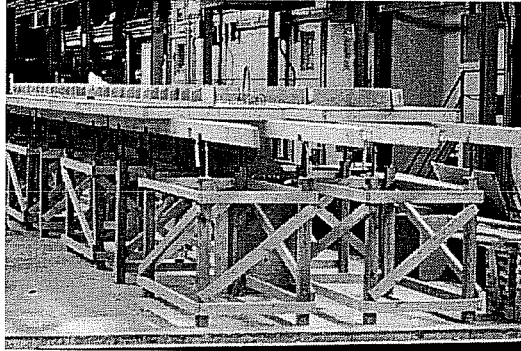
**Figure 3.11: Placement of Deck Forms**
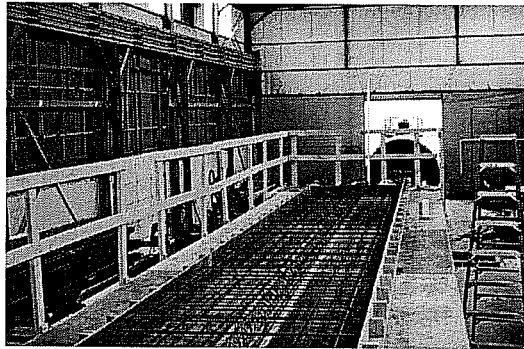


**Figure 3.12: Mild Steel Reinforcement in Place**
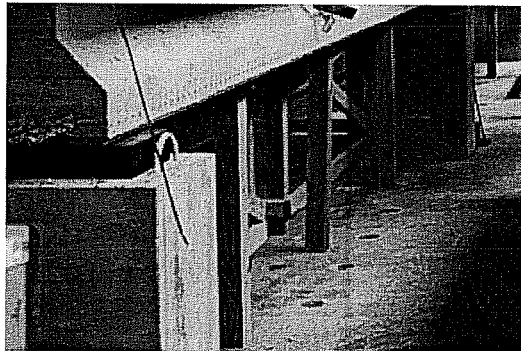


**Figure 3.13: Placement of Shores**

27

After the forms were in place and the beam was shored, placement of the concrete could commence. Concrete was supplied by Capital Aggregates of Austin, Texas. A slump test was performed on the concrete after arrival to ensure workability. A slump of 75 mm (3 in) was used.

The concrete was placed using a bucket and overhead crane. The casting procedure consisted of the concrete being placed, vibrated and screeded. After all of the concrete was screeded, the slab was floated and trowel finished to ensure a relatively smooth surface. The slab was covered with plastic during a curing period of approximately one week. This procedure can be seen in Figures 3.14 through 3.16.
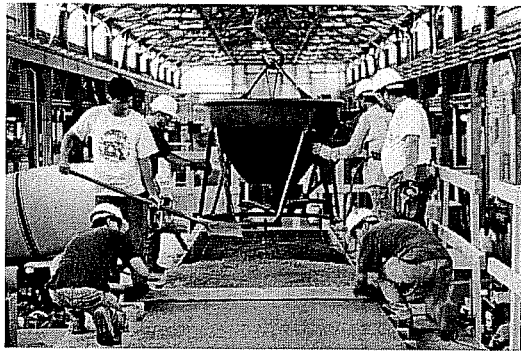


**Figure 3.14: Placement, Vibration and Screeding of Deck Concrete**
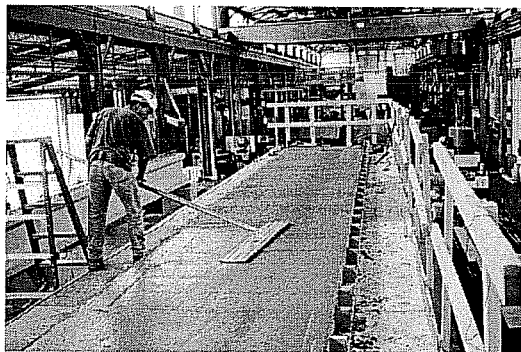


**Figure 3.15: Floating of the Concrete Deck**

28

**Figure 3.16: Trowel Finishing of the Deck Surface**

Concrete test cylinders were prepared at the same time as the slab was being cast. The cylinders were covered to simulate the curing conditions of the beam. Cylinder compressive strength and modulus of elasticity tests were performed after approximately two days to ensure sufficient strength and stiffness to remove the forms and shores. The same procedure was used to cast the second slab in each pair, reusing the same set of forms.

# CHAPTER FOUR

## Transfer Length Testing

### 4.1    INTRODUCTION

Transfer lengths were measured using two sets of readings taken before and after transfer of the prestressing force: surface concrete strains and the draw-in of the strands. This chapter will discuss the instrumentation and procedure used to measure the transfer lengths. Short- and long-term readings were taken, and the results were compared to determine what effect time had on transfer lengths.

### 4.2    INSTRUMENTATION AND MEASUREMENTS

#### 4.2.1    DEMEC Strain Gage Method

The primary system used for determination of transfer lengths was the Detachable Mechanical (DEMEC) Strain Gage System. This system has been used quite successfully in several previous research projects[1,10,24], both in the laboratory and in the field.

The DEMEC system measures the distance between two points before and after transfer of the prestressing force. The points are metallic discs with a machined hole in the center that is used to receive the DEMEC gage. The points were epoxied at a height of 63.5 mm (2.5 in) from the bottom of the beam. The initial point was placed 25 mm (1.0 in) from the vertical face of the beam and the subsequent points were placed with a spacing of 50 mm (2.0 in). Points were placed along each face of each end of the beam throughout the transfer zone as shown in Figure 4.1. The points were applied along a sufficient length to ensure that the entire transfer length could be monitored. For this study, the points were applied over a length of 4570 mm (180 in), or 1830 mm (72 in) beyond the longest debond length.

The points were applied with a fast-setting, two-part epoxy. Measurements were made with a ruler to determine the location of the four initial points at each beam end. The points were placed four at a time on each of the four beam ends before returning to the initial end to place the subsequent four points. This allowed sufficient time for the epoxy to set before the points were used in setting the next group of points, which might cause the epoxy bonding to be disturbed.

30

The subsequent four points were placed relative to the initial four points using a 200 mm (7.87 in) gage bar to ensure a consistent spacing. This process was continued until all points were placed on each face.
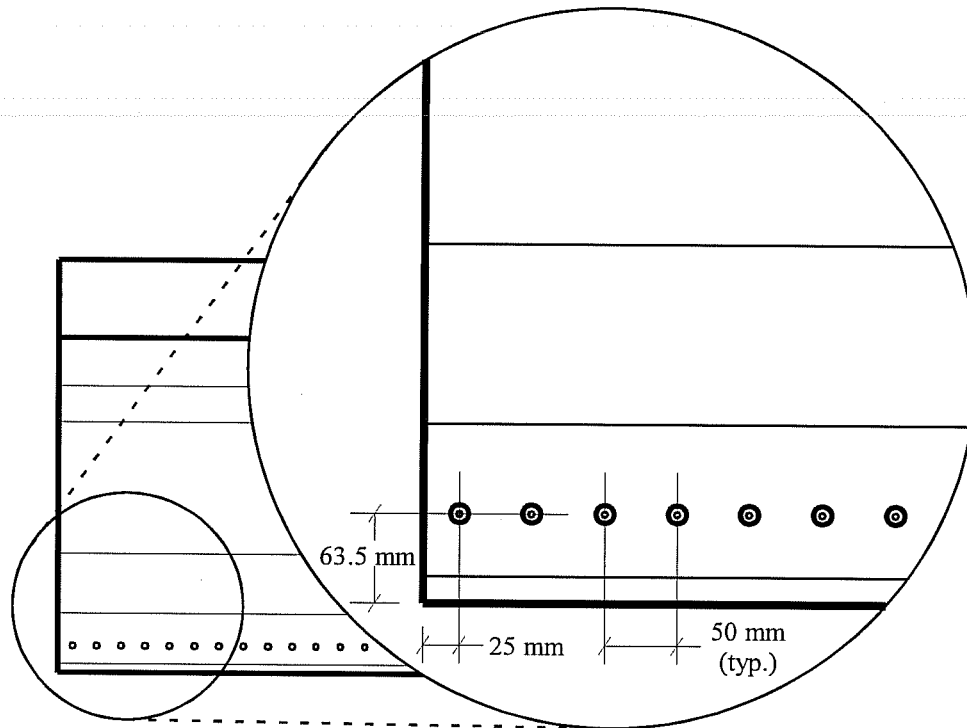


**Figure 4.1: Placement of DEMEC Points**

After all of the DEMEC points had been applied and prior to the release of the prestressing force, the initial readings were taken with the DEMEC gage. The gage measures the distance between a pair of points relative to a standard gage length of approximately 200 mm (7.87 in) with a precision of 0.00016 mm ($6.30 \times 10^{-6}$ in). The measured value was used to determine the actual distance between the points when compared to the reading for the 200 mm (7.87 in) standard.

Each set of readings were taken starting at the beam end and progressing toward the middle of the beam. The relative distance between each pair of points was read twice and recorded. The two readings were required to be within two gage units of each other. Otherwise, the readings were repeated. This resulted in a tolerance of 0.00032 mm ($1.26 \times 10^{-5}$ in) between the two readings. Figure 4.2 shows a DEMEC gage being employed.

31
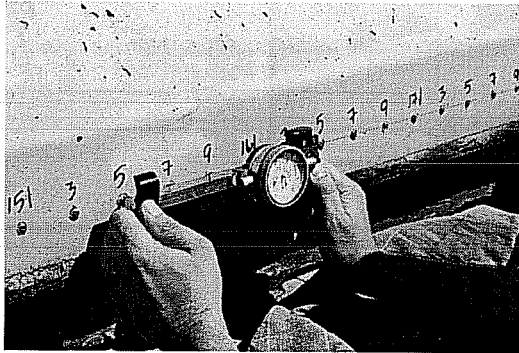
**Figure 4.2: DEMEC Gage Being Employed**

After all of the initial gage readings were taken, the prestress force was released and the transfer readings were taken. The same procedure was used to measure the transfer readings as was used for the initial readings.

The gage readings were performed in two-person teams. One member read the gage while the other member recorded the measurements and checked the differential trend. The team members switched duties after each beam end was completed. The same person performed the initial and transfer readings on each beam end in an attempt to reduce the human error. Readings were then used to calculate the concrete surface strains over each gage length; change in length divided by the initial gage length gave the strain at each position as described in Section 4.3.

### 4.2.2    Draw-In Method

An additional method of calculating the transfer length is based on the draw-in of the prestressing strand after release of the prestress force. The transfer length is a function of the draw-in and the initial prestressing force.

Draw-in of the strand was determined by painting a mark on the strand and then measuring the distance from the mark to the face of the beam end. Masking tape was wrapped around the strand prior to painting to provide a sharp reference point on the strand. A non-water soluble paint was used to ensure that the paint would not wash off before long-term measurements could be made. Hose clamps were attached to the strands to prevent them from fraying when the prestress force was transferred.

Measurements of the distance to the paint mark on the strand from the face of the concrete at the beam end were performed before and after the transfer of the prestressing force

32

with a metal ruler. Measurements were averaged from three wires of each strand, because there was often differential displacement between the wires. Readings were made to the nearest 0.25 mm (0.01 in). Long-term readings were also taken before the beams were shipped to the research lab. The difference between the initial measurement and the transfer or long-term measurement was the strand draw-in. The debonded strand readings had to be adjusted to compensate for the elastic shortening of strand, which took place within the debonded length.

## 4.3    REDUCTION OF DEMEC DATA

DEMEC readings were taken on both faces of each beam end. The results of both faces were averaged to construct the concrete strain profile for that beam end. The average results were used to help counteract the thermal effects due to the sun shining on one side of the beam, but not the other, as well as the scatter in readings which occurs in collecting these data.

The difference between the initial and transfer reading was multiplied by the gage factor to determine the differential strain. Each DEMEC reading covered a span of five DEMEC points. The differential strain is simply the average strain over the entire gage length. Therefore, the stain was assigned to the location of the middle DEMEC point, which is located at the center of the gage distance. Also, the strain due to the beam weight was calculated at every point and subtracted from the measured strains. This helped to more clearly indicate the strain plateau due only to prestressing, which is necessary to locate when determining the transfer length.

The raw data strain profile shows the measured strains corresponding to each point. A smoothing procedure was used to remove some of the scatter that is inherent in the raw data. Determination of the smoothed value was accomplished by taking the average of three measurements: the measurement at the point in question, and at the two points on either side of it, as seen in Figure 4.3. This process can also be seen in Equation (4-1). A comparison of the raw and smoothed data is shown in Figure 4.4.

$$\varepsilon_{i,smoothed} = \frac{\varepsilon_{i-1} + \varepsilon_i + \varepsilon_{i+1}}{3} \qquad (4\text{-}1)$$

33
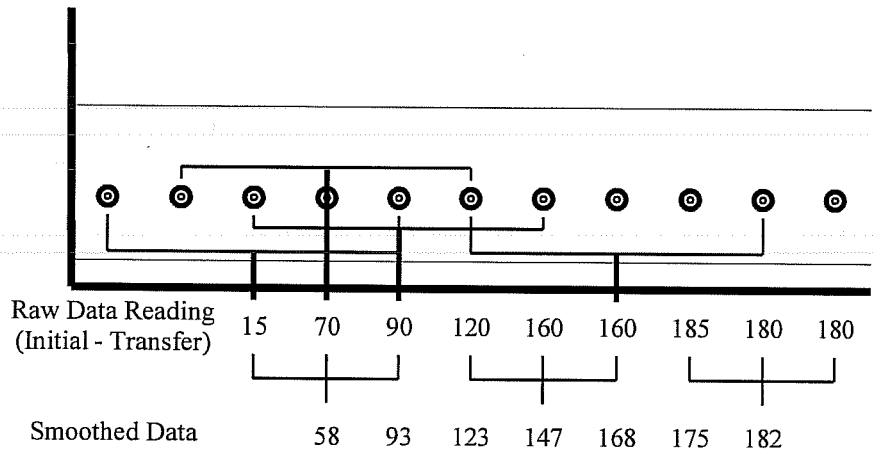
Figure 4.3: Smoothing Procedure
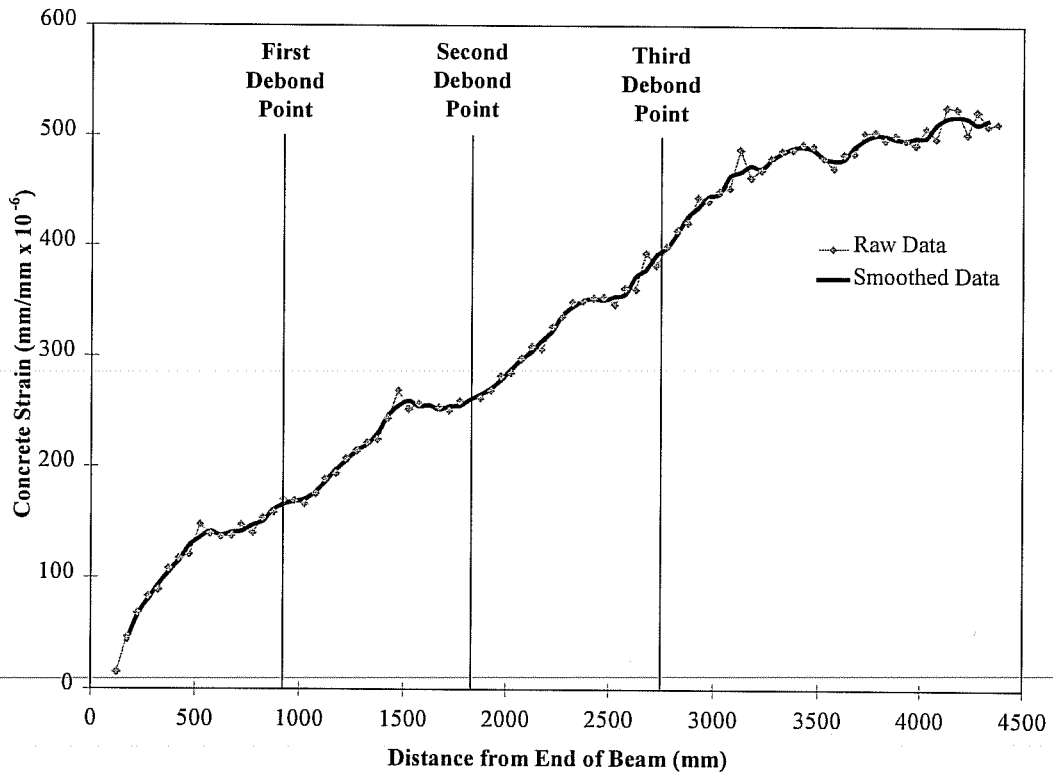


Figure 4.4: Typical Strain Profile

34

After data from the two faces of the beam end were "smoothed," they were averaged to determine the strain profile for the beam end. This procedure was used to determine the strain profiles for the initial and long-term cases. The resulting beam end profiles were used to determine the transfer lengths. All of the beam end strain profiles are located in Appendix E.

## 4.4    CALCULATING THE TRANSFER LENGTH

### 4.4.1    The 95% Average Maximum Strain Method

In the 95% Average Maximum Strain (AMS) method, the transfer length is defined as the point where a line corresponding to 95% of the average maximum strain intersects the strain profile[10], as seen in Figure 4.5. The AMS is determined by averaging the values on the plateau of the strain profile. The plateau that yields the maximum strain is determined by a trial and error method. The reason for using 95% AMS is because of the round off at the intersection of the transition region and the plateau[19]. This round off is introduced due to smoothing and the use of the average strain over the gage distance. This procedure yields a slightly longer transfer length then the idealized model.
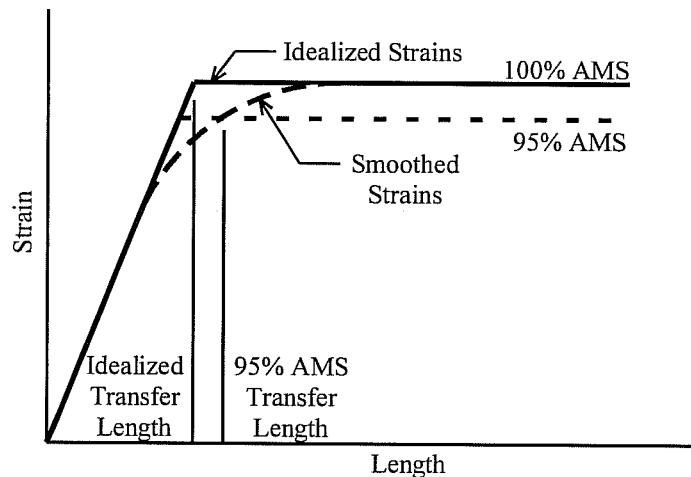


**Figure 4.5: Smoothing at the Transition Point**

The 95% AMS was determined by taking 95% of the strain increment from the previous plateau to the plateau under consideration. Thus, the reduction in strain is five percent of the

increase from one strain plateau to the next. The same reduction that was calculated for the initial strain profile was also used for the long-term profile. Figure 4.6 illustrates this procedure.
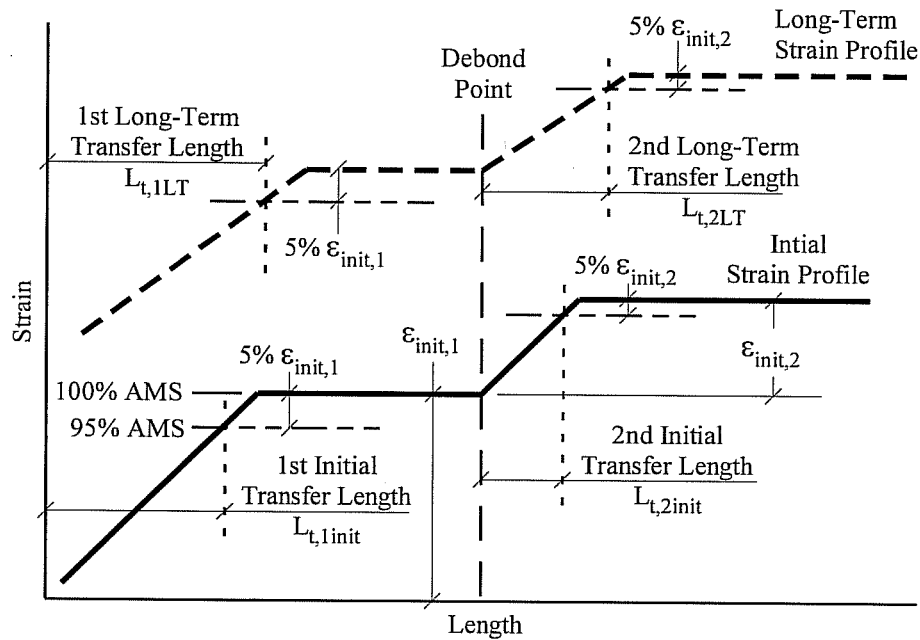


**Figure 4.6: Calculation of 95% AMS**

The presentation and discussion of the results of the transfer length measurements using the 95% AMS method can be found in Sections 7.2.1 and 7.3.1 of this thesis. In addition to the presentation of the calculated transfer lengths for each specimen, the effects of such variables as concrete strength, time, debonding and method of release on the transfer length will be discussed.

### 4.4.2    The Draw-In Method

Another way to estimate the transfer length is by the Draw-In Method. This method estimates the transfer length when the draw-in of the strand after release and the initial prestress of the strand are known[25]. This procedure was initially developed for fully bonded beams, but it can be modified for use with debonded specimens. To do this, the draw-in of the strand must be corrected for the elastic shortening that occurs in the free end of any unbonded strand length, as seen in Equation (4-2). This elastic shortening must be subtracted from the measured draw-in of

the strand in Equation (4-3). This corrected draw-in is then used to calculate the transfer length with Equation (4-4).

$$\text{Elastic Shortening, } ES = \frac{(f_{si})(\text{Free End})}{E_{ps}} \tag{4-2}$$

$$\text{Draw-In, } g = (\text{Measured Draw-In}) - ES \tag{4-3}$$

$$\text{Transfer Length, } L_t = \alpha \frac{E_{ps}}{f_{si}} g \tag{4-4}$$

The $\alpha$ coefficient in the transfer length equation (4-4) is based on the assumed shape of the bond stress distribution throughout the transfer region[25]. Two types of bond contribute to the value of the coefficient: friction bond and elastic bond. Friction bond produces a constant stress distribution which results in $\alpha = 2$. Elastic bond produces a linear stress distribution and results in $\alpha = 4$. Both bond mechanisms contribute to the stress distribution and therefore a value of $\alpha = 3$ is used to determine the transfer length.

To determine the transfer length for each transfer region, first the draw-in was calculated for each strand of each specimen. Figure 4.7 shows the corrected initial and long-term strand draw-in for a typical specimen.
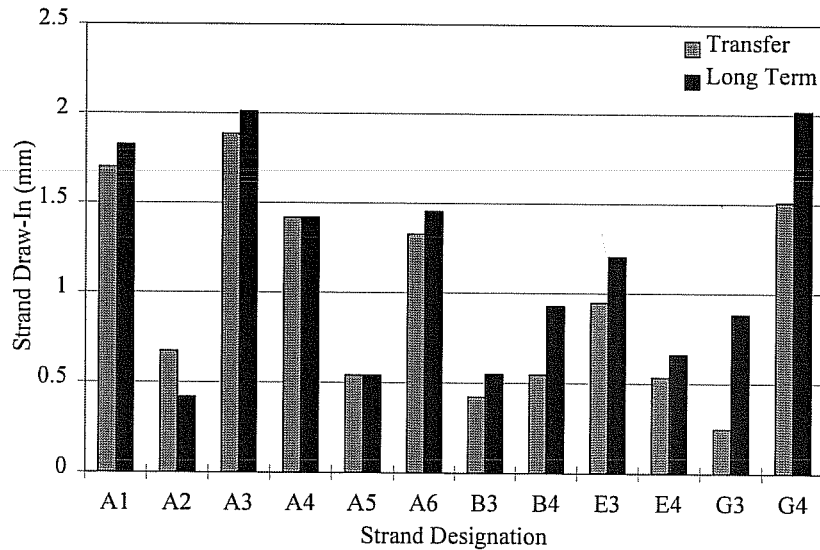


Figure 4.7: Corrected Initial and Long-Term Strand Draw-In

Once the corrected draw-in was calculated for each strand, the transfer length of each strand was determined. The transfer length for each transfer region was then calculated by averaging the transfer length of all strands in each transfer region. The corrected strand draw-in diagrams for each beam end are presented in Appendix F.

The presentation and discussion of the results of the transfer length measurements using the Draw-In method can be found in Section 7.2.2 and 7.3.2 of this thesis. In addition to the presentation of the calculated transfer lengths for each specimen, a comparison of the results with the 95% AMS results will be made.

# CHAPTER FIVE

## Development Length Testing

### 5.1    INTRODUCTION

After all transfer length data had been acquired in Victoria, Texas, the beams were transported approximately 130 miles to the Ferguson Structural Engineering Laboratory (FSEL) in Austin, where development length testing was conducted. The two beams that were cast simultaneously were shipped as a pair to FSEL. All testing was completed on each pair of beams prior to the next pair being delivered.

After the beams were delivered to FSEL, they were placed on pedestals and neoprene bearing pads. Before testing could commence, the concrete deck slab had to be placed per Section 3.5. In addition, preliminary investigation and analysis had to be performed to determine the location of load points, placement of instrumentation, and predicted beam behavior.

This chapter will discuss the preparation and performance of the development length testing. Critical parameters will be introduced and the means used to monitor them will be presented.

### 5.2    TEST SETUP

The test setup completion involved several tasks. First, the embedment length, $L_e$, of the first test had to be determined. The first test embedment length was initially chosen based on code requirements. It is important to remember that for debonded specimens the embedment length is measured from the end of the longest debonded length, $L_b$, to the critical section.

An adequate development length could be determined by adjusting subsequent test lengths based on the results of prior testing. If a test suffered a bond failure, then a longer embedment length was used in the ensuing test, and if a test yielded a flexural failure, a shorter length would be used.

The first three tests were performed with different embedment lengths for each test. The fourth test was always performed on the beam end that contained the H-bar horizontal web

39

reinforcement detail. This test was performed using the shortest embedment length of the first three tests. This test was performed to investigate whether the presence of the H-bar detail improved the bond performance of the beam.

Once the test embedment length was determined, the other test variables could be determined. The required test span length, $L_s$, had to be determined. Since both ends of the beam were to be tested, the beam end that was not being testing was cantilevered to avoid damage to that portion of the beam. The test span length had to be long enough to eliminate any possibility of a shear failure, yet short enough to limit the amount of damage in the potion of the beam which would be within the span of the second test.
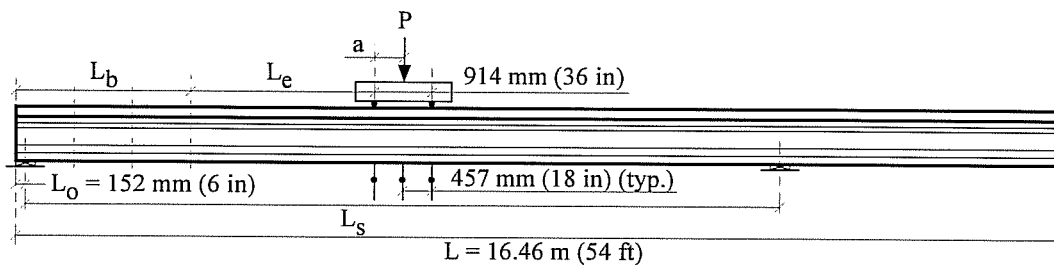


**Figure 5.1: Development Length Test Setup**

The test setup used for development length testing can be seen in Figure 5.1. The load was applied to the specimen with a hydraulic ram, which was attached to a steel loading frame. The frame was securely fastened to the FSEL Elevated Testing Slab with heavy bolts that were tensioned to prevent frame movement under test loads. A load spreader beam was placed on two load points to distribute the load from the ram. The spreader beam was supported on the load points by steel rollers. The load points were placed so that the rollers were centered 914 mm (36 in) apart, with the roller closest to the beam end being located at the critical section for the test embedment length.

The resulting two-point loading created a constant moment region during testing. Because the load points were not always located at the midspan, the hydraulic ram had to be offset to produce the desired constant moment. This offset distance, a, also had to be determined before testing could begin. All calculated testing variables related to the test setup lengths shown in Figure 5.1 are presented in Table 5.1 for the three beam series.

40

**Table 5.1: Development Length Test Variables**

| Test I.D. | Longest Debonded Length, $L_b$ mm (in) | Embedment Length, $L_e$ mm (in) | Test Span Length, $L_s$ mm (in) | Ram Location, a mm (in) |
|-----------|-----------|-----------|-----------|-----------|
| L6B-1 | 2743 (108) | 2438 (96) | 10973 (432) | 476 (18.75) |
| L6B-2 | 2743 (108) | 2896 (114) | 11887 (468) | 476 (18.75) |
| L6B-3 | 2743 (108) | 2134 (84) | 10363 (408) | 470 (18.5) |
| L6B-4 | 2743 (108) | 2134 (84) | 10363 (408) | 470 (18.5) |
| M9B-1 | 2743 (108) | 4572 (180) | 12192 (480) | 606 (23.875) |
| M9B-2 | 2743 (108) | 2438 (96) | 10973 (432) | 467 (18.375) |
| M9B-3 | 2743 (108) | 2896 (114) | 11887 (468) | 470 (18.5) |
| M9B-4 | 2743 (108) | 2438 (96) | 10973 (432) | 470 (18.5) |
| H9B-1 | 2743 (108) | 4572 (180) | 12192 (480) | 606 (23.875) |
| H9B-2 | 2743 (108) | 2438 (96) | 10973 (432) | 470 (18.5) |
| H9B-3 | 2743 (108) | 2438 (96) | 10973 (432) | 467 (18.375) |
| H9B-4 | 2743 (108) | 2438 (96) | 10973 (432) | 470 (18.5) |

After the loading frame was in place, the beam was instrumented with measuring devices. The devices were used to monitor the applied load, beam and support displacement, strand slip and the strain of the top concrete fibers of the deck. The instrumentation of the test specimen is explained in further detail in Section 5.3. Figure 5.2 shows the complete test setup in the laboratory.
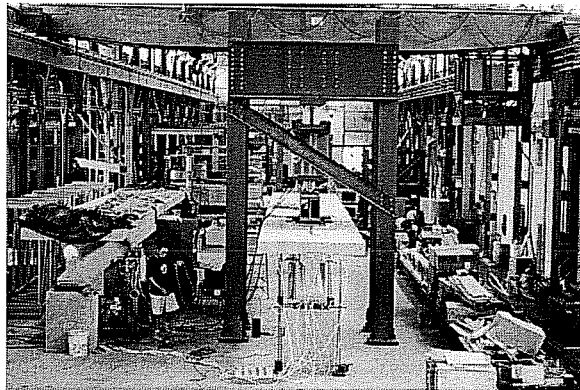


**Figure 5.2: Test Setup in Laboratory**

Following the testing of the first beam end, the process was duplicated for testing of the second end, with the pedestals repositioned to give the lengths shown in Table 5.1. After both beams were tested, they were cut into lengths that could be lifted with the laboratory overhead crane, were removed from the lab, and then the next pair of beams was delivered.

## 5.3    INSTRUMENTATION

As discussed in the previous section, several parameters were measured during the development length testing of the specimens. The measuring devices that were used to monitor these parameters are discussed in the following sections.

### 5.3.1    Measurement of the Applied Load

The applied load was monitored by two devices: a load cell and a pressure transducer. The load cell was the primary measuring device. It was attached to the hydraulic ram and monitored the load that was applied by the ram to the spreader beam. The pressure transducer served mainly as a backup device. It was attached to the hydraulic pump and monitored the pressure of the hydraulic fluid in the hoses between the pump and the ram. Both devices were connected to the electronic data acquisition system, which converted the recorded signal voltages to units of force.

### 5.3.2    Measurement of Beam and Support Displacement

The displacement of the beam was monitored with three measuring instruments: linear potentiometers, a tension wire system, and a dial gage. The primary instrumentation consisted of the linear potentiometers. Three potentiometers were used to record the beam displacement. One was placed under each of the two load points and the third was centered between the load points. The three potentiometers were connected to the data acquisition system, which converted the recorded signal voltages to units of displacement.

42
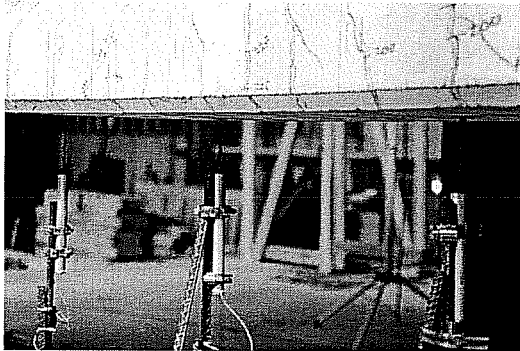
**Figure 5.3: Linear Potentiometers Measuring Beam Deflection**

The tension wire system served as the backup to the potentiometers for measuring beam deflections. In this system, anchor bolts were embedded into the beam over the centerline of the bearings and a length of wire was strung between the two bolts. One end of the wire was secured to the first anchor bolt, while the other end of the wire was draped over the second anchor bolt with a steel weight suspended to tension the wire. A ruler was then attached to the beam at the center of the load points. Readings were taken manually using a mirror to align the wire, thus avoiding any error due to parallax. This measurement yielded the "true" displacement of the beam because it was relative to the bearing height, which was not constant during testing.

The dial gage was used to monitor the displacements early in the testing procedure. It was placed at center of the load points. The primary use of the dial gage was to check the potentiometer readings. Figure 5.4 shows the dial gage along with the potentiometers and tension wire measuring system.
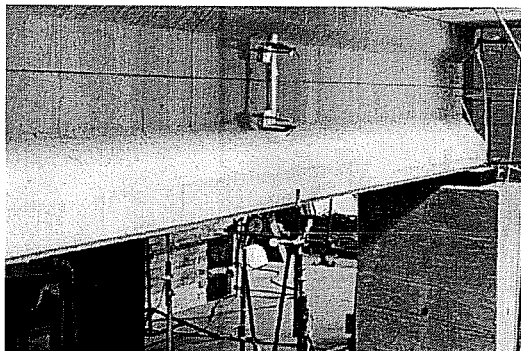


**Figure 5.4: Linear Potentiometers, Piano Wire and Dial Gage**

43

As discussed above, the tension wire reading gives a "true" displacement, because it did not include the effects of the bearing displacement. To compensate for bearing displacements when using data from the linear potentiometers, additional potentiometers were placed under the deck slab at the centerline of the bearings and on both sides of the beam to monitor any vertical displacement at the supports. This allowed the relative displacement of the bearings to be determined. The "true" beam displacement could then be calculated by adjusting the displacement measured from the center beam potentiometer, located midway between the load points as shown in Figure 5.1.

### 5.3.3    Measurement of Strand End Slip

Strand end slips were monitored to assist in the identification of the failure mode. If large end slips were observed and the beam did not reach the predicted maximum load, it could be assumed that a bond failure had occurred. Also, if no slip was observed it could be assumed that the beam had not failed in bond.

The measurement of strand end slips was performed with linear potentiometers. Special fasteners were used to securely clamp the potentiometers to the strands. Potentiometers were attached to the free end of each strand. Glass slides were epoxied to the beam end face to ensure a smooth, level surface from which to make readings.
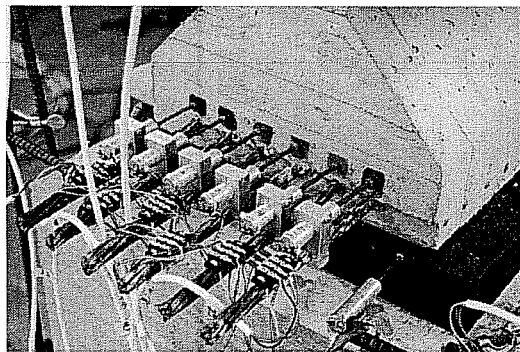


**Figure 5.5:  Linear Potentiometers Measuring Strand End Slip**

### 5.3.4 Measurement of Concrete Deck Top Fiber Strains

Monitoring of the top concrete fiber strain of the deck was necessary to assist with the identification of the failure mode. Electronic Resistance Strain Gages (ERSG) were bonded to the top of the slab to determine the top fiber strains. Spalling of the concrete deck occurred after sufficient rotation was induced into the specimen; therefore, it was desirable to monitor the concrete strains at the top of the slab. Spalling would generally occur when the compressive strain of the concrete became greater then 0.003. The maximum concrete strains were expected to be located within the constant moment region, therefore the ERSG's were placed within this region.

Spalling of the top deck concrete was typically an indicator of a flexural failure, however spalling could also occur in bond failures. The applied load, strain in the prestressing strand, and end slips also needed to be investigated to determine the failure mode. If the predicted load and required strand strain was achieved and no end slip was observed, then a flexural failure could be assumed.

The ERSG's were connected to the data acquisition system, which converted the signal voltages to strains. The strains could be checked during testing to indicate when and where spalling of the slab might be expected to occur.
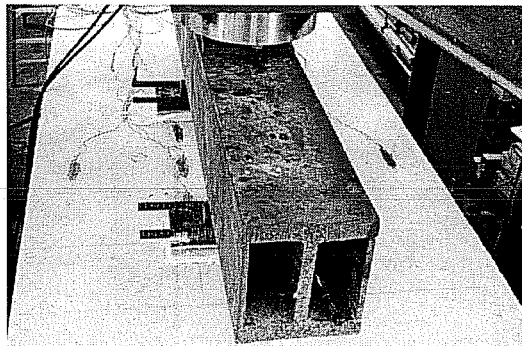


**Figure 5.6: Placement of Electronic Resistance Strain Gages**

### 5.3.5 The Data Acquisition System

The data acquisition system was necessary to convert the voltages from all of the electronic measuring instruments to engineering units. The system consisted of two DC voltage

sources (one 2 Volts and one 10 Volts), one quarter-bridge box, two full-bridge boxes, an IBM personal computer, and a Hewlett Packard scanner. The voltages were scanned for each instrument at several intervals during the test. The voltages were then converted to engineering units using the HPDAS2 conversion program.

In addition to the equipment listed above, a printer was used to produce a hard copy of the data during testing. The hard copy was used to monitor the readings which were being made by the instruments during testing and served as backup data in the event of a computer failure. A pen plotter was also used to produce the load-deflection curve. This plot was used to ensure that realistic beam response was being recorded during testing.



Figure 5.7: The Data Acquisition System

## 5.4 DEVELOPMENT LENGTH TEST PROCEDURE

After all test setup procedures were completed and all instrumentation was in place, development length testing could begin. An initial reading was made on each manual measuring device to establish a datum, and electronic devices were zeroed before the beam was loaded.

The development length testing comprised several load steps. Before cracking of the beam, when the beam stiffness was high, the load steps were made in increments of the applied load. After cracking, when the beam stiffness was reduced, the load steps were made in increments of the beam deflection.

At the end of each load step, the electronic instruments were scanned, and the manual instruments were read and recorded on data sheets. The load and deflection were recorded, and the beam was inspected for any cracking. All cracks were marked before the next load step was

46

begun.  Important events, such as the first flexure or shear crack, first crack in a transfer region and the final load, were noted and photographed.  Also, crack widths were measured at certain points in the constant moment region and the transfer regions.

Testing continued until one of three general failure modes was observed.  The three failure modes are flexural, bond and hybrid failures.  The flexural failure mode is defined as the beam reaching the calculated flexural capacity without any significant strand end slip being observed.  Bond failure is defined as a failure where excessive strand end slip prevented the beam from reaching the calculated flexural capacity.  The hybrid failure mode is a combination of the flexural and bond failure modes.  A hybrid failure is defined as any failure where the beam is able to reach the calculated flexural capacity, but significant strand end slip and cracking in the transfer regions are present prior to failure.

After testing was completed, the beam was unloaded and readings were taken a final time to determine any residual deflection.  The test data was used to produce plots of load versus deflection, strand end slip versus deflection and concrete strain versus applied load.  The plots for each development length test can be found in Appendices G and H.  In addition, the crack pattern for each beam test can be found in Appendix I.

The presentation and discussion of the results of the development length testing can be found in Sections 7.4 and 7.5 of this thesis.

# CHAPTER SIX

## Strand Pull-Out Testing

### 6.1   INTRODUCTION

Strand pull-out testing was developed to determine the quality of bond between the concrete and strand. Previous pull-out testing has established a benchmark for the required pull-out load/bond stress for which adequate transfer and development lengths can be expected. All of the prior testing had been performed with 12.7 mm (0.5 in) strand; therefore pull-out tests were performed to determine if the same bond stress would be sufficient to produce adequate bond with 15.2 mm (0.6 in) strand.

In 1974, Saad Moustafa[26] developed the strand pull-out test at the Concrete Technical Commission (CTC), in Tacoma, Washington. These tests were performed using 12.7 mm (0.5 in) diameter strand with an embedment length of 457 mm (18 in). An average pull-out force of 170 kN (38.2 kips) was observed. Further pull-out testing with 12.7 mm (0.5 in) strand in May 1996 by Logan[27], accompanied transfer and development length testing of beams. This enabled pull-out test results to be compared to transfer and development test results. These tests showed that strand with a pull-out force greater than 160 kN (36 kips) performed well in development length testing.

The bond stress resulting from a pull-out force of 160 kN for 12.7 mm strand is 6.58 MPa (0.955 ksi). Using this bond stress, a required pull-out force for 15.2 mm (0.6 in) strand with the same 457 mm (18 in) embedment length can be calculated. The corresponding pull-out force for 15.2 mm (0.6 in) diameter strand is 192 kN (43.2 kips). Pull-out test results from this study were checked to see if adequate transfer and development is achieved in beams with companion tests showing pull-out forces greater than 192 kN.

### 6.2   PREPARATION OF THE PULL-OUT TEST BLOCK

Each pull-out test block was prepared and cast at the same time as a pair of beams at the Texas Concrete Company in Victoria, Texas. The prestressing strand and concrete used in the test block were identical to those used in the beams. The test block consisted of six strands that were embedded 457 mm (18 in) into the concrete block that measured 914 mm (36 in) long, 610 mm (24 in) wide, and 610 mm (24 in) deep. Each strand was placed to ensure 152 mm (6 in) of cover

and 305 mm (12 in) of center-to-center strand spacing. Figure 6.1 shows the dimensions of the block and placement of the strands.
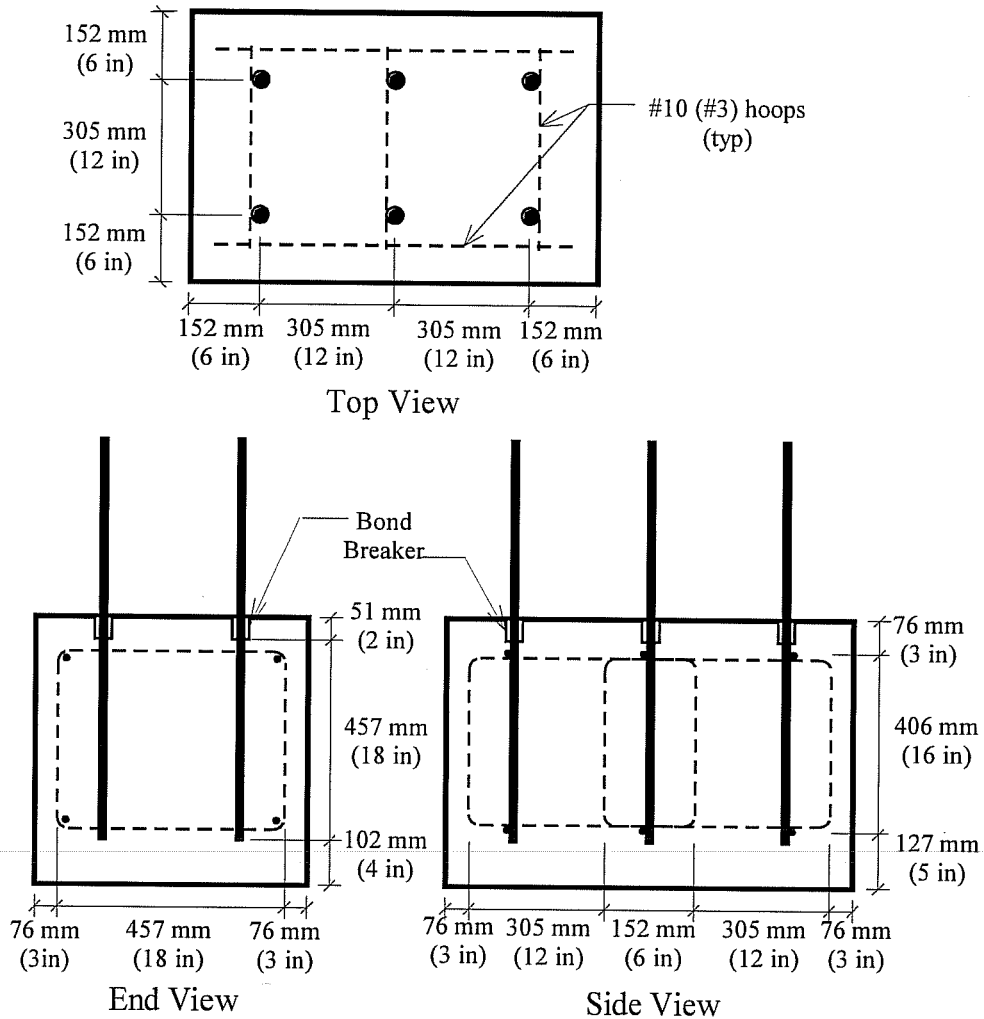


**Figure 6.1: Pull-Out Test Block Dimensions**

A mild steel reinforcement cage was used to hold the strand in place, as seen in Figures 6.1 and 6.2. Also, a piece of plastic sleeve was attached to strand and extended 51 mm (2 in) into the top of the block. The reason for this was to act as a bond breaker and eliminate the effects of surface spalling, which hindered the measurement of the pull-out length. Figures 6.3 and 6.4 show the concrete being placed and the finished test block.
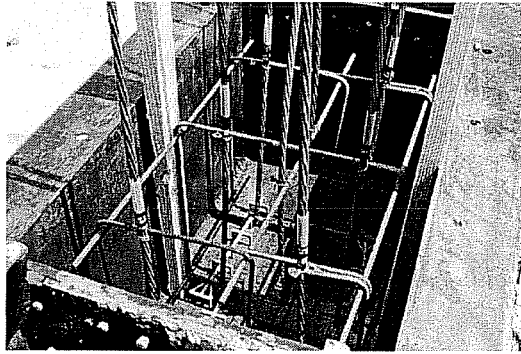
**Figure 6.2: Prestressing Strands Tied to Reinforcing Cage**
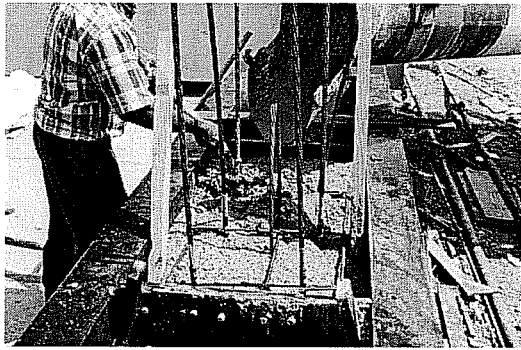


**Figure 6.3: Concrete Being Placed for Pull-Out Test Block**
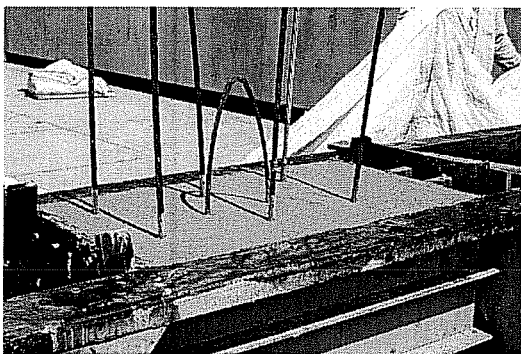


**Figure 6.4: Finished Pull-Out Test Block**

## 6.3    TEST SETUP AND INSTRUMENTATION

Pull-out testing typically took place two days after the block was cast. Testing took place at Texas Concrete in Victoria, Texas.

Test set-up preparation began by removing any exposed plastic sleeve from around the strand at the top of the test block. A steel stand was then placed around the strand as shown in Figure 6.5. The stand was used to avoid any direct stress concentration to the concrete surface around the strand, as well as to allow an unobstructed view of the strand during testing. The stand supported a load cell and hydraulic ram. A strand chuck was then placed on the strand for the ram to bear against.

The ram was then connected to a hydraulic pump, and the load cell was attached to a DC power supply. A voltmeter was attached to the load cell to read the voltage. Finally, a reference mark was placed on the strand to monitor strand slip and an initial reading was made with a metal ruler. Figure 6.5 shows the test block with a strand that is ready to be tested.
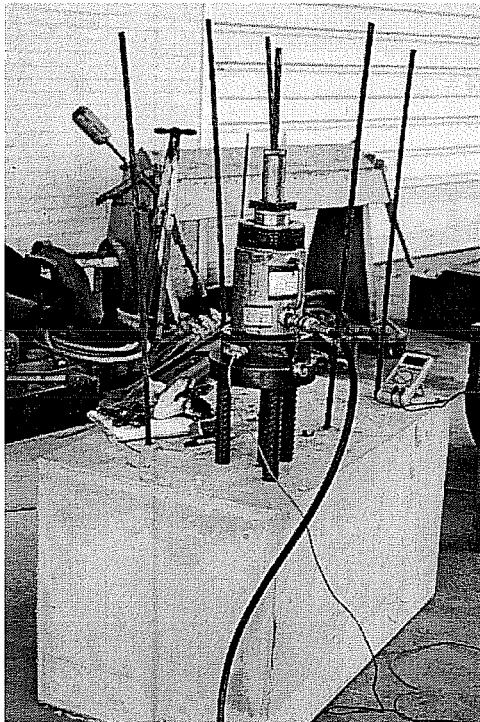


**Figure 6.5: Pull-Out Test Set-Up**

51

## 6.4   PULL-OUT TEST PROCEDURE

The strand was loaded at a rate of 89 kN (20 kips) per second. The strand was loaded at a constant rate until one of three failure modes was observed. The three failure modes were: fracture of one or more wires, sudden slip of the strand and gradual slip of the strand until no increase in load was observed.

The voltage was recorded at first apparent slip as well as the peak voltage. The pull-out length was recorded at voltage intervals throughout loading and at the peak load. After a failure mode was observed and all readings were recorded, the strand was unloaded, and the procedure was repeated until all six strands were tested. The recorded voltages were later converted to usable engineering units of kN and kips.

The results of the pull-out testing are presented and discussed in Sections 7.6 and 7.7.

# CHAPTER SEVEN

# Presentation and Discussion of Test Results

## 7.1    INTRODUCTION

The results of the transfer and development length, and strand pull-out testing are presented and discussed in this chapter. Measured results are presented and the effects of the different variables investigated. In addition, comparisons of the test data with current code requirements and the results of previous research are included.

## 7.2    TRANSFER LENGTH TEST RESULTS

Transfer lengths were measured using two methods: 95% Average Maximum Strain (AMS) Method and Strand Draw-In Method. The transfer length results of each method are presented in Sections 7.2.1 and 7.2.2 for the 95% AMS method and the draw-in method, respectively. Both the initial and the long-term transfer lengths will be presented for each method.

The initial transfer length measurements were performed on the day of prestress release. Long-term transfer lengths were taken prior to the beam pair being transported to Ferguson Structural Engineering Laboratory. The age of the beams at the time when the long-term measurements were made varied for each beam series. Long-term measurements were made at 138, 26, and 83 days for the L6B, M9B, and H9B beam series, respectfully.

Some of the prestressing strands in the beams were debonded to control tensile forces in the top concrete fibers of the beam ends. A predetermined number of strands were debonded in one of three lengths: 914 mm (36 in), 1829 mm (72 in), and 2743 mm (108 in). These three sets of debonded strands plus the fully bonded strands combined to create four distinct transfer regions. Transfer lengths were measured for each transfer region and each length is reported for both measurement methods.

## 7.2.1    Transfer Length Results of the 95% AMS Method

The initial and long-term transfer lengths as measured using the 95% Average Maximum Strain method as described in Section 4.4.1 are presented in Tables 7.1 and 7.2, respectively. The transfer lengths are calculated for each of the four transfer regions of each beam end. Average transfer lengths were determined for each beam end and for each transfer region of each beam series. In addition, an average transfer length for each beam series was determined. A discussion of the results follows in Section 7.3.1.

**Table 7.1:  Initial Transfer Lengths Using 95% AMS Method**

| Beam End | Transfer Region | | | | Beam-end Average mm (in) |
|---|---|---|---|---|---|
| | First mm (in) | Second mm (in) | Third mm (in) | Fourth mm (in) | |
| L6B-1 | 550 (22.0) | 630 (25.0) | 470 (18.5) | 550 (21.5) | 540 (21.5) |
| L6B-2 | 510 (20.0) | 550 (21.5) | 550 (21.5) | 550 (21.5) | 530 (21.0) |
| L6B-3 | 560 (22.0) | 550 (21.5) | 590 (23.0) | 480 (19.0) | 570 (21.5) |
| L6B-4 | 640 (25.0) | 580 (23.0) | 650 (25.5) | 550 (22.0) | 630 (24.0) |
| Avg. L6B | 560 (22.0) | 580 (22.5) | 560 (22.0) | 530 (21.0) | 560 (22.0) |
| M9B-1 | 600 (23.5) | 690 (27.0) | 560 (22.0) | 410 (16.0) | 560 (22.0) |
| M9B-2 | 660 (26.0) | 610 (24.0) | 580 (22.5) | 370 (14.5) | 550 (22.0) |
| M9B-3 | 570 (22.5) | 470 (18.5) | 440 (17.0) | 370 (14.5) | 460 (18.0) |
| M9B-4 | 550 (21.5) | 470 (18.5) | 510 (20.0) | 350 (13.5) | 470 (18.5) |
| Avg. M9B | 590 (23.5) | 560 (22.0) | 520 (20.5) | 370 (14.5) | 510 (20.0) |
| H9B-1 | 440 (17.0) | 530 (20.5) | 600 (23.5) | 410 (16.0) | 490 (19.5) |
| H9B-2 | 420 (16.5) | 640 (25.5) | 560 (22.0) | 410 (16.0) | 510 (20.0) |
| H9B-3 | 440 (17.5) | 600 (23.5) | 470 (18.5) | 470 (18.5) | 500 (19.5) |
| H9B-4 | 460 (18.0) | 560 (22.0) | 420 (16.5) | 420 (16.5) | 470 (18.5) |
| Avg. H9B | 440 (17.5) | 580 (23.0) | 520 (20.5) | 430 (17.0) | 490 (19.5) |

54

**Table 7.2: Long-Term Transfer Lengths Using 95% AMS Method**

| Beam End | Transfer Region | | | | Beam-end Average mm (in) |
|---|---|---|---|---|---|
| | First mm (in) | Second mm (in) | Third mm (in) | Fourth mm (in) | |
| L6B-1 | 600 (23.5) | 620 (24.5) | 520 (20.5) | 560 (22.0) | 580 (22.5) |
| L6B-2 | 440 (17.5) | 520 (20.5) | 520 (20.5) | 560 (22.0) | 510 (20.0) |
| L6B-3 | 530 (21.0) | 560 (22.0) | 570 (22.5) | 580 (23.0) | 560 (22.0) |
| L6B-4 | 630 (25.0) | 670 (26.0) | 660 (26.0) | 560 (22.0) | 630 (24.5) |
| Avg. L6B | 550 (21.5) | 590 (23.5) | 570 (22.5) | 560 (22.0) | 570 (22.5) |
| M9B-1 | 600 (23.5) | 690 (27.0) | 650 (25.5) | 420 (16.5) | 590 (23.0) |
| M9B-2 | 630 (25.0) | 570 (22.5) | 580 (22.5) | 370 (14.5) | 540 (21.0) |
| M9B-3 | 650 (25.5) | 520 (20.5) | 400 (15.5) | 400 (15.5) | 490 (19.5) |
| M9B-4 | 550 (21.5) | 460 (18.0) | 500 (19.5) | 400 (15.5) | 470 (18.5) |
| Avg. M9B | 610 (24.0) | 560 (22.0) | 530 (21.0) | 400 (15.5) | 520 (20.5) |
| H9B-1 | 530 (21.0) | 600 (23.5) | 620 (24.5) | 470 (18.5) | 560 (22.0) |
| H9B-2 | 420 (16.5) | 630 (25.0) | 560 (22.0) | 520 (20.5) | 530 (21.0) |
| H9B-3 | 400 (15.5) | 580 (23.0) | 470 (18.5) | 460 (18.0) | 480 (19.0) |
| H9B-4 | 430 (17.0) | 570 (22.5) | 510 (20.0) | 460 (18.0) | 490 (19.5) |
| Avg. H9B | 450 (17.5) | 600 (23.5) | 540 (21.0) | 480 (19.0) | 510 (20.0) |

Due to the somewhat arbitrary method of determining the maximum average strain, it is unreasonable to expect an "exact" transfer length. Therefore, the transfer lengths have been reported to the closest 10 mm (0.5 in).

## 7.2.2 Transfer Length Results of the Draw-In Method

The initial and long-term transfer lengths measured using the Strand Draw-In method, as described in Section 4.4.2, are presented in Tables 7.3 and 7.4, respectively. The transfer lengths are calculated for each of the four transfer regions of each beam end. Average transfer lengths were determined for each beam end and for each transfer region of each beam series. In addition, an average transfer length for each beam series was determined. A discussion of the results follows in Section 7.3.2

**Table 7.3: Initial Transfer Lengths Using Draw-In Method**

| Beam End | Transfer Region | | | | Beam-end Average mm (in) |
| --- | --- | --- | --- | --- | --- |
| | First mm (in) | Second mm (in) | Third mm (in) | Fourth mm (in) | |
| L6B-1 | 400 (16) | -50 (-2) | 200 (8) | -300 (-12) | 50 (2) |
| L6B-2 | 450 (18) | 750 (30) | 300 (12) | 150 (6) | 400 (16) |
| L6B-3 | 200 (8) | 50 (2) | 100 (4) | -750 (-30) | -100 (-4) |
| L6B-4 | 700 (28) | 250 (10) | 250 (10) | 500 (20) | 450 (18) |
| Avg. L6B | 450 (18) | 250 (10) | 200 (8) | -100 (-4) | 200 (8) |
| M9B-1 | 500 (20) | 100 (4) | 400 (16) | -550 (-22) | 100 (4) |
| M9B-2 | 600 (24) | 450 (18) | 150 (6) | -50 (-2) | 300 (12) |
| M9B-3 | 500 (20) | 400 (16) | 400 (16) | -50 (-2) | 300 (12) |
| M9B-4 | 350 (14) | 150 (6) | -1650 (-66) | -500 (-20) | -400 (-16) |
| Avg. M9B | 500 (20) | 250 (10) | -200 (-8) | -300 (-12) | 50 (2) |
| H9B-1 | 650 (26) | 250 (10) | 700 (28) | 250 (10) | 450 (18) |
| H9B-2 | 350 (14) | 800 (32) | -1450 (-58) | 900 (36) | 150 (6) |
| H9B-3 | 650 (26) | 300 (12) | 650 (26) | 400 (16) | 500 (20) |
| H9B-4 | 450 (18) | 500 (20) | -1350 (-54) | 300 (12) | -50 (-2) |
| Avg. H9B | 500 (20) | 450 (18) | -350 (-14) | 450 (18) | 250 (10) |

**Table 7.4: Long-Term Transfer Lengths Using Draw-In Method**

| Beam End | Transfer Region | | | | Beam-end Average mm (in) |
| | First mm (in) | Second mm (in) | Third mm (in) | Fourth mm (in) | |
|---|---|---|---|---|---|
| L6B-1 | 600 (24) | -50 (-2) | 200 (8) | -300 (-12) | 100 (4) |
| L6B-2 | 350 (14) | 750 (30) | 300 (12) | 150 (6) | 400 (16) |
| L6B-3 | 300 (12) | 50 (2) | 100 (4) | -750 (-30) | -100 (-4) |
| L6B-4 | 800 (32) | 250 (10) | 100 (4) | 300 (12) | 350 (14) |
| Avg. L6B | 500 (20) | 250 (10) | 150 (6) | -150 (-6) | 200 (8) |
| M9B-1 | 600 (24) | 400 (16) | 350 (14) | -100 (-4) | 300 (12) |
| M9B-2 | 750 (30) | 500 (20) | 0 (0) | -300 (-12) | 250 (10) |
| M9B-3 | 650 (26) | 400 (16) | 450 (18) | -50 (-2) | 350 (14) |
| M9B-4 | 300 (12) | 300 (12) | -700 (-30) | -750 (-30) | -200 (-10) |
| Avg. M9B | 600 (24) | 400 (16) | 0 (0) | -300 (-12) | 200 (8) |
| H9B-1 | 750 (30) | 400 (16) | 700 (30) | 250 (10) | 550 (22) |
| H9B-2 | 500 (20) | 900 (36) | -1650 (-66) | 850 (34) | 150 (6) |
| H9B-3 | 600 (24) | 450 (18) | 800 (32) | 400 (16) | 550 (22) |
| H9B-4 | 650 (26) | 650 (26) | -600 (-24) | 250 (10) | 250 (10) |
| Avg. H9B | 650 (26) | 600 (24) | -200 (-8) | 450 (18) | 350 (16) |

The ruler used to measure the strand draw-in had a precision to the nearest 0.127 mm (0.005 in). Using this length in Equation 4-4, which was used to calculate the draw-in transfer length, results in a length of 53.6 mm (2.11 in). Due to this possible error, the draw-in transfer lengths were reported to the closest 50 mm (2.0 in)

## 7.3 Discussion of Transfer Length Results

This section concentrates on the discussion of the transfer length test results that were presented in Sections 7.2.1 and 7.2.2. Discussion of the test results from the 95% AMS method and the draw-in method is presented in Sections 7.3.1 and 7.3.2, respectively. The results of the 95% AMS method will be discussed initially, and then the results of the draw-in method will be discussed and compared to the 95% AMS results.

### 7.3.1    95% Average Maximum Strain

The transfer length test results, as measured by the 95% AMS method, are discussed in this section. The effects of four variables on the transfer length are addressed in the following sections. These variables are time, concrete strength, debonding, and method of prestress release.

#### 7.3.1.1    Effects of Time

Figure 7.1 shows the average initial and long-term transfer length for each beam series using data from Tables 7.1 and 7.2. It can be seen from Figure 7.1 that the transfer length in each beam series increased slightly with the passage of time. It can also be seen that the amount of change in transfer length increased with increased concrete strength.
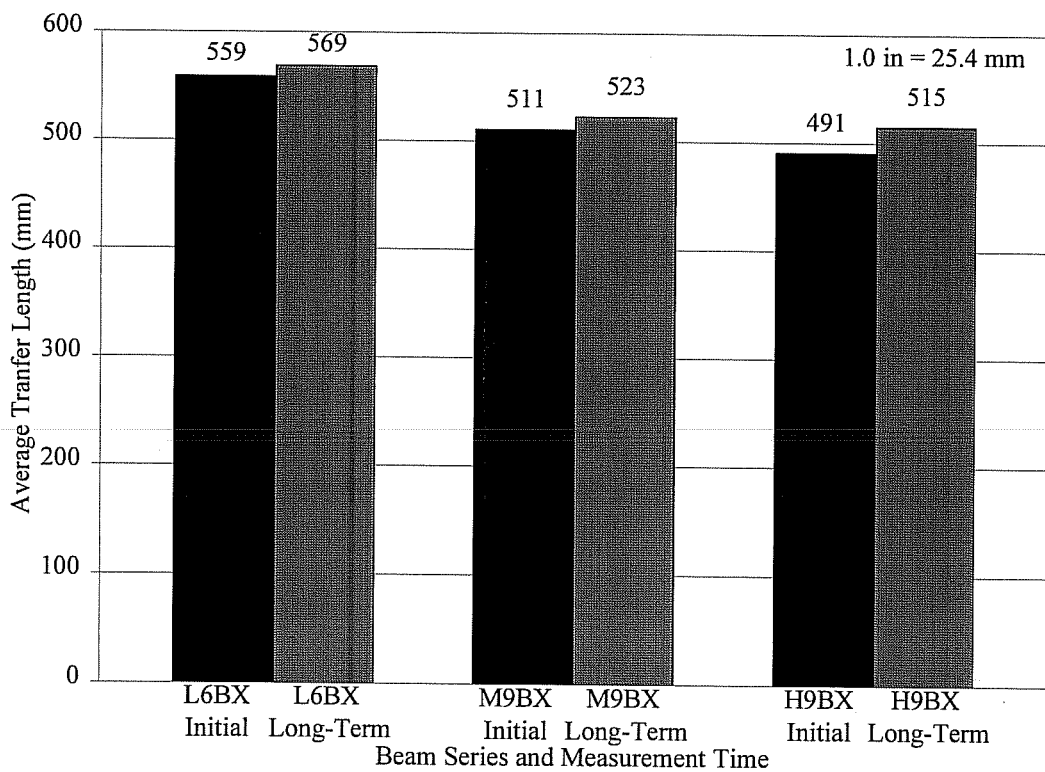


**Figure 7.1:  Change of Transfer Length with Concrete Strength**

In Table 7.5, the initial and long-term transfer lengths are reported along with the change between the two readings. It can be seen that the percent increase of the transfer length over time increased as the concrete strength increased. The high strength concrete series had a transfer length increase of 4.1% compared to increases of 2.0% and 1.8% for the medium and low strength concrete series, respectively. The change in length of the initial and long-term transfer length ranges from 10 to 20 mm (0.5 to 1.0 in). This change is rather negligible when considering the precision of the readings was only to the nearest 10 mm (0.5 in).

**Table 7.5: Change of Transfer Length with Time**

| Beam Series | Average Transfer Length, mm (in) | | Δ Length mm (in) | % Increase |
|:---:|:---:|:---:|:---:|:---:|
| | Initial | Long-Term | | |
| L6B | 560 (22.0) | 570 (22.5) | 10 (0.5) | 1.8 |
| M9B | 510 (20.0) | 520 (20.5) | 10 (0.5) | 2.0 |
| H9B | 490 (19.5) | 510 (20.0) | 20 (1.0) | 4.1 |

### 7.3.1.2 Effects of Concrete Strength

Previous research[16,17,28] has shown that the transfer length decreases as the concrete strength of the specimen increases. The effects of concrete strength on the measured transfer lengths of this study can be seen in Figure 7.1. Both the initial and long-term transfer lengths decreased as the concrete strength increased.

**Table 7.6: Change of Transfer Length with Concrete Release Strength, $f'_{ci}$**

| Beam Series | Release Concrete Strength, $f'_{ci}$ MPa (psi) | Average Transfer Length, mm (in) | |
|:---:|:---:|:---:|:---:|
| | | Initial | Long-Term |
| L6B | 32.5 (4710) | 560 (22.0) | 570 (22.5) |
| M9B | 54.4 (7890) | 510 (20.0) | 520 (20.5) |
| H9B | 59.5 (8630) | 490 (19.5) | 510 (20.0) |
| % Change from L6B to M9B | | 9.8 | 9.6 |
| % Change from M9B to H9B | | 4.1 | 2.0 |

Table 7.6 shows the transfer lengths for each beam series as well as the percent change of the length between beam series. As the concrete strength increased, the change in transfer length

between beam series decreased. Also, the change in transfer length between beam series decreased for the long-term measurements.

### 7.3.1.3 Effects of Debonding

Table 7.7 shows the average initial and long-term transfer length that was measured for each transfer region as well as an average for each beam end. The first transfer region consists of the fully-bonded strands, and the second, third and fourth transfer regions contain the strands that were debonded 914 mm (36 in), 1829 mm (72 in), and 2743 mm (108 in), respectively. There was no great disparity between the transfer lengths of the fully-bonded and debonded strands.

**Table 7.7: Change of Transfer Length with Debonding**

| Beam Series Measurement | | Transfer Region | | | | Series Average mm (in) |
|---|---|---|---|---|---|---|
| | | First mm (in) | Second mm (in) | Third mm (in) | Fourth mm (in) | |
| Avg. L6B | Initial | 560 (22.0) | 580 (22.5) | 560 (22.0) | 530 (21.0) | 560 (22.0) |
| | Long-Term | 550 (21.5) | 590 (23.5) | 570 (22.5) | 560 (22.0) | 570 (22.5) |
| Avg. M9B | Initial | 590 (23.5) | 560 (22.0) | 520 (20.5) | 370 (14.5) | 510 (20.0) |
| | Long-Term | 610 (24.0) | 560 (22.0) | 530 (21.0) | 400 (15.5) | 520 (20.5) |
| Avg. H9B | Initial | 440 (17.5) | 580 (23.0) | 520 (20.5) | 430 (17.0) | 490 (19.5) |
| | Long-Term | 450 (17.5) | 600 (23.5) | 540 (21.0) | 480 (19.0) | 510 (20.0) |

The average transfer lengths in the L6B series were approximately the same for all transfer regions. The transfer lengths were within 60 mm (2.5 in) of each other for all of the transfer regions.

In the M9B series, the first transfer region had the longest transfer length and then the transfer length decreased with each subsequent transfer region. In this series the first three transfer regions had transfer lengths within 90 mm (3.5 in) of each other, but the fourth transfer region had a much shorter transfer length. The initial and long-term transfer lengths of the fourth transfer region were 220 mm (9.0 in) and 210 mm (8.5 in) shorter than the transfer lengths for the fully-bonded strands of the first transfer region.

In the H9B series, the transfer lengths of the first and fourth transfer regions were similar. The transfer lengths of the second and third transfer regions were longer than the first and fourth. The second transfer region had the longest transfer lengths, which were 140 mm (5.5 in) and 150 mm (6.0 in) longer than the fully-bonded strands of the first transfer region.

Russell[10] reported in his study that the transfer lengths for debonded strands were shorter than the transfer lengths for fully-bonded strands. Table 7.8 shows Russell's results compared to the results of this study. The transfer lengths reported are an average of all measured transfer lengths. The results from this study clearly show no significant effect of debonding on the transfer length. The transfer lengths for 15.2 mm (0.6 in) strand measured in this study was less than that in Russell's study, which had material from a different supplier.

**Table 7.8: Comparison of Average Transfer Length of Bonded and Debonded Strands**

|  | Russell 12.7 mm Strand mm (in) | Russell 15.2 mm Strand mm (in) | Measured* mm (in) |
|---|---|---|---|
| Fully Bonded Strands | 762 (30.0) | 1039 (40.9) | 530 (21.0) |
| Debonded Strands | 719 (28.3) | 807 (31.8) | 520 (20.5) |
| Change | 43 (1.7) | 232 (9.1) | 10 (0.5) |

* Only 15.2 mm (0.6 in) strands were used in this study

### 7.3.1.4 Effects of Prestress Release

During the release of prestress, two methods of release were used: three-point and single-point. Three-point release was used on the L6B series specimens. As described in Section 3.4, each strand was flame-cut at three points simultaneously until all strands were released. The three points of release were at the outer end of each beam and between the beam pair. This method of prestress release distributes the release impulse evenly to all of the beam ends.

Single-point release was used with the M9B and H9B series specimens. The strands were flame-cut at a single point between the two beams in this method, as described in Section 3.4. The beam end where the strands are cut experiences a sudden prestress transfer and is referred to as the live end, while the opposite end has a more gradual prestress transfer and is referred to as the dead end.

It has been suggested[2,16,28] that the release method may effect the transfer length. The sudden release of the prestress that is incurred during flame cutting may cause cracking in the transfer region and result in longer transfer lengths. The live end of the single-point release specimens is considered to represent a worst case release scenario. The dead end is considered to be similar to the gradual release achieved with hydraulic prestressing beds, which is the preferred method of release. Additional research by Castrodale[1] has shown that this may be less prominent in high strength concrete specimens.

61

The transfer lengths for each beam series are presented in Table 7.9. For the M9B and H9B series, the average live and dead end transfer lengths are presented along with the total average transfer length for all of the regions in each of the two beam series. The transfer lengths for the L6B series, with three-point release, are presented to compare with the results of the M9B and H9B series, which had single-point release.

**Table 7.9: Effect of Prestress Release on Transfer Length**

| Beam Series | Release Method | Transfer Region | | | |
|---|---|---|---|---|---|
| | | First mm (in) | Second mm (in) | Third mm (in) | Fourth mm (in) |
| L6B | 3-point | 560 (22.0) | 580 (22.5) | 560 (22.0) | 530 (21.0) |
| M9B | Live | 610 (24.0) | 540 (21.5) | 550 (21.5) | 360 (14.0) |
| | Dead | 580 (23.0) | 580 (23.0) | 500 (19.5) | 390 (15.5) |
| | All | 590 (23.5) | 560 (22.0) | 520 (20.5) | 370 (14.5) |
| H9B | Live | 440 (17.5) | 600 (23.5) | 490 (19.5) | 420 (16.5) |
| | Dead | 440 (17.5) | 560 (22.0) | 530 (21.0) | 440 (17.5) |
| | All | 440 (17.5) | 580 (23.0) | 520 (20.5) | 430 (17.0) |

The results in Table 7.9 show that there is no distinguishable difference in the transfer lengths for the different release methods. Contrary to previous results, the live release ends did not produce consistently longer transfer lengths in this study.

The concrete release strength of the M9B and H9B specimens was quite high in both cases. The M9B and H9B specimens had release strengths of 54.4 MPa (7890 psi) and 59.5 MPa (8630 psi), respectively. These results may help to support the claim that high strength concrete reduces the effect of the prestress release on the transfer length.

## 7.3.2 Draw-In Method

The transfer length results calculated using the draw-in method are discussed in this section. The results are compared with the results of the 95% AMS method. In addition, the effect of time on the draw-in transfer lengths is investigated.

### 7.3.2.1 Comparison to 95% AMS Results

Due to the large scatter that was observed in the draw-in transfer length calculations, a comparison of the average draw-in transfer lengths is made with the average 95% AMS transfer lengths. Table 7.10 shows the average initial transfer lengths for each beam series for both methods.

**Table 7.10: Average Transfer Lengths for 95% AMS and Draw-In Methods**

| Beam Series | Method | Transfer Region | | | |
| | | First mm (in) | Second mm (in) | Third mm (in) | Fourth mm (in) |
|---|---|---|---|---|---|
| L6B | 95% AMS | 563 (22.2) | 577 (22.7) | 563 (22.2) | 532 (20.9) |
| | Draw-In | 444 (17.5) | 239 (9.4) | 210 (8.3) | -91 (-3.6) |
| M9B | 95% AMS | 594 (23.4) | 558 (22.0) | 518 (20.4) | 374 (14.7) |
| | Draw-In | 488 (19.2) | 261 (10.3) | -178 (-7.0) | -288 (-11.4) |
| H9B | 95% AMS | 439 (17.3) | 580 (22.8) | 515 (20.3) | 428 (16.9) |
| | Draw-In | 517 (20.4) | 448 (17.6) | -370 (-14.5) | 455 (17.9) |

For the most part, the draw-in transfer lengths did not agree with the 95% AMS transfer lengths. However, the transfer lengths in the first transfer region are similar for both methods. This should be expected considering that the first transfer region consists of the fully-bonded strands and the transfer length equation used in the draw-in method was derived from test data that used specimens with fully-bonded strands.

The average transfer lengths for the draw-in method tended to be less than the transfer lengths from the 95% AMS method for the debonded strands. This may be accredited to the strands not being completely frictionless over the entire debonded length. When the prestress is released at transfer the strand diameter returns to it original size, however the plastic sheathing used to prevent bond may restrict the draw-in of the strand once it returns to its original size. This is particularly evident in the L6B and M9B series where the calculated transfer length became shorter with increased debond length, even to the point where the strands with the longest debonding had calculated transfer lengths that were negative. Clearly there was friction along to debonded length and the strand was not perfectly free to regain its initial length within the debonded region as the draw-in transfer length method assumes.

63

### 7.3.2.2 Effect of Time

In this section the effect of time on the average initial and long-term transfer lengths that were calculated using the draw-in method is investigated for each beam series. Even with the unexpected results from the draw-in method, the effect of time should be similar to that of the results from the 95% AMS method. Table 7.11 shows the average initial and long-term transfer lengths that were calculated by the draw-in method.

**Table 7.11: Change of Transfer Length with Time**

| Beam Series | Reading | Transfer Region | | | |
|---|---|---|---|---|---|
| | | First mm (in) | Second mm (in) | Third mm (in) | Fourth mm (in) |
| L6B | Initial | 444 (17.5) | 239 (9.4) | 210 (8.3) | -91 (-3.6) |
| | Long-Term | 519 (20.4) | 239 (9.4) | 172 (6.8) | -148 (-5.8) |
| M9B | Initial | 488 (19.2) | 261 (10.3) | -178 (-7.0) | -288 (-11.4) |
| | Long-Term | 577 (22.7) | 404 (15.9) | 9 (0.4) | -281 (-11.1) |
| H9B | Initial | 517 (20.4) | 448 (17.6) | -370 (-14.5) | 455 (17.9) |
| | Long-Term | 625 (24.6) | 604 (23.8) | -185 (-7.3) | 447 (17.6) |

In most cases, the long-term transfer length is slightly longer than the initial transfer length. This is consistent with the 95% AMS results. This helps to confirm that the draw-in measurements were taken correctly.

## 7.3.3 Transfer Length Results Compared to Suggested Equations

In this section the measured transfer lengths from this study are compared with the values calculated from suggested equations of current codes and prior studies. Due to the sporadic transfer length results that were calculated using the draw-in method, only the 95% AMS transfer lengths are used for comparison to the suggested equation results.

Figure 7.2 shows the distribution of normalized transfer lengths and how they compare to the suggested transfer lengths from the AASHTO Standard, AASHTO LRFD, and ACI 318 specifications as reported in Table 2.3. The transfer lengths were normalized by dividing them by the strand diameter.
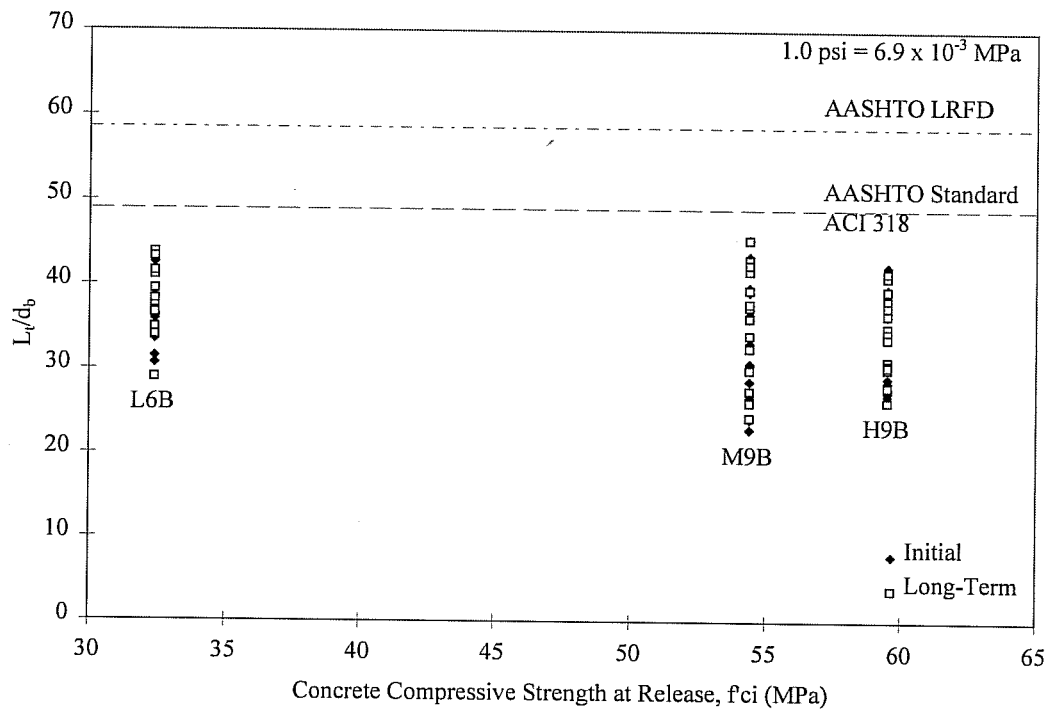
**Figure 7.2: Comparison of Measured Transfer Lengths to Code Equations**

The initial and long-term transfer lengths from all transfer regions of all beam series, as presented in Tables 7.1 and 7.2, were plotted to show the distribution throughout the beam series. The largest scatter was seen in the M9B series, however the L6B and M9B series experienced similar scatter, but to a lesser degree.

Several transfer length equations have been developed from previous research. A partial list of these equations can be found in Table 2.3 of this thesis. Table 7.12 compares transfer lengths using some of these equations with the actual test results of this study. The equations that were selected were those that considered the release strength of the concrete, because of the obvious influence of the concrete strength that was observed in Figure 7.1 and discussed in Section 7.3.1.2.

**Table 7.12: Suggested Equations from Previous Research Compared to Measured Results**

| Beam Series | Release Strength, $f'_{ci}$ MPa (psi) | Zia[16] and Mostafa mm (in) | Cousins[3] et al mm (in) | Mitchell[17] et al mm (in) | Measured 95% AMS mm (in) |
|---|---|---|---|---|---|
| L6B | 32.5 (4710) | 866 (34.1) | 1125 (44.3) | 821 (32.3) | 560 (22.0) |
| M9B | 54.4 (7890) | 470 (18.5) | 897 (35.3) | 634 (25.0) | 510 (20.0) |
| H9B | 59.5 (8630) | 420 (16.5) | 860 (33.9) | 607 (23.9) | 490 (19.5) |

From Table 7.12, it can be seen that the Cousins equation for transfer length predicted almost twice the measured length. The equations from Zia and Mitchell yielded transfer lengths that were much closer to the measured transfer lengths for this study. In both cases, the predicted transfer length for the L6B series was approximately 50% higher than the measured length. However, the predicted values were very close to the measured lengths for the M9B and H9B series.

The equation from Zia predicted transfer lengths that were within 75 mm (3.0 in) of the measured values. These predicted transfer lengths were less than the measured lengths and may be considered unconservative as an upper limit boundary. The predicted transfer lengths from the equation by Mitchell were within approximately 115 mm (4.5 in) of the measured values. These predicted transfer lengths were greater than the measured lengths. Therefore, the Mitchell equation would be a better option if an upper limit boundary was desired.

## 7.4 PRESENTATION OF DEVELOPMENT LENGTH TEST RESULTS

The results of the development length tests are presented in Tables 7.13 and 7.14. A discussion of the results follows in Section 7.5.

Table 7.13 contains the test embedment length, the ratio of the embedment length to the AASHTO required development length for fully-bonded strand, the ultimate applied load, the ratio of the ultimate applied moment to the ultimate calculated moment, and the mode of failure. The calculated AASHTO development length is from AASHTO LRFD[6] Section 5.11.4.1. This is the required development length for fully-bonded strand, NOT for debonded strand.

**Table 7.13: Development Length Test Results**

| Test | Embedment Length, $L_e$ mm (in) | Development Length, $L_{d,AASHTO}$ mm (in) | $\dfrac{L_e}{L_{d,AASHTO}}$ | Applied Load, $P_{u,app}$ kN (kips) | $\dfrac{M_{u,app}}{M_{u,calc}}$ | Failure Mode |
|------|------|------|------|------|------|------|
| L6B-1 | 2438 (96) | 2266 (89) | 1.08 | 750 (169) | 1.06 | Hybrid |
| L6B-2 | 2896 (114) | 2265 (89) | 1.28 | 635 (143) | 1.00 | Flexure |
| L6B-3 | 2134 (84) | 2274 (90) | 0.94 | 780 (175) | 1.00 | Hybrid |
| L6B-4 | 2134 (84) | 2274 (90) | 0.94 | 790 (178) | 1.02 | Hybrid |
| M9B-1 | 4572 (180) | 2207 (87) | 2.07 | 825 (186) | 1.03 | Flexure |
| M9B-2 | 2438 (96) | 2225 (88) | 1.10 | 875 (197) | 1.00 | Hybrid |
| M9B-3 | 2896 (114) | 2230 (88) | 1.30 | 805 (181) | 1.02 | Hybrid |
| M9B-4 | 2438 (96) | 2237 (88) | 1.09 | 915 (206) | 1.04 | Hybrid |
| H9B-1 | 4572 (180) | 2261 (89) | 2.02 | 820 (185) | 1.01 | Flexure |
| H9B-2 | 2438 (96) | 2269 (89) | 1.07 | 855 (192) | 0.98 | Bond |
| H9B-3 | 2896 (114) | 2269 (89) | 1.28 | 800 (180) | 1.02 | Hybrid |
| H9B-4 | 2438 (96) | 2274 (90) | 1.07 | 895 (202) | 1.02 | Hybrid |

**Table 7.14: Development Length Test Concrete and Strand Strains**

| Test | Maximum Concrete Strain, $\varepsilon_{cu}$ | Neutral Axis at Failure, c mm (in) | Initial Strand Strain, $\varepsilon_{ps}$ | Maximum Strand Strain, $\varepsilon_{su}$ |
|------|------|------|------|------|
| L6B-1 | 0.00327 | 57 (2.25) | 0.00630 | 0.05031 |
| L6B-2 | 0.00327 | 64 (2.50) | 0.00629 | 0.04553 |
| L6B-3 | 0.00305 | 60 (2.35) | 0.00628 | 0.04538 |
| L6B-4 | 0.00343 | 51 (2.00) | 0.00627 | 0.05854 |
| M9B-1 | 0.00367 | 76 (3.00) | 0.00655 | 0.04266 |
| M9B-2 | 0.00257 | 71 (2.80) | 0.00650 | 0.03376 |
| M9B-3 | 0.00332 | 56 (2.20) | 0.00648 | 0.05216 |
| M9B-4 | 0.00378 | 57 (2.25) | 0.00646 | 0.05728 |
| H9B-1 | 0.00315 | 69 (2.70) | 0.00641 | 0.04117 |
| H9B-2 | 0.00198 | 88 (3.45) | 0.00640 | 0.02306 |
| H9B-3 | 0.00288 | 71 (2.80) | 0.00639 | 0.03693 |
| H9B-4 | 0.00353 | 66 (2.60) | 0.00638 | 0.04699 |

Table 7.14 contains the maximum measured concrete strain measured on the top surface of the deck slab, the depth to the measured neutral axis at failure, the initial strain in the prestressing strand before load was applied, and the calculated maximum strain in the prestressing strand. The neutral axis was determined by measuring the deck slab cracks after testing. The distance from the top of the slab to the tip of the slab crack that propagated the farthest through that slab is the depth to the neutral axis. Since the concrete strain of the top slab fiber and the neutral axis were known, the strand strains could then calculated by strain compatibility assuming linear strain over the depth of the beam

## 7.5 DISCUSSION OF DEVELOPMENT LENGTH TEST RESULTS

### 7.5.1 Introduction

The results of the development length testing of this study are discussed in Section 7.5.2. The effects of the beam concrete strength, test embedment length, and strand slip on the beam performance are investigated to help determine an adequate development length. In addition, the effect of the horizontal web reinforcement, H-bar, on the test behavior of the specimen is investigated.

The most important result of the development length testing is the mode of failure. Three types of failures were identified during testing: flexural, hybrid, and bond. The desired mode of failure is the flexural failure. This is because flexural failures are easy to predict and provide some warning before failure. Flexural failures are identified by the test specimen reaching the predicted nominal moment and NO cracking or strand slip occurring in the transfer region.

Bond failures, on the other hand, are difficult to predict and can result in sudden collapse. The reason that the bond failure is difficult to predict is because it is difficult to determine the stresses in the prestressing strand after they begin to slip. Bond failures are identified by the test specimen NOT reaching the predicted nominal moment, as well as the presence of significant cracking and strand slip in the transfer region.

Hybrid failures are identified by the test specimen reaching the predicted nominal moment, with the presence of cracking and strand slip in the transfer region. The problem with hybrid failures is determining what amount of strand slip is acceptable when trying to determine an adequate development length. An investigation of the test results will help to solve this problem.

## 7.5.2    Estimating the Development Length

The embedment length required to provide adequate development of the prestressing strand must be greater than the sum of the transfer bond length and the flexure bond length as described in Section 2.3.1.4.  Since the transfer lengths that were calculated in this study showed some influence of the concrete strength, it would seem likely that the development length would also be affected.

Figure 7.3 shows the normalized ultimate test moment versus the embedment length for each beam end tested.  The moments were normalized by dividing the maximum applied moment by the calculated nominal moment.  In addition, the calculated AASHTO[6] required development lengths for specimens with fully bonded and debonded strands, per Section 5.11.4.1 and 5.11.4.2, have been labeled.
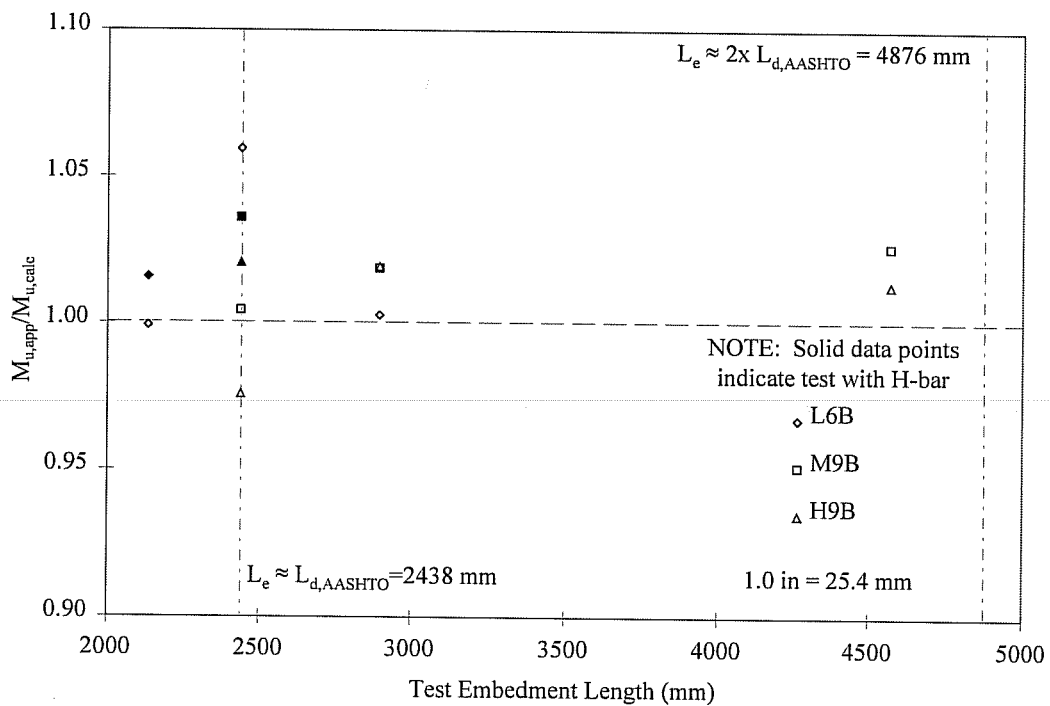


**Figure 7.3:  Normalized Ultimate Moment of All Tests vs Test Embedment Lengths**

It can be seen in Figure 7.3 that the majority of the tests reached the nominal calculated moment. Only one test, H9B-2, had a maximum applied moment less than 99% of the calculated nominal moment. However, there is no clear indication of any influence of the concrete strength on the ability of the specimen to reach the nominal moment.

As discussed above, the definition of a flexural failure is that the specimen must reach the predicted nominal moment without the presence of any cracking in the transfer region. Figure 7.3 shows that most of the specimens were able to reach the predicted nominal moment. Of those specimens to reach their nominal moment only two had no cracking in the transfer region: M9B-1 and H9B-1. The remaining specimens sustained hybrid failures, except H9B-2, which suffered a bond failure.
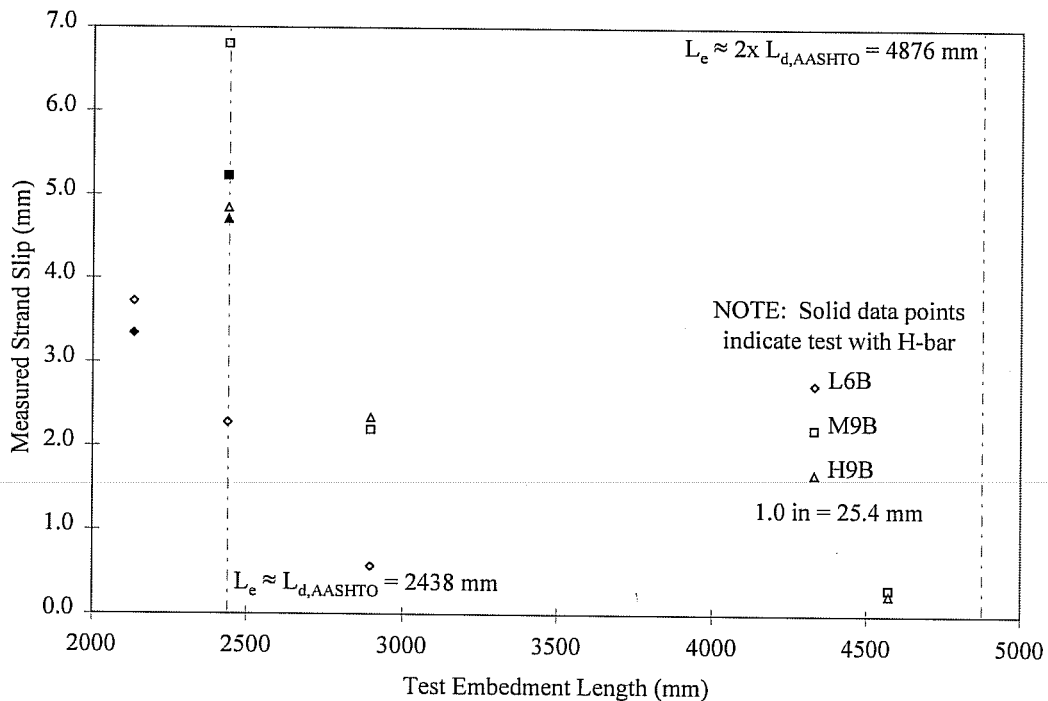


Figure 7.4: Measured Strand Slips for All Tests vs Test Embedment Length

Figure 7.4 shows the maximum measured prestressing strand slip of each test plotted at the test embedment length. From Figure 7.4, we can see that the strand slip increased with decreased embedment length in each test series. Also, for tests using the same embedment length,

the measured slip of the M9B and H9B series specimens was greater than the slips of the L6B series specimens.

This can be explained by looking at the strand configuration used in each of the series, as seen in Figure 3.2. The M9B and H9B series have two additional strands in the last transfer region. This results in additional flexural capacity in these beams without any additional precompression in the transfer region. Therefore, the strands in the L6B series have less increased bond stress demand in the transfer region at the nominal capacity, resulting in less strand slip.

Hybrid failures experienced maximum strand slips that ranged from 0.571 mm (0.022 in) to 6.804 mm (0.268 in). This leads us back to the question of how much slip in a hybrid failure is too much to be considered safe.

From an inspection of the measured slips and the cracking patterns (Appendix I) of specimens that experienced hybrid failures, it can be seen that the specimens that experienced the most severe cracking in the transfer region also had the highest strand slips. These specimens included L6B-3, L6B-4, M9B-2, M9B-4, M9B-2, and M9B-4. It is obvious that, due to the severe cracking in the transfer region and large strand slips, the test embedment lengths used for these specimens were inadequate.

Other specimens that experienced hybrid failures had cracking at the beginning of the transfer region. Since this cracking took place in the region before transfer had begun, the effect of this cracking does not add any additional stress to the strand in the transfer region. These specimens, L6B-1, M9B-3, and H9B-3, contained one crack in at least one of each of the transfer zones. Strand slips in these specimens were significantly less than the slips in the specimens with severe cracking. It is the embedment lengths of these tests that will be investigated more closely to determine if the strand slips are acceptable.

During the development length testing, crack widths were measured at intervals along the specimen. The crack widths that developed in the transfer region were among those that were measured. When cracks were first detected in the transfer region it was observed that the measured strand slip was equal to the crack width, indicating that there was no actual strand slip being measured, only the width of the crack. Therefore, when the total crack widths in the transfer region were subtracted from the measured strand slips the "actual" strand slip could be determined. The "actual" strand slip of the specimens that failed in flexure could then be compared to the slip of the specimens that experienced a hybrid failure with limited cracking.

The maximum measured strand slip and the total sum of all the crack widths in the third and fourth transfer regions for each test are presented in Table 7.15. In addition, the calculated "actual" strand slip for both transfer regions is shown. The total measured crack widths were not

recorded for all of the tests. The practice of measuring the total crack widths began with test M9B-3, but by observing the trends from the available data a prediction of the performance can be made. Prior tests with limited cracking could be evaluated by looking at the crack patterns. For example, test L6B-2 had only one crack and it was behind the transfer region, and M9B-1 had no cracking in the transfer regions. The remaining tests had significant cracking in the transfer region and can be assumed to have unacceptable strand slips.

Table 7.15: "Actual" Strand Slips

| Test | Maximum Strand Slip per Transfer Region mm (in) | | Total Crack Widths in Transfer Region mm (in) | | "Actual" Strand Slip per Transfer Region mm (in) | |
|---|---|---|---|---|---|---|
| | Third | Fourth | Third | Fourth | Third | Fourth |
| L6B-1 | 0.970 (0.038) | 2.229 (0.088) | N/A | N/A | N/A | N/A |
| L6B-2 | 0.199 (0.008) | 0.571 (0.022) | 0.00 (0.000) | 0.00 (0.000) | 0.199 (0.008) | 0.571 (0.022) |
| L6B-3 | 2.366 (0.093) | 3.725 (0.147) | N/A | N/A | N/A | N/A |
| L6B-4 | 2.075 (0.082) | 3.353 (0.132) | N/A | N/A | N/A | N/A |
| M9B-1 | 0.215 (0.008) | 0.310 (0.012) | 0.00 (0.000) | 0.00 (0.000) | 0.215 (0.008) | 0.310 (0.012) |
| M9B-2 | 2.991 (0.118) | 6.846 (0.270) | N/A | N/A | N/A | N/A |
| M9B-3 | 1.205 (0.047) | 2.196 (0.086) | 0.55 (0.022) | 0.00 (0.000) | 0.655 (0.025) | 2.196 (0.086) |
| M9B-4 | 3.333 (0.131) | 5.227 (0.206) | 0.95 (0.037) | 3.50 (0.138) | 2.383 (0.094) | 1.727 (0.068) |
| H9B-1 | 0.139 (0.005) | 0.243 (0.010) | 0.00 (0.000) | 0.00 (0.000) | 0.139 (0.005) | 0.243 (0.010) |
| H9B-2 | 4.443 (0.175) | 4.845 (0.191) | 2.10 (0.083) | 5.05 (0.199) | 2.343 (0.092) | -0.205 (-0.008) |
| H9B-3 | 1.268 (0.050) | 2.341 (0.092) | 0.80 (0.031) | 1.65 (0.065) | 0.468 (0.019) | 0.691 (0.027) |
| H9B-4 | 2.769 (0.109) | 4.709 (0.185) | 1.00 (0.039) | 2.90 (0.114) | 1.769 (0.070) | 1.809 (0.071) |

From the two specimens that produced a flexural failure, H9B-1 and M9B-1, a basis for an allowable strand slip can be made. The strand slip for the specimens with a flexural failure was

72

less than 0.310 mm (0.012 in). Strand slips for the hybrid failure specimens should be close to the slips for the flexural failure specimens. It can be seen that for the three hybrid failure specimens, L6B-2, M9B-3, and H9B-3, which had an embedment length of 2896 mm (114 in), the actual strand slips are fairly close to the flexural failure specimens. It appears that specimens with maximum strand slips of approximately 1.20 mm (0.050 in) in the third transfer region, and 2.40 mm (0.100 in) in the fourth transfer region performed well in the development length testing.

Strand slips in the hybrid failure specimen, L6B-1, with embedment length of 2438 mm (96 in) are also close to the flexural failure specimen slips. This specimen was the only one out of five with an embedment length of 2438 mm (96 in) that had small strand slips. However, L6B-1 had a low strength beam concrete and the other four tests had medium and high strength beam concrete. This reaffirms what was seen in Figure 7.4, that the low strength specimens had smaller strand slips than the medium and high strength specimens.

This would also indicate that the pattern of the strand layout and debonding should be considered when determining an adequate development length. The AASHTO LRFD Bridge Design Specification[6], in Section 5.11.4.2, restricts the use of debonded strands to less than 25% of the total number of strands and less than 40% of the strands in any one row. The specimens tested in this study contained 60% of the total number of strands debonded in the L6B series and 75% of the total number debonded in the M9B and H9B series. Furthermore, all series contained rows with greater than 40% of the strands debonded.

After investigating all of the development length test data, it appears that an adequate development length for this series of beams was roughly 2896 mm (114 in). This is equivalent to approximately 1.2 times the AASHTO recommended development length for fully bonded strands, which is much less than the current code requirement of 2.0 times the fully-bonded length. In addition, the AASHTO restrictions on debonding appear to be overconservative.

### 7.5.3    Effects of the Horizontal Web Reinforcement, H-bar

Specimens with and without the H-bar detail were tested with the same embedment length to determine if the detail enhanced the performance of the specimen. The H-bar test used the shortest embedment length of the three previous tests for each beam series. This was to ensure that enough damage occurred in the transfer region to evaluate the benefits of the H-bar detail. In each series, the test without the H-bar detail resulted in either an unacceptable hybrid failure or a bond failure.

The results of the tests with and without the H-bar detail are compared in Table 7.16. The effects of the H-bar detail are shown in Figures 7.3 and 7.4. It can be seen that the test that included the H-bar detail had a higher ultimate applied moment to calculated moment ratio and had less strand slip in all cases. In addition, from Table 7.16, it is seen that the H-bar detail helped reduce the maximum crack width in the transfer region in two of the three series. These results show that the H-bar detail was beneficial to the test performance of the specimen, but did not prevent an unacceptable hybrid failure.

**Table 7.16: Comparison of Identical Embedment Lengths With and Without H-bar Detail**

| Test | H-bar | $\dfrac{M_{u,app}}{M_{u,calc}}$ | Maximum Strand Slip mm (in) | Maximum Crack Width In Transfer Region mm (in) | Failure Mode |
|------|-------|------|------|------|------|
| L6B-3 | N | 0.999 | 3.725 (0.147) | 1.00 (0.039) | Hybrid |
| L6B-4 | Y | 1.016 | 3.344 (0.132) | 0.90 (0.035) | Hybrid |
| % Difference | | 1.7 | 10.2 | 10 | |
| M9B-2 | N | 1.004 | 6.804 (0.268) | 0.70 (0.028) | Hybrid |
| M9B-4 | Y | 1.036 | 5.227 (0.268) | 1.10 (0.043) | Hybrid |
| % Difference | | 3.1 | 23.2 | -57.1 | |
| H9B-2 | N | 0.976 | 4.845 (0.191) | 1.10 (0.043) | Bond |
| H9B-4 | Y | 1.021 | 4.709 (0.185) | 0.85 (0.033) | Hybrid |
| % Difference | | 4.4 | 2.8 | 22.7 | |

## 7.5.3    Development Length Results Compared to Suggested Equations

The suggested equations that were selected to be compared with the findings of this study were from the same sources as those used for comparison of the transfer lengths. Once again, these equations considered the concrete strength as a variable when computing the development length. Table 7.17 contains the calculated results of the three suggested equations as well as the measured development lengths from this study.

None of the development lengths that were calculated with the suggested equations compared favorably with the results of this study. The Zia and Mitchell equations both predicted development lengths that were much shorter than the measured lengths, and the Cousins equation predicted lengths that were much greater than the measured values.

74

**Table 7.17: Suggested Equations from Previous Research Compared to Measured Results**

| Beam Series | Conc. Comp. Strength, $f'_c$ MPa (psi) | Zia[16] and Mostafa mm (in) | Cousins[3] et al mm (in) | Mitchell[17] et al mm (in) | Measured mm (in) |
|---|---|---|---|---|---|
| L6B | 49.2 (7140) | 2699 (106.2) | 4590 (180.7) | 1930 (76.0) | 2896 (114) |
| M9B | 80.8 (11710) | 2173 (85.5) | 3459 (136.2) | 1448 (57.0) | 2896 (114) |
| H9B | 88.8 (12880) | 2182 (85.9) | 3390 (133.5) | 1413 (55.6) | 2896 (114) |

All three of these equations were based on studies using fully-bonded strands. This would explain the shorter calculated lengths of the Zia and Mitchell equations. Specimens with fully-bonded strands have been shown to have a shorter development length than specimens with debonded strands.

The tests that Cousins used as the basis for his equation for development length, resulted in much longer development lengths than had previously been seen. This would explain the long development lengths that were calculated using this equation.

As discussed earlier, the concrete strength did not significantly affect the development length that was measured in this study; all specimen series had a similar development length. The measured development length was approximately 1.2 times the AASHTO recommended length for fully-bonded strands. Using this 1.2 multiplier with the results from the Zia equation, would give a development length close to what was measured in this study.

## 7.6 PRESENTATION OF PULL-OUT TEST RESULTS

The pull-out test data are presented in this Section. Six strands were tested for each beam series as discussed in Section 6.4. The peak load and steel stress, pull-out length at peak load, and the mode of failure are presented in Table 7.18.

There were three failure modes that were observed during the pull-out testing. The first failure mode was the fracture of any of the wires in the strand. Gradual slip of the strand until the peak pull-out load was achieved was the second failure mode. The final pull-out failure mode was a sudden strand slip of approximately 10 mm (0.375 in).

A discussion of the results follows in Section 7.7.

### Table 7.18: Pull-Out Test Data

| Strand ID | Peak Load kN (kips) | Peak Strand Stress GPa (ksi) | Pull-Out Length at Peak Load mm (in) | Failure Mode |
|---|---|---|---|---|
| L6B-A | 213 (47.8) | 1.52 (220) | 6 (0.25) | Pull-out |
| L6B-B | 210 (47.3) | 1.50 (218) | 3 (0.125) | Pull-out |
| L6B-C | 214 (48.0) | 1.53 (221) | 3 (0.125) | Pull-out |
| L6B-D | 208 (46.8) | 1.49 (216) | 3 (0.125) | Pull-out |
| L6B-E | 206 (46.3) | 1.47 (213) | 3 (0.125) | Pull-out |
| L6B-F | 215 (48.3) | 1.53 (223) | 3 (0.125) | Pull-out |
| M9B-A | 258 (58.0) | 1.84 (267) | 19 (0.75) | Fracture 2 |
| M9B-B | 264 (59.3) | 1.88 (273) | 18 (0.72) | Fracture 1 |
| M9B-C | 260 (58.5) | 1.86 (270) | 20 (0.78) | Fracture 6 |
| M9B-D | 265 (59.5) | 1.89 (274) | 27 (1.05) | Fracture 6 |
| M9B-E | 262 (59.0) | 1.87 (272) | 38 (1.50) | Sudden Slip |
| M9B-F | 258 (58.0) | 1.84 (267) | 28 (1.10) | Fracture 6 |
| H9B-A | 228 (51.3) | 1.63 (236) | 33 (1.30) | Pull-out |
| H9B-B | 265 (59.5) | 1.89 (274) | 43 (1.70) | Sudden Slip |
| H9B-C | 256 (57.5) | 1.83 (264) | 28 (1.10) | Pull-out |
| H9B-D | 246 (55.3) | 1.76 (255) | 15 (0.61) | Pull-out |
| H9B-E | 255 (57.3) | 1.82 (264) | 24 (0.93) | Pull-out |
| H9B-F | 252 (56.8) | 1.80 (262) | 29 (1.13) | Pull-out |

Note: The number after "Fracture" is the number of wires that fractured.

## 7.7    DISCUSSION OF PULL-OUT TEST RESULTS

Pull-out testing is used to predict the bond performance of prestressing strand. Studies by Logan[27] have resulted in the proposal of a minimum pull-out force for which acceptable bond performance can be expected. A minimum pull-out force of 160 kN (36 kips) was established for 12.7 mm (0.5 in) strand with an embedment of 457 mm (18 in). From this, a minimum pull-out force can be determined for 15.2 mm (0.6 in) strand by calculating the pull-out force required to achieve the same bond stress. This results in a minimum pull-out force of 192 kN (43.2 kips) for 15.2 mm (0.6 in) strand with an embedment of 457 mm (18 in).

Figure 7.5 shows the distribution of the pull-out forces for all of the strands that were tested. In addition, two lines have been placed to identify the minimum pull-out force for 15.2 mm (0.6 in) and 12.7 mm (0.5 in) strands. As can be seen in Figure 7.5, all of the tests had pull-

out forces greater than 192 kN (43.2 kips), therefore adequate bond performance was expected. The flexural tests clearly showed that the bond performance of the strand used in these beams was excellent.
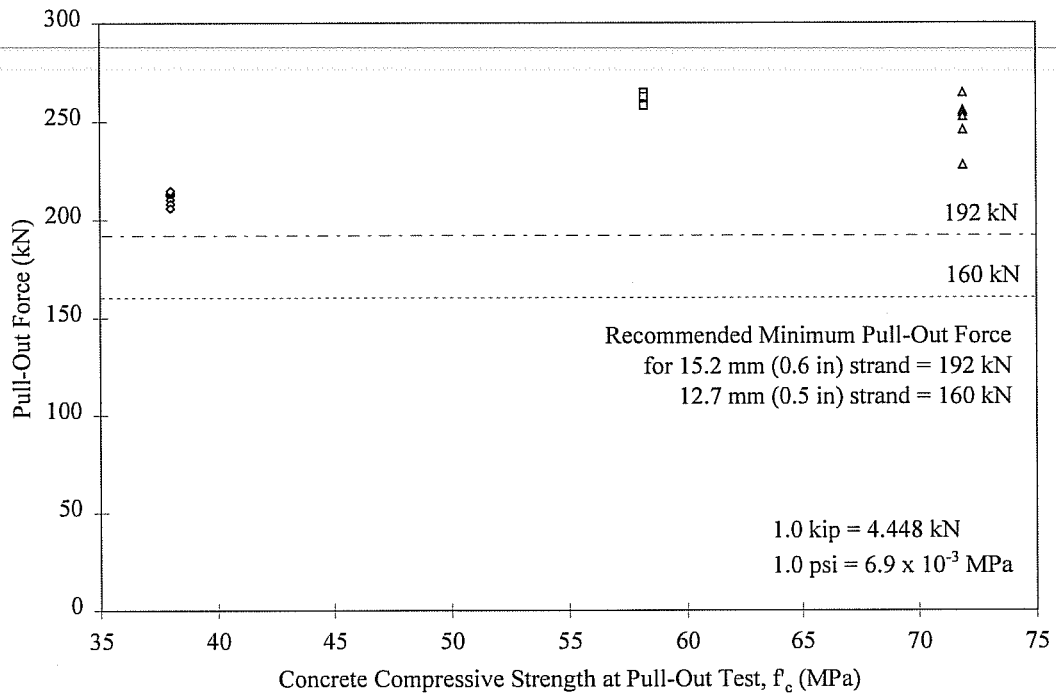


**Figure 7.5: Measured Pull-Out Forces and Recommended Minimum**

The conservative results of transfer and development lengths in this study, compared to ACI and AASHTO recommendations, leave little doubt that adequate bond performance was present for the prestressing strand used in this study. These results reinforce the credibility of the Moustafa Pull-Out Test as an accurate indicator of acceptable bond performance of prestressing strand.

# CHAPTER EIGHT

## Summary and Conclusions

### 8.1    INTRODUCTION

This chapter contains the summary and conclusions from the testing that was performed in this study. A summary of the testing and results is in Section 8.2 and the conclusions are in Section 8.3.

### 8.2    SUMMARY

The objective of this study was to determine the transfer and required development length of 15.2 mm (0.6 in) prestressing strands with a bright surface condition in prestressed pretensioned concrete specimens with more than 60% of the total number of strands debonded. The specimens that were tested in this study consisted of six AASHTO Type I prestressed concrete composite girders. Three concrete strengths were used for the precast prestressed specimens. Two beams were cast with each concrete mix that ranged from 49.2 MPa (7140 psi) to 88.8 MPa (12,880 psi). In addition, the benefit of horizontal web reinforcement was investigated in three of the twelve development length tests.

The test specimens were cast at the Texas Concrete Company in Victoria, Texas. Transfer length and pull-out testing were also performed at the Texas Concrete Company. The specimens were then delivered to the Ferguson Structural Engineering Laboratory (FSEL) where a concrete deck slab with a strength of approximately 41 MPa (6000 psi) was cast on each beam, and the development length testing took place. Both ends of each beam were tested to measure transfer and development lengths.

### 8.2.1    Transfer Length Testing

Three debonded strand lengths were used in the specimens of this study. Four transfer regions were present in each beam end due to the three sets of debonded strands plus the fully-bonded strands. Transfer lengths were determined for each transfer region of each beam end.

Transfer lengths were calculated using two methods. The first method measured the external concrete strains in the transfer region of each beam end at the height corresponding to the center of gravity of the prestressing strand. The strains in the concrete were measured using the DEMEC system. The strain profiles were plotted and the transfer lengths were determined from these plots using the 95% Average Maximum Strain method as shown in Appendix E.

The second method is the Strand Draw-In method. The draw-in of each strand at prestress release is measured for this method. The transfer lengths are determined as a function of the strand draw-in and the initial prestressing force for each individual strand. The calculated lengths of all strands in each transfer region were averaged to determine the transfer length for each region.

## 8.2.2    Development Length Testing

Development length testing was performed on both ends of each specimen. The test embedment length was varied for each test, and the performance of the specimen during testing was evaluated to determine an acceptable development length. The criteria that was used to judge an acceptable development length was that the nominal moment capacity was achieved at the critical section without the presence of excessive strand slip. In addition, the contribution of horizontal web reinforcement was assessed.

## 8.2.3    Strand Pull-Out Testing

Direct tension pull-out testing was performed to predict the bond performance of the prestressing strand that was used in the test specimens. The pull-out test block was cast at the same time as the test specimens and consisted of the same concrete and strand.

## 8.3    CONCLUSIONS

Several conclusions can be made based on the test results of this study. Conclusions concerning transfer and development length, and pull-out testing are present in the following sections.

### 8.3.1 Transfer Length Testing

1. The average measured transfer lengths for this study ranged from 490 mm (19.5 in) for specimens with high strength concrete to 560 mm (22.0 in) for specimens with low strength concrete. The AASHTO recommended transfer lengths of 760 mm (30 in) for the Standard Specification[5] and 910 mm (36 in) for the LRFD Specification[6] were much higher than the average transfer lengths of this study. From the results of this study, it can be seen that the AASHTO requirement for transfer length is conservative.

2. Specimens with a higher concrete strength at the release of prestress have shorter measured transfer lengths than specimens with lower release strengths. High strength concrete specimens, which had a release strength of 59.5 MPa (8630 psi), had an average transfer length of 490 mm (19.5 in). Similarly, the medium and low strength specimens, which had release strengths of 54.4 MPa (7890 psi) and 32.5 MPa (4710 psi), had measured average transfer lengths of 510 mm (20.0 in) and 560 mm (19.5 in), respectfully.

3. Results from this study showed that the effect of the release of the prestressing force on the transfer length was negligible. Measured transfer lengths from beam-ends with sudden and gradual prestress release were similar and showed no trends for either method.

4. No significant change in the transfer length was observed when strands were debonded. Transfer lengths measured for debonded strands were similar to the lengths for fully bonded strands.

5. The increase in transfer length over time was found to be insignificant. Increases in the average transfer length from the initial measurements to the long-term measurements ranged from 10 mm (0.5 in) to 20 mm (1.0 in).

6. Transfer lengths calculated with the Strand Draw-In method produced results similar to the 95% AMS results for the fully bonded transfer region only. However, the draw-in transfer lengths for the debonded strands were much less than the 95% AMS values. The draw-in measurements indicated that the debonded strand was not perfectly free to move over the debond length, resulting in incorrect transfer lengths from calculations with the Strand Draw-In method.

7. Suggested transfer lengths from the Zia and Mostafa[16] equation were 420 mm (16.5 in), 470 mm (18.5 in), and 866 mm (34.1 in) for high, medium and low strength concretes, respectively. These predicted lengths compared well to the measured lengths of this study, however the predicted length was unconservative as an upper bound for the high and medium strength concrete. The equation from Mitchell[17] et al predicted transfer lengths of 607 mm

(23.9 in), 634 mm (25.0 in), and 821 mm (32.3 in) for high, medium and low strength concretes, respectively. These predicted lengths compared well to the measured lengths of this study, and they serve as a conservative upper bound.

### 8.3.2    Development Length Testing

1. The required development length for specimens with debonded 15.2 mm (0.6 in) prestressing strands was determined in this study. At least 60% of the total number of strands were debonded up to 2743 mm (108 in). The required development length for these specimens as determined in this study is approximately 2896 mm (114 in). This results in a development length that is approximately 1.2 times the AASHTO[5,6] required development length for fully-bonded strands. The AASHTO development length requirement for debonded strands is 2.0 times the fully-bonded requirement. From the results of this study, it can be seen that the AASHTO requirement for the necessary development length of specimens with debonded strands is conservative.

2. The maximum measured strand slips was one of the governing factors in the selection of an adequate development length for specimens that experienced a hybrid failure. Comparison of the measured strand slips of the flexural failure specimens with the hybrid failure specimens led to a selection of an acceptable maximum strand slip. The maximum measured strand slips that were deemed acceptable in this study were: 1.20 mm (0.050 in) for strands in the third transfer region and 2.40 mm (0.100 in) for strands in the fourth transfer region.

3. The configuration of the prestressing strands influenced the strand slips that were measured during the development length testing. The low strength concrete test specimens contained two fewer prestressing strands then the medium and high strength concrete specimens. The strand slips in the low strength specimens were smaller then the slips in the medium and high strength specimens when tested at the same embedment length.

4. The presence of the horizontal web reinforcement, H-bar, did not reduce the development length of the test specimens. It did reduce the crack widths in the transfer region, but did not reduce the amount of cracking in the transfer region. In comparison of the results of identical tests of specimens with and without the H-bar, no significant changes were observed.

### 8.3.3    Strand Pull-Out Testing

The conservative results of the transfer and development length testing compared to the AASHTO requirements indicate that excellent bond of the prestressing steel to the concrete was present. All strand pull-out tests resulted in a peak pull-out load that exceeded the recommended load[27] of 192 kN (43.2 kips) for 0.6 in diameter prestressing strand. For these beams, the pull-out test properly indicated that the bond properties of the strand were quite good, as reflected by measured transfer and development lengths, which were well within AASHTO[5,6] requirements.

# APPENDIX A

## Notation

| | |
|---|---|
| a | Distance from outside load point to location of the hydraulic ram |
| $A_{ps}$ | Area of a prestressing strand |
| B | Bond Modulus |
| b | Width of the deck slab |
| c | Neutral Axis |
| $d_b$ | Diameter of a prestressing strand |
| $E_c$ | Modulus of elasticity of concrete |
| $E_{ci}$ | Modulus of elasticity of concrete at transfer |
| $E_{ps}$ | Modulus of elasticity of the prestressing strand |
| ES | Elastic shortening |
| f'c | Concrete compressive strength |
| $f'_{ci}$ | Concrete compressive strength at release |
| $f_{ps}$ | Steel stress at failure |
| $f_{se}$ | Effective prestress after losses |
| $f_{si}$ | Prestress immediately after transfer |
| g | Strand draw-in |
| $L_b$ | Longest debonded length of the strand |
| $L_d$ | Development length |
| $L_{d,AASHTO}$ | AASHTO recommended development length for fully bonded strand |
| $L_e$ | Embedment Length |
| $L_s$ | Test Span Length |
| $L_t$ | Transfer Length |
| $M_{u,app}$ | Maximum applied moment at the critical section |
| $M_{u,clac}$ | Maximum calculated moment at the critical section |
| $P_{u,app}$ | Maximum applied load |
| $U'_d$ | Plastic bond stress coefficient for development |
| $U'_t$ | Plastic bond stress coefficient |
| $\alpha$ | Coefficient indicating shape of bond stress distribution in transfer zone |
| $\varepsilon_{cu}$ | Maximum top fiber concrete strain |
| $\varepsilon_{ps}$ | Strand strain before load is applied |
| $\varepsilon_{su}$ | Maximum strand strain |

# APPENDIX B

## Concrete Mix Designs

**Table B1: Low Strength Concrete Mix Design**

| Material | Quantity per cubic yard |
|---|---|
| Type III Cement | 528 lb |
| Fly Ash | 205 lb |
| Water | 242 lb |
| Coarse Aggregate | 1799 lb |
| Fine Aggregate | 1120 lb |
| Air | 5% |
| Admixtures | High Range Water Reducer |
| | Air Entraining Agent |

**Table B2: Medium Strength Concrete Mix Design**

| Material | Quantity per cubic yard |
|---|---|
| Type III Cement | 564 lb |
| Fly Ash | 162 lb |
| Water | 202 lb |
| Coarse Aggregate | 1999 lb |
| Fine Aggregate | 1153 lb |
| Air | 2% |
| Admixtures | High Range Water Reducer |
| | Air Entraining Agent |

**Table B3: High Strength Concrete Mix Design**

| Material | Quantity per cubic yard |
|---|---|
| Type III Cement | 671 lb |
| Fly Ash | 319 lb |
| Water | 246 lb |
| Coarse Aggregate | 1882 lb |
| Fine Aggregate | 1052 lb |
| Air | 2% |
| Admixtures | High Range Water Reducer |
| | Air Entraining Agent |

# APPENDIX C

## Material Properties
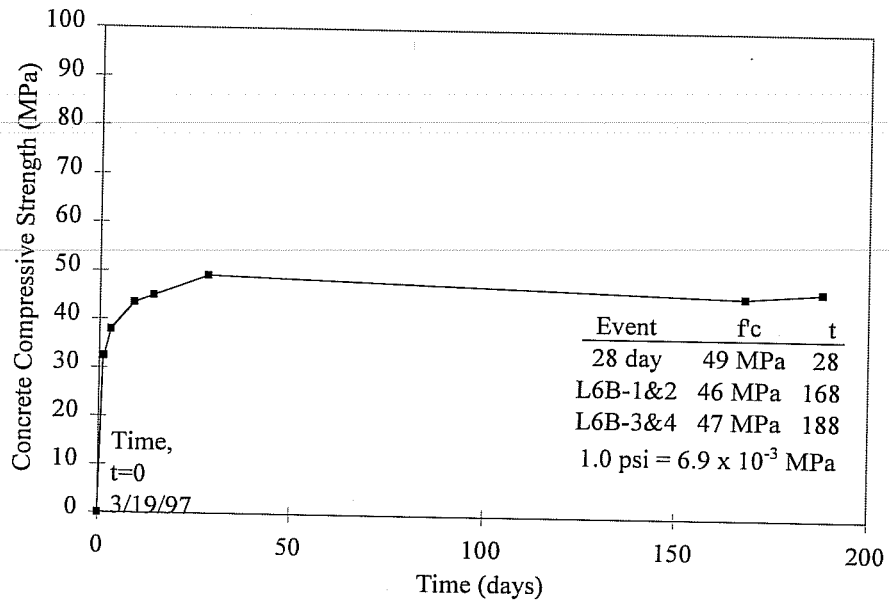
Figure C.1:  Beam Concrete Strength versus Time for L6B Series
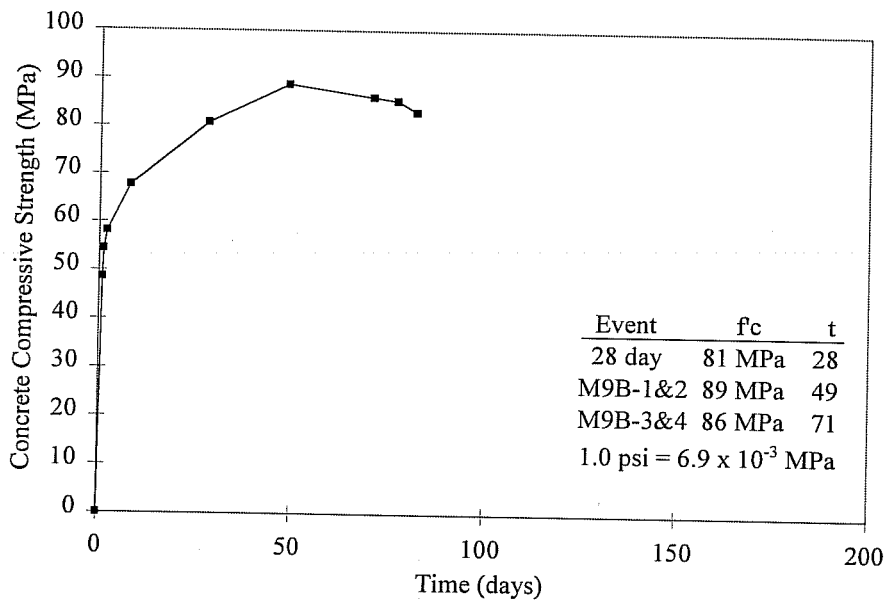


Figure C.2: Beam Concrete Strength versus Time for M9B Series

88
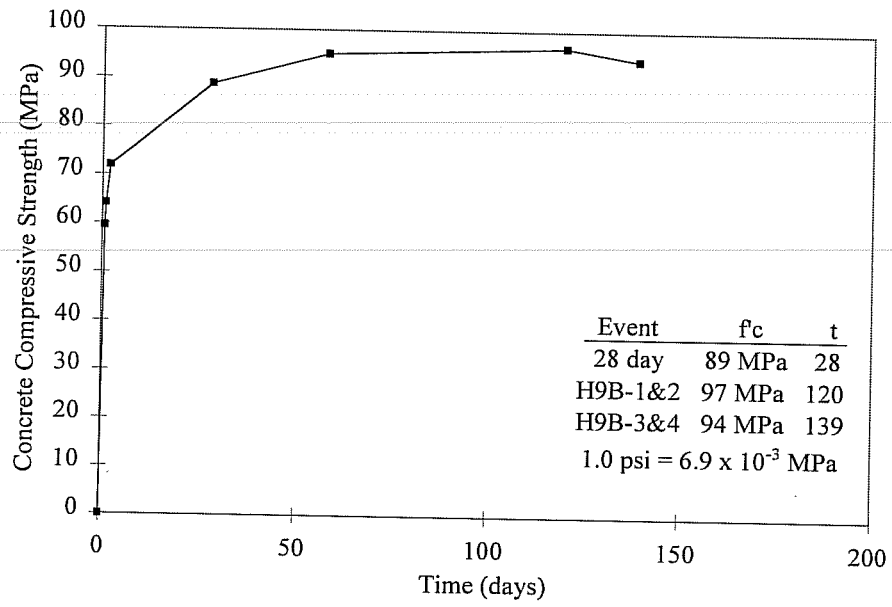
**Figure C.3: Beam Concrete Strength versus Time for H9B Series**

| Event | f'c | t |
|-------|-----|---|
| 28 day | 89 MPa | 28 |
| H9B-1&2 | 97 MPa | 120 |
| H9B-3&4 | 94 MPa | 139 |
| 1.0 psi = 6.9 x $10^{-3}$ MPa | | |

89
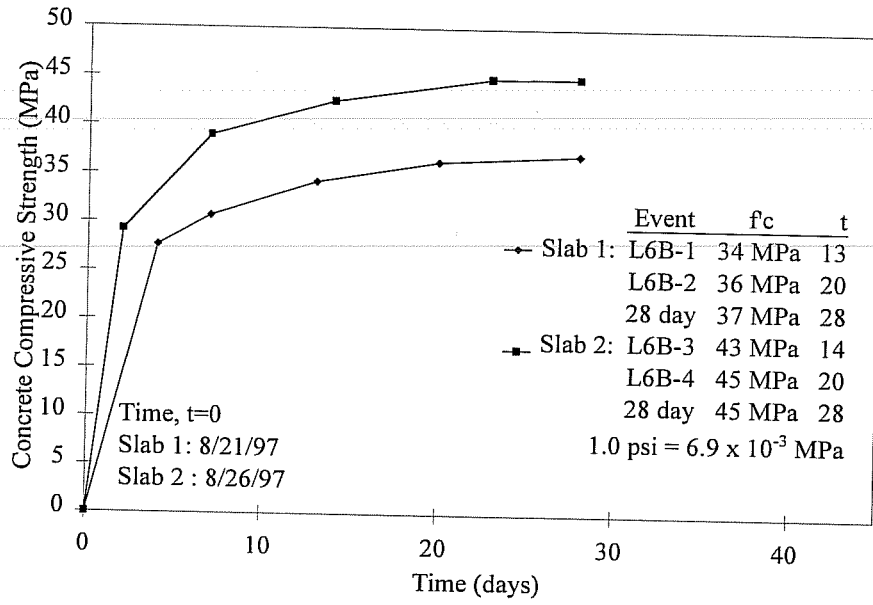
**Figure C.4: Deck Slab Concrete Strength versus Time for L6B series**
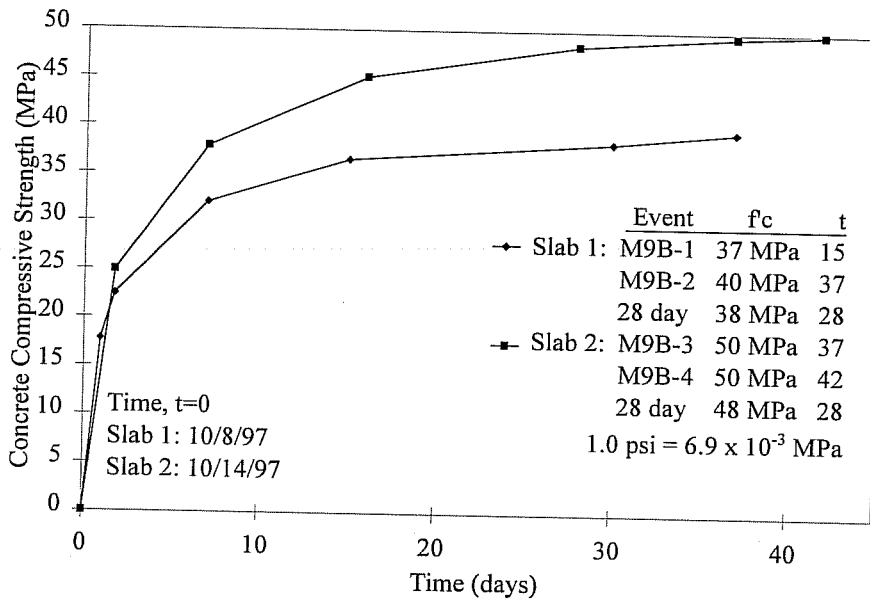


**Figure C.5: Deck Slab Concrete Strength versus Time for M9B Series**
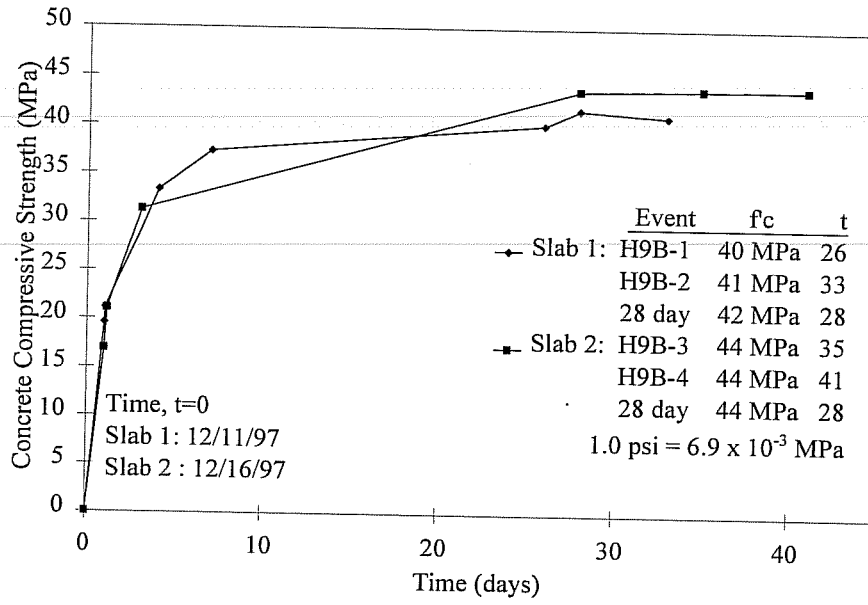
**Figure E.6: Deck Slab Concrete Strength versus Time for H9B series**

The chart shows Concrete Compressive Strength (MPa) on the y-axis (0 to 50) versus Time (days) on the x-axis (0 to 40).

Legend and data table:

| Event | | f'c | t |
|---|---|---|---|
| Slab 1: | H9B-1 | 40 MPa | 26 |
| | H9B-2 | 41 MPa | 33 |
| | 28 day | 42 MPa | 28 |
| Slab 2: | H9B-3 | 44 MPa | 35 |
| | H9B-4 | 44 MPa | 41 |
| | 28 day | 44 MPa | 28 |

$1.0 \text{ psi} = 6.9 \times 10^{-3} \text{ MPa}$

Time, t=0
Slab 1: 12/11/97
Slab 2 : 12/16/97

91

# APPENDIX D

## Texas Department of Transportation Prestressed Concrete Beam

### Mild Steel Reinforcement Details
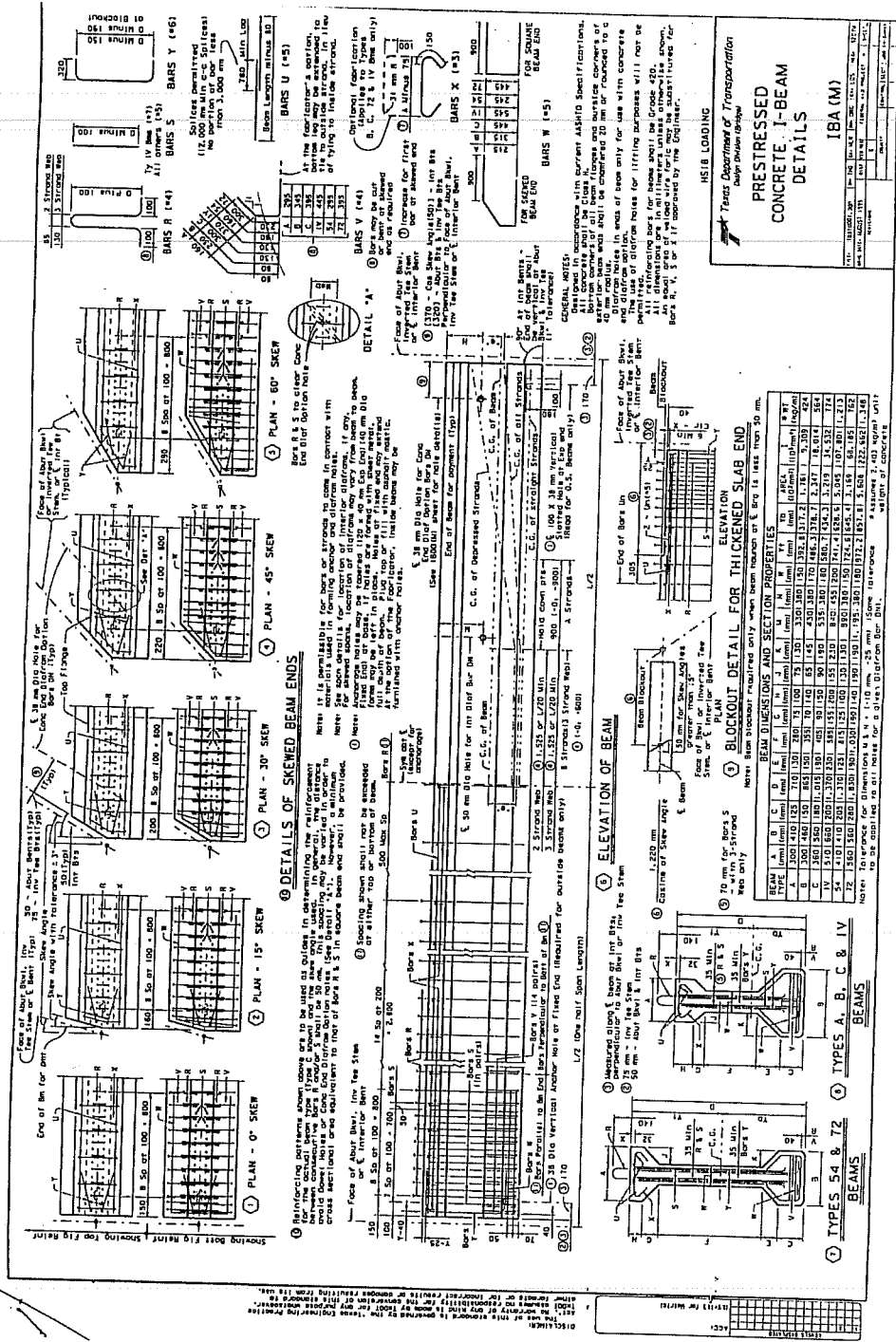
Figure D1: TxDOT Prestressed Concrete Beam Mild Steel Reinforcement Detail IBA (M)

Figure D2: TxDOT Prestressed Concrete Beam Mild Steel Reinforcement Detail IBNS (M)

94

# APPENDIX E

## Transfer Length Strain Profiles
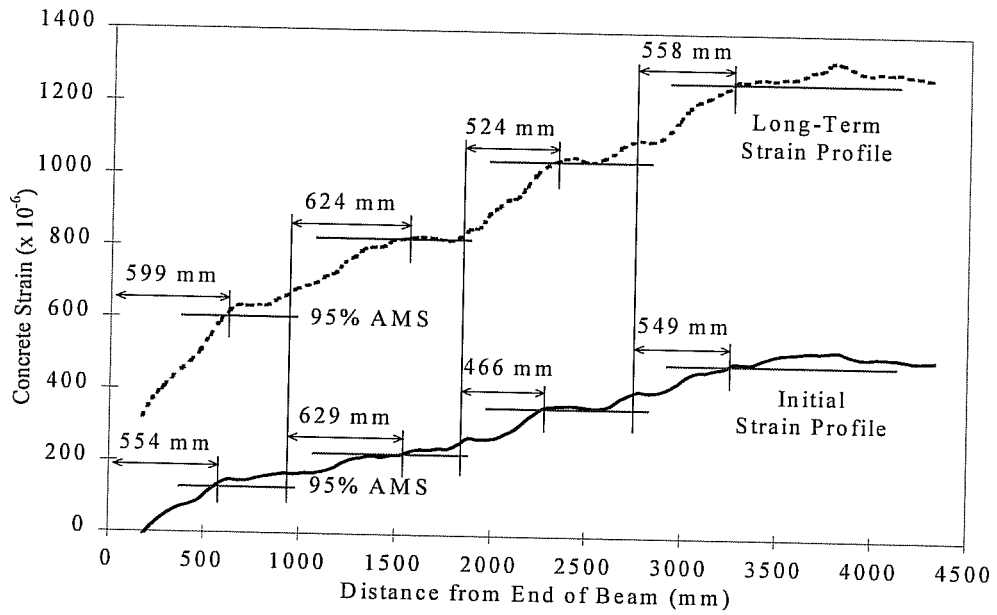
**Figure E.1: Concrete Strain Profile for Specimen L6B-1**
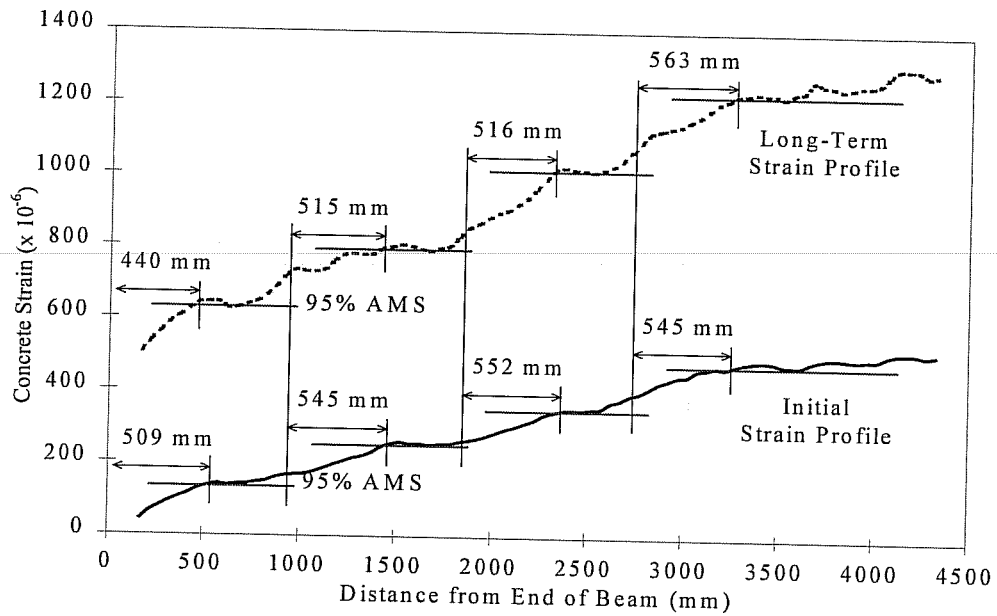


**Figure E.2: Concrete Strain Profile for Specimen L6B-2**
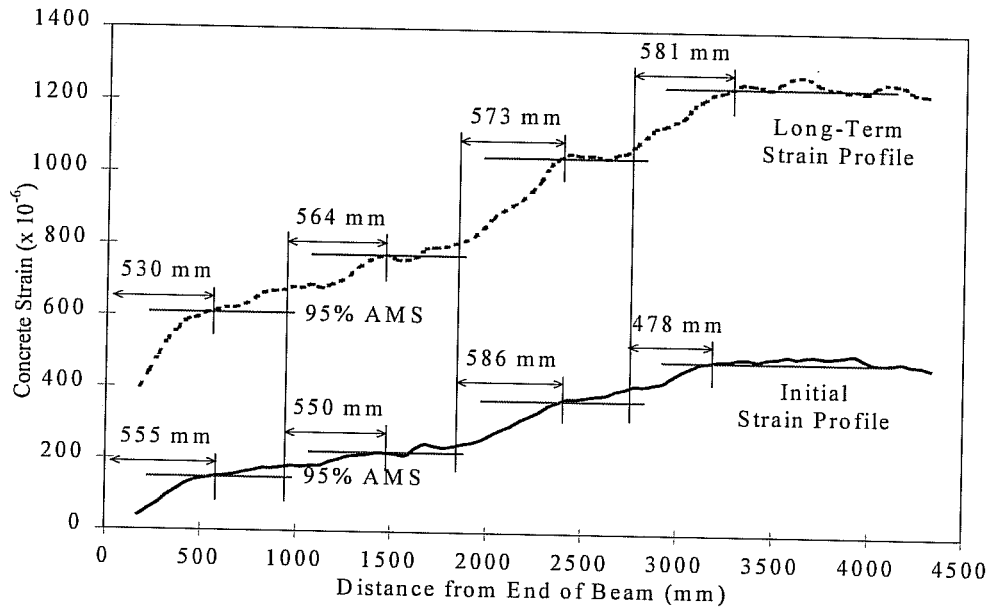
**Figure E.3: Concrete Strain Profile for Specimen L6B-3**
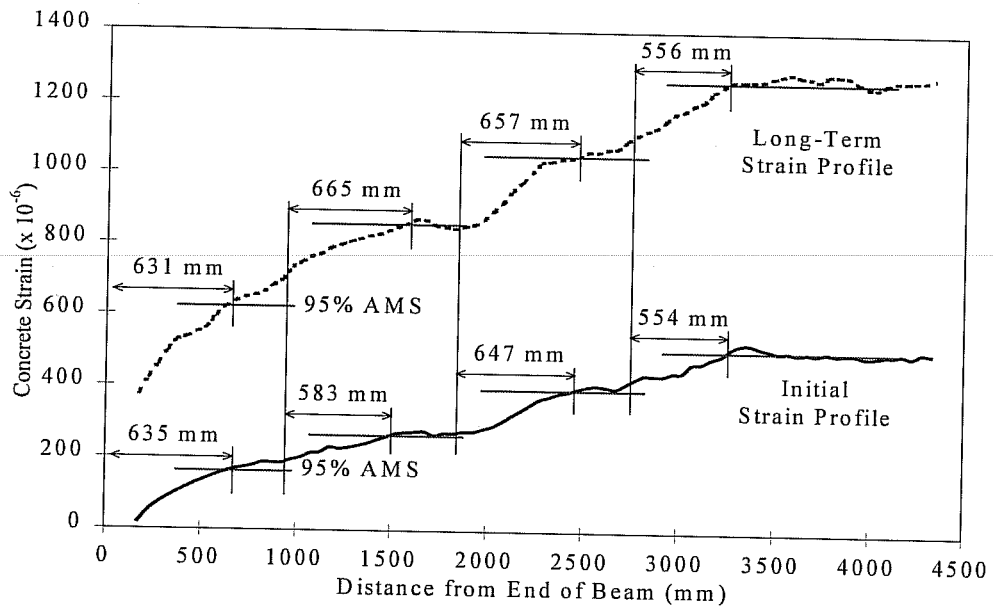


**Figure E.4: Concrete Strain Profile for Specimen L6B-4**

97
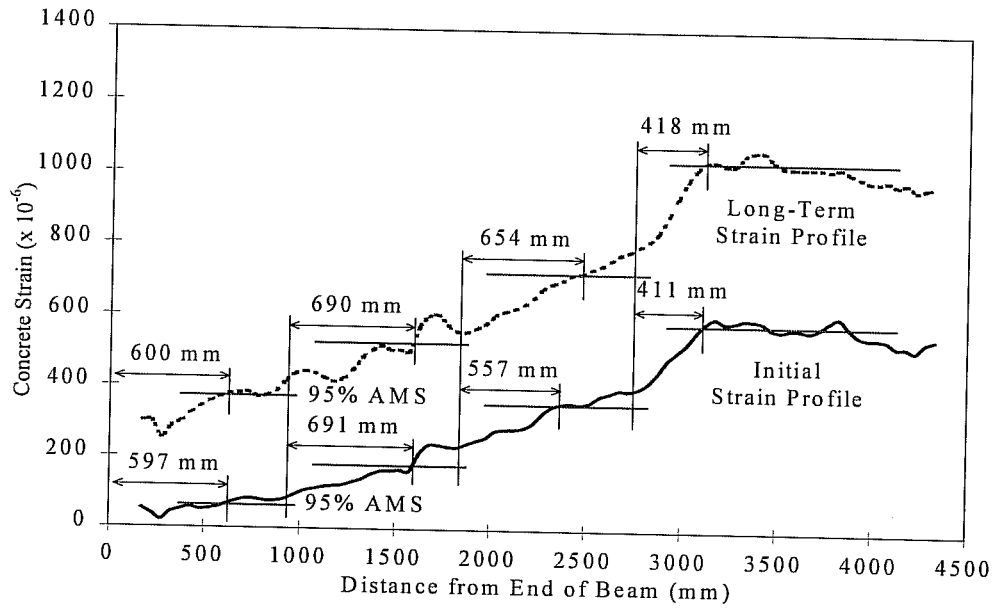
**Figure E.5: Concrete Strain Profile for Specimen M9B-1**
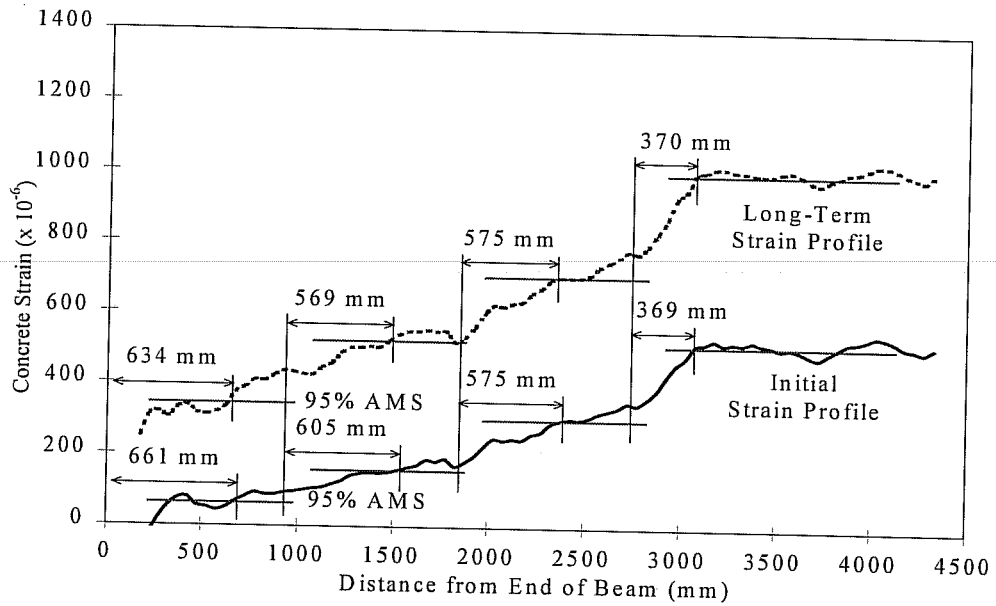


**Figure E.6: Concrete Strain Profile for Specimen M9B-2**
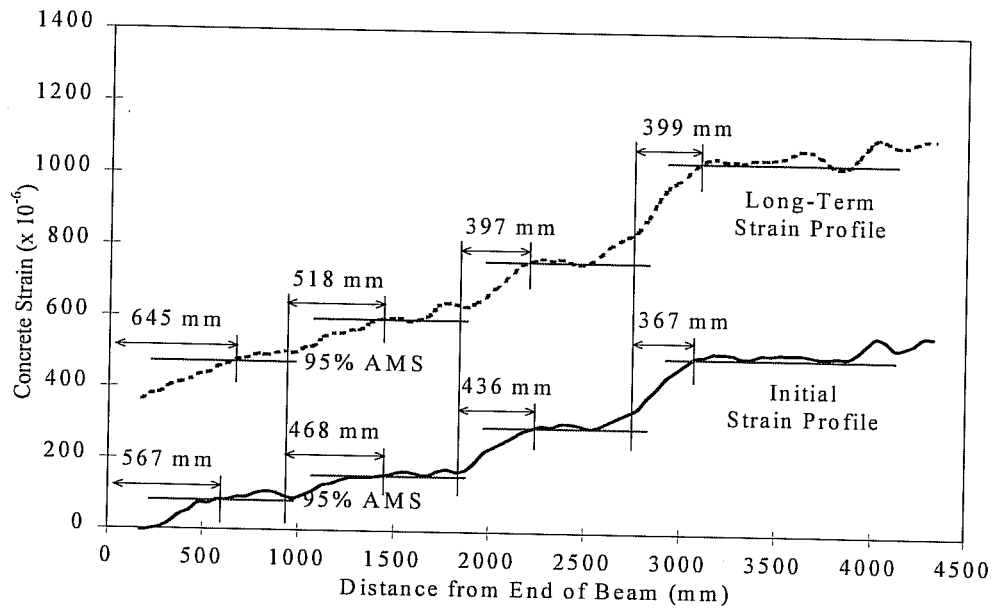
**Figure E.7: Concrete Strain Profile for Specimen M9B-3**
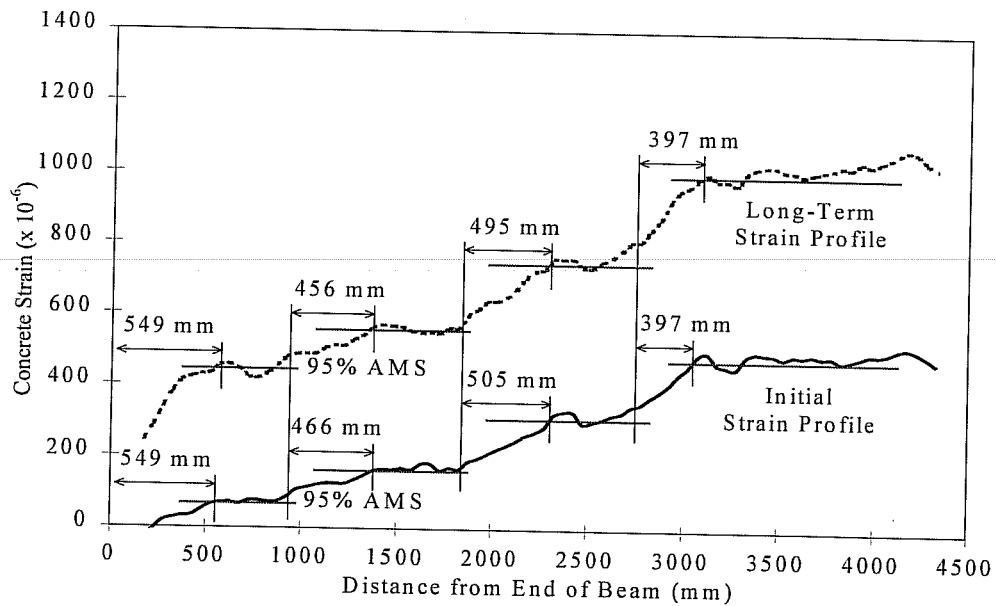


**Figure E.8: Concrete Strain Profile for Specimen M9B-4**

99
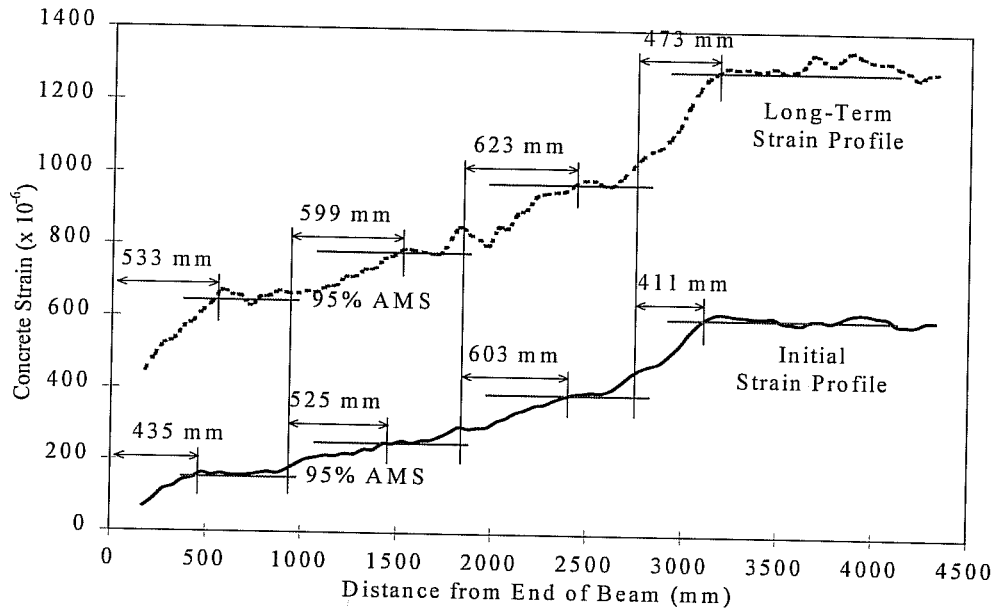
**Figure E.9: Concrete Strain Profile for Specimen H9B-1**
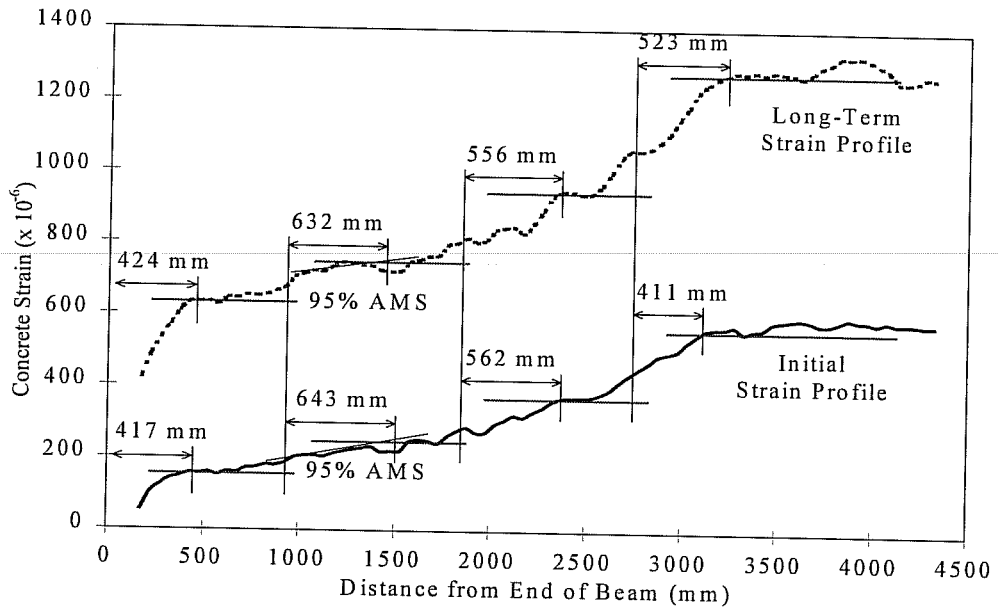


**Figure E.10: Concrete Strain Profile for Specimen H9B-2**

100
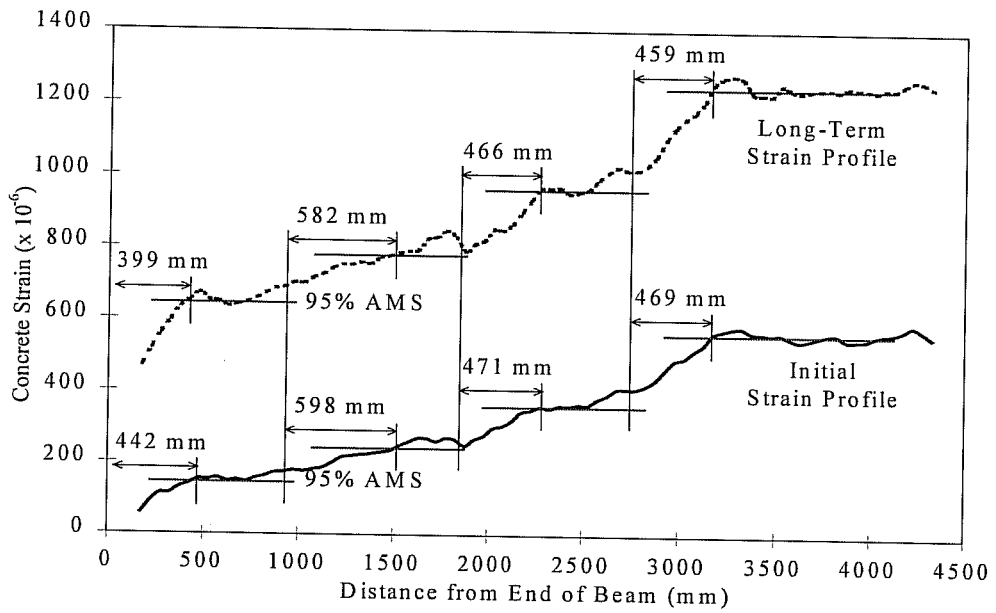
**Figure E.11: Concrete Strain Profile for Specimen H9B-3**
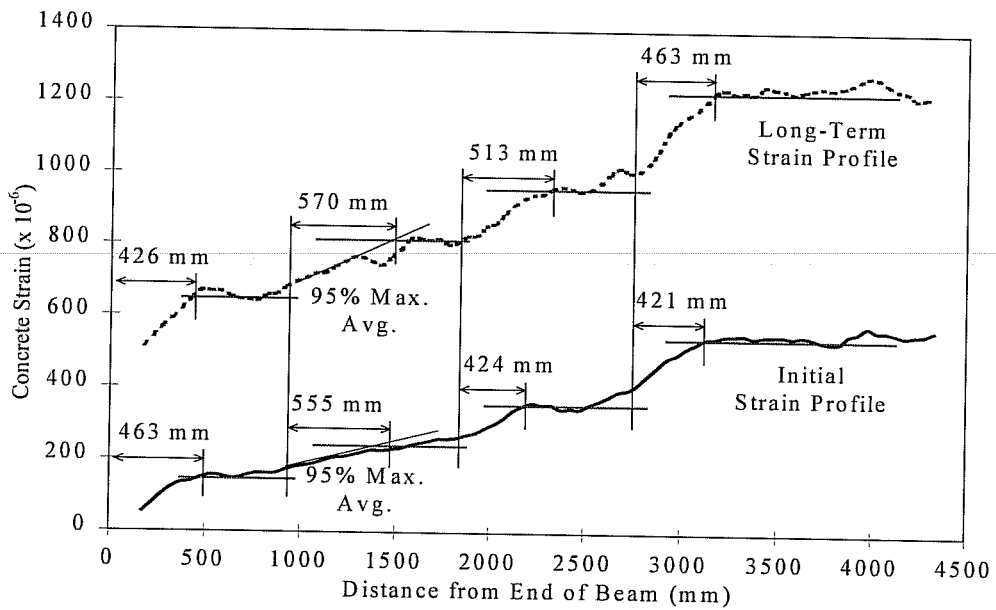


**Figure E.12: Concrete Strain Profile for Specimen H9B-4**

101

# APPENDIX F

## Corrected Strand Draw-In Measurements
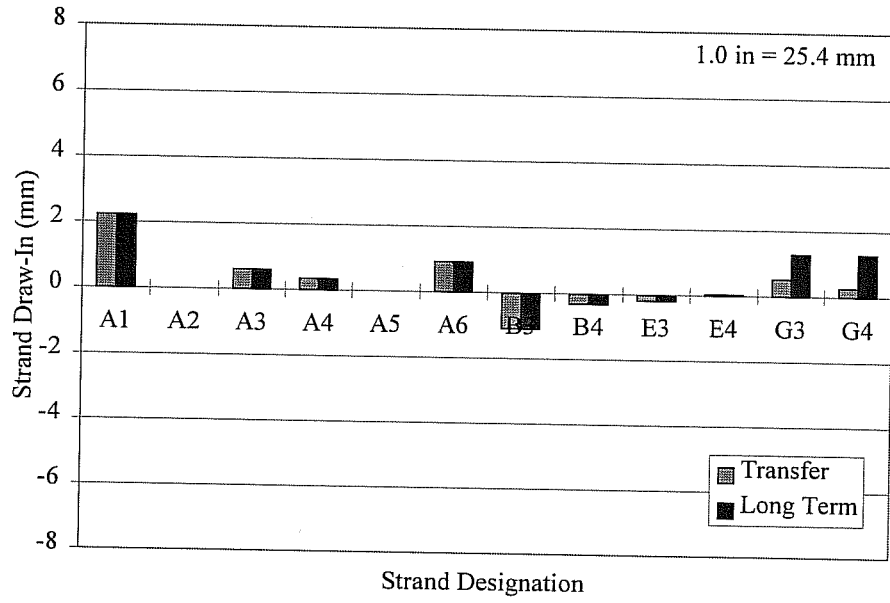
**Figure F.1: Corrected Strand Draw-In for Specimen L6B-1**
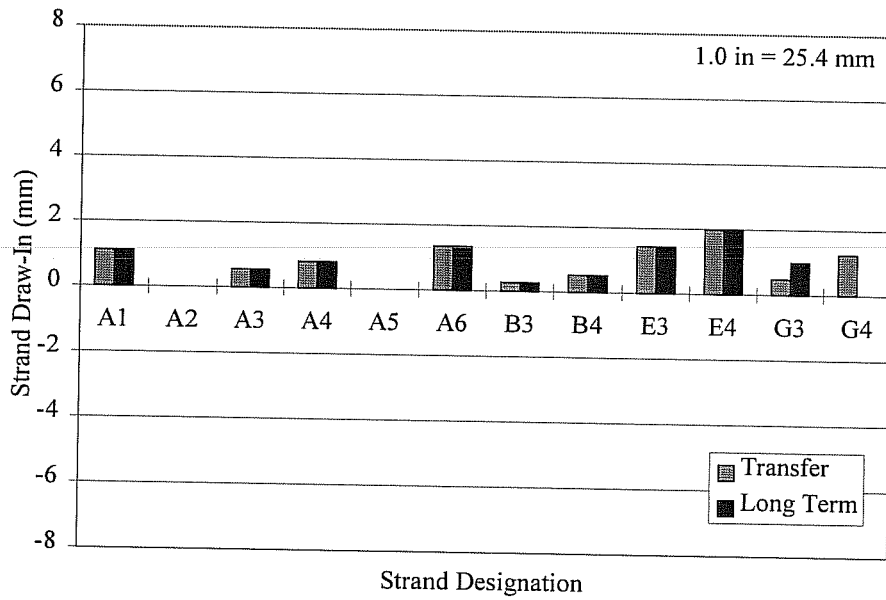


**Figure F.2: Corrected Strand Draw-In for Specimen L6B-2**

103
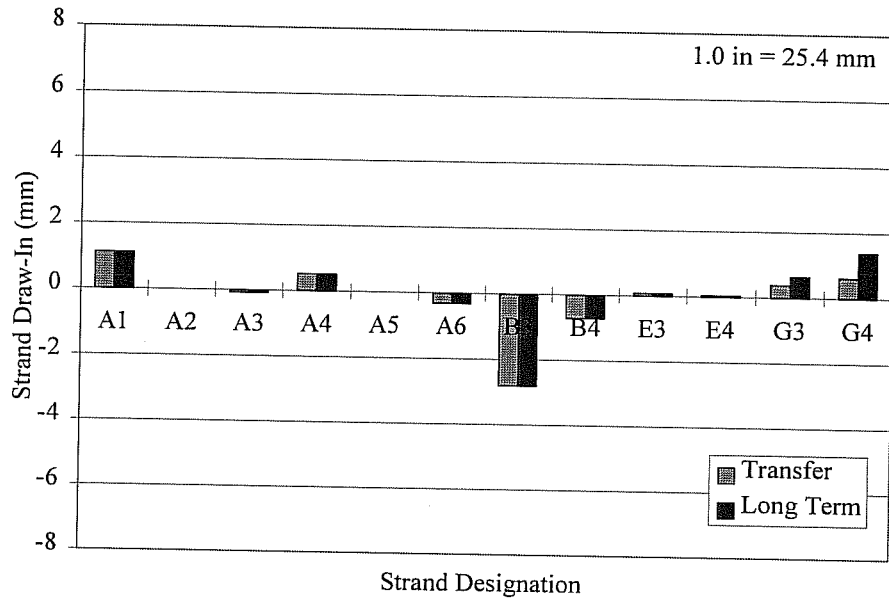
**Figure F.3:  Corrected Strand Draw-In for Specimen L6B-3**
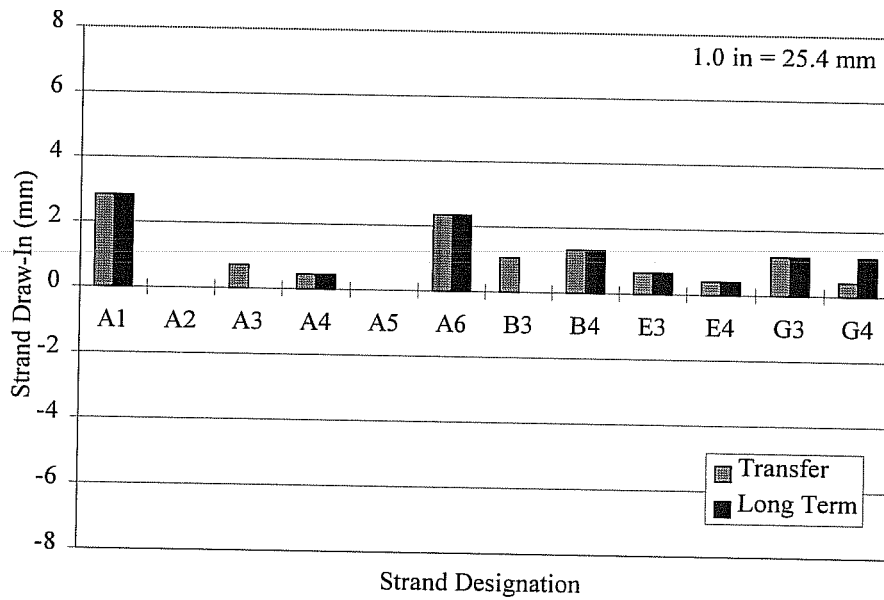


**Figure F.4:  Corrected Strand Draw-In for Specimen L6B-4**
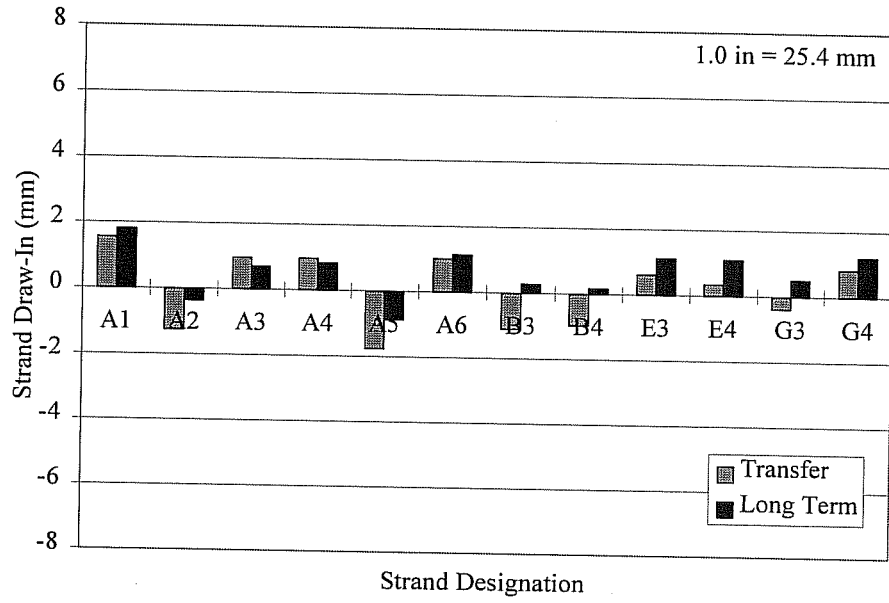
**Figure F.5: Corrected Strand Draw-In for Specimen M9B-1**
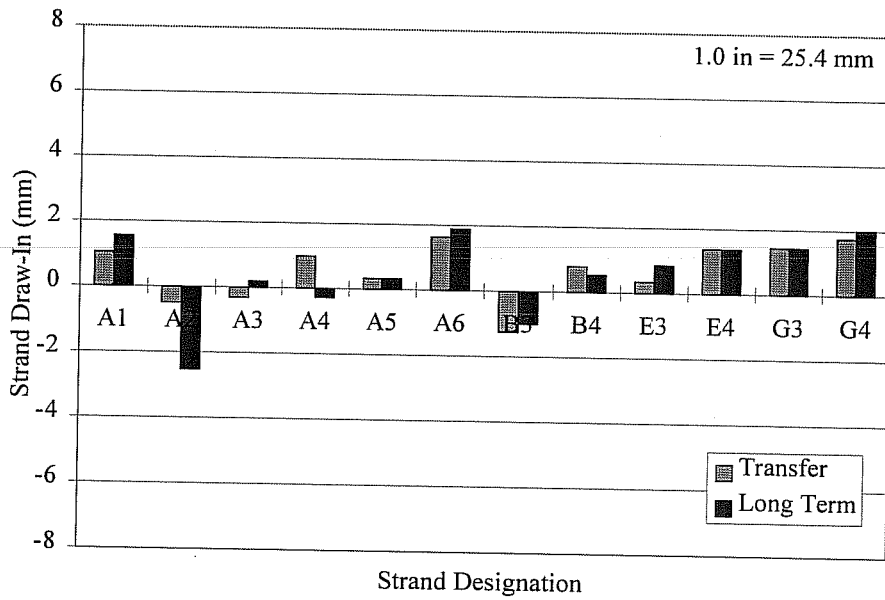


**Figure F.6: Corrected Strand Draw-In for Specimen M9B-2**
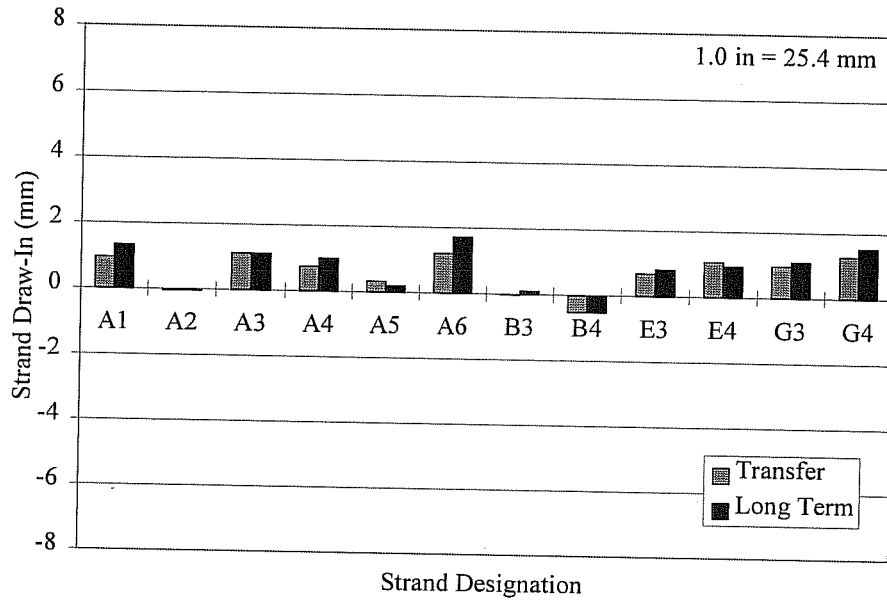
**Figure F.7:  Corrected Strand Draw-In for Specimen M9B-3**
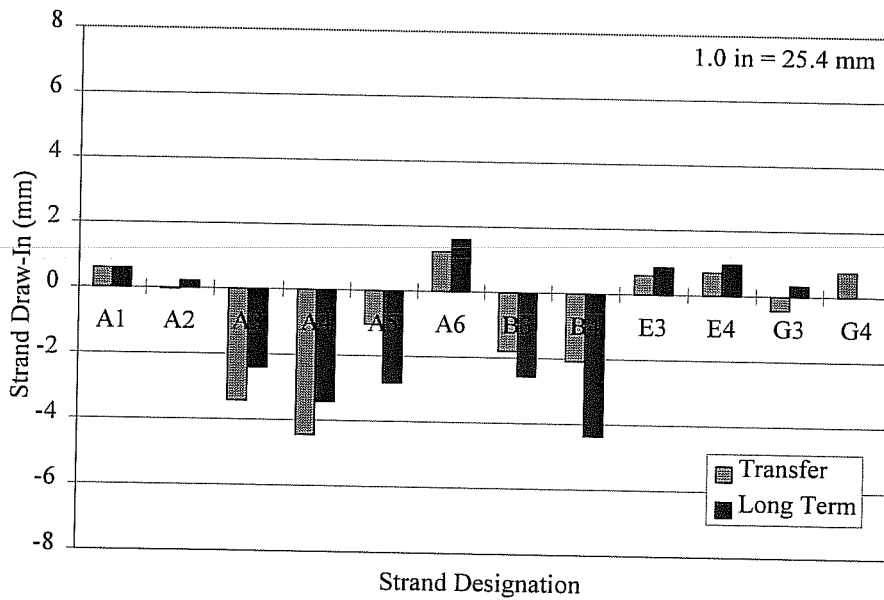


**Figure F.8:  Corrected Strand Draw-In for Specimen M9B-4**
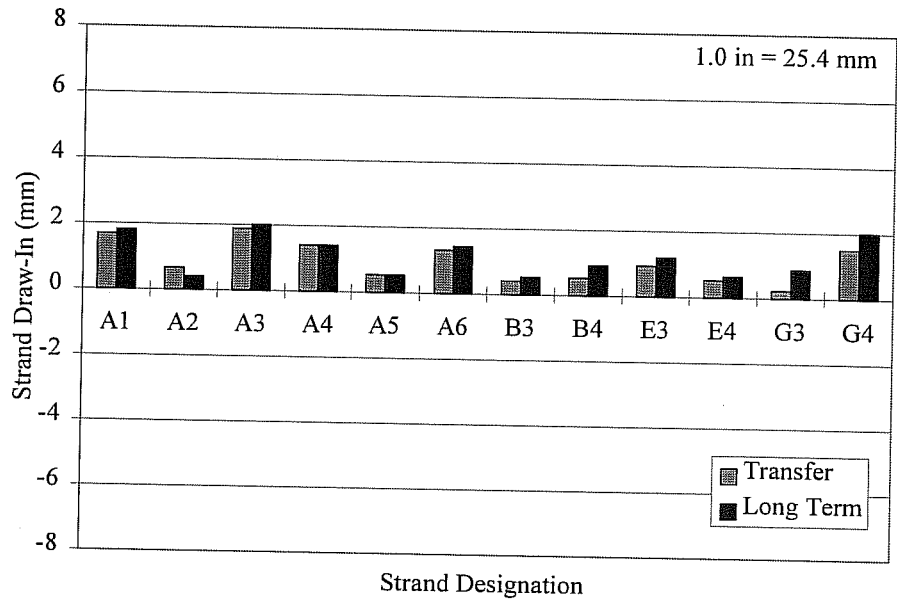
**Figure F.9: Corrected Strand Draw-In for Specimen H9B-1**
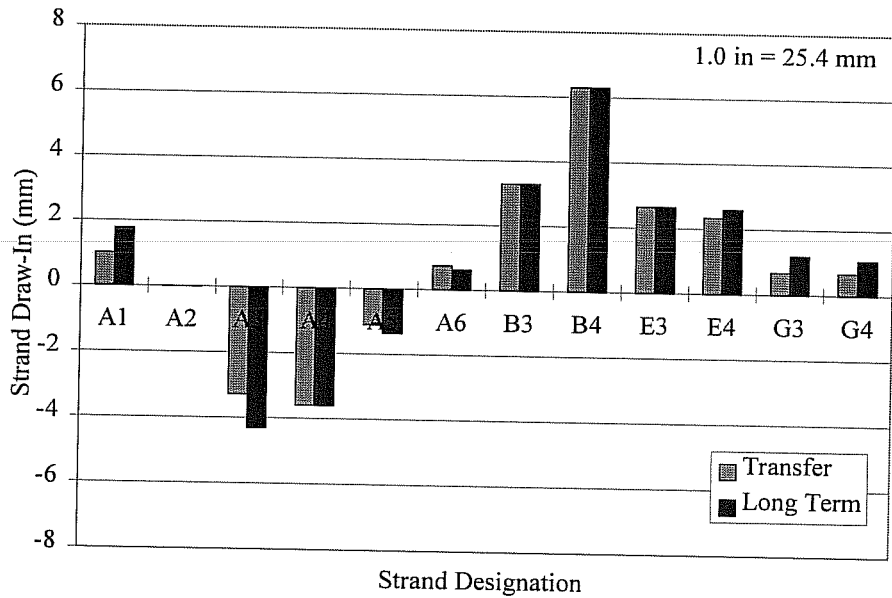


**Figure F.10: Corrected Strand Draw-In for Specimen H9B-2**
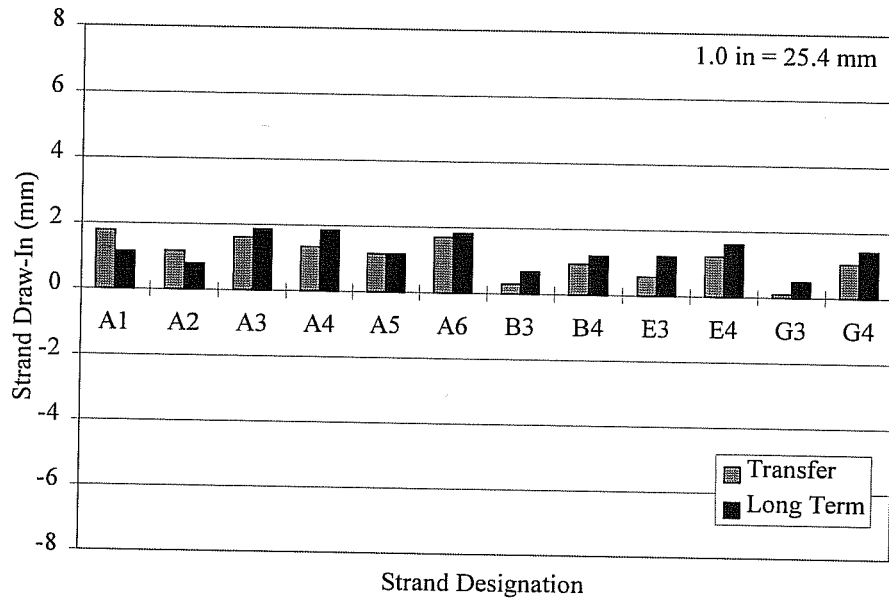
**Figure F.11: Corrected Strand Draw-In for Specimen H9B-3**
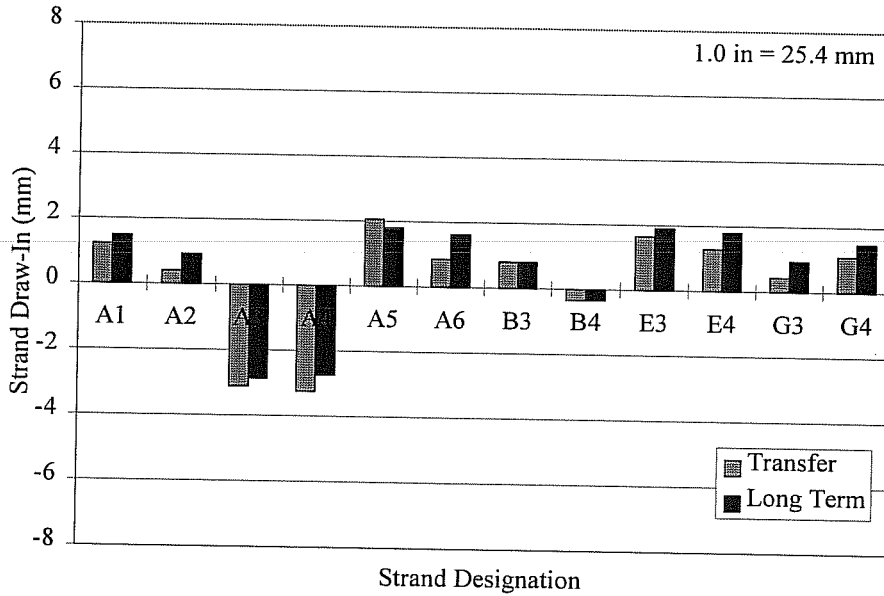


**Figure F.12: Corrected Strand Draw-In for Specimen H9B-4**

108

# APPENDIX G

## Normalized Load and Strand End Slip vs Beam Displacement Plots
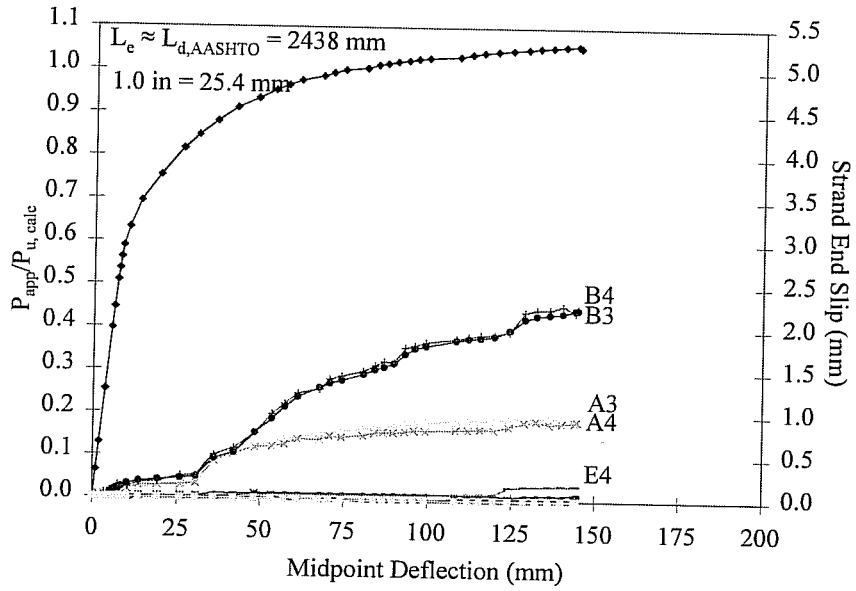
**Figure G.1: Normalized Load and Strand Slip vs Beam Displacement for Specimen L6B-1**
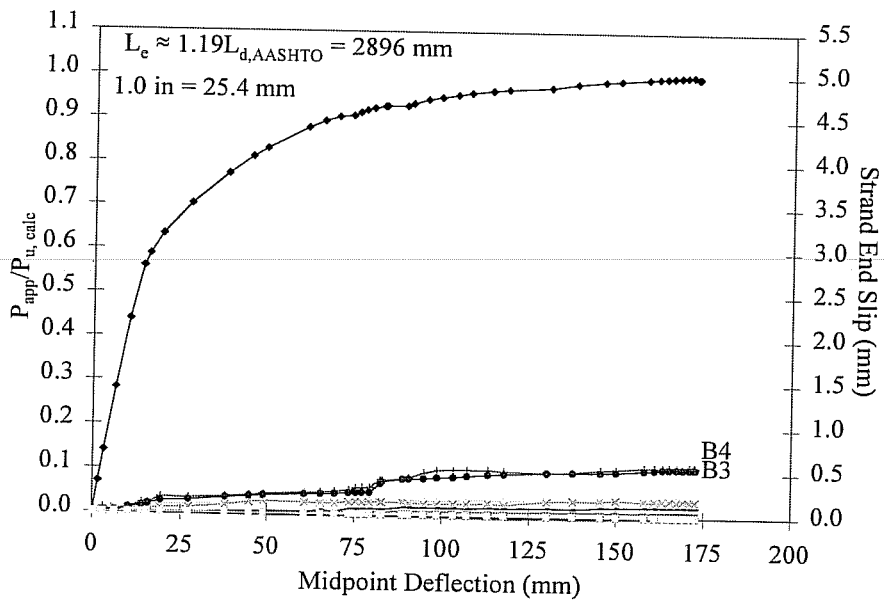


**Figure G.2: Normalized Load and Strand Slip vs Beam Displacement for Specimen L6B-2**

110
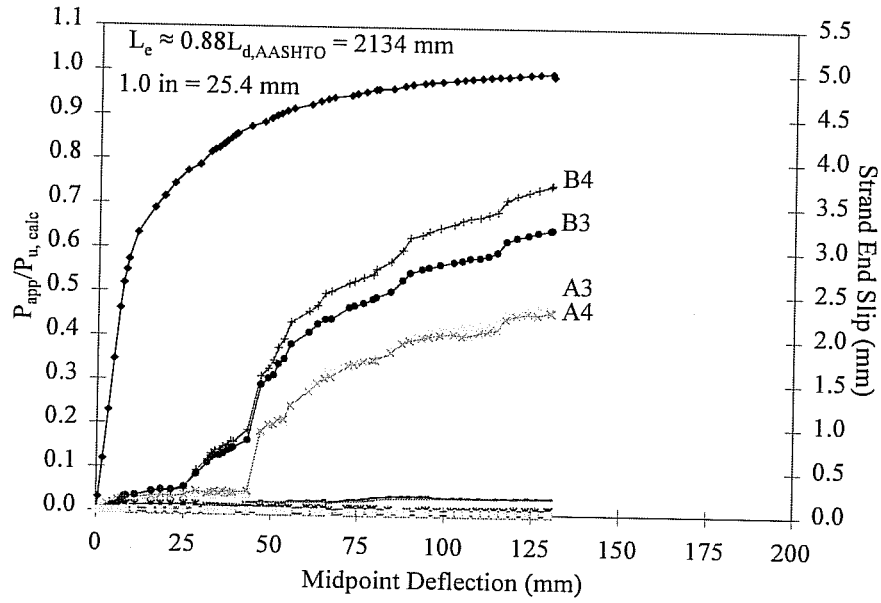
**Figure G.3: Normalized Load and Strand Slip vs Beam Displacement for Specimen L6B-3**
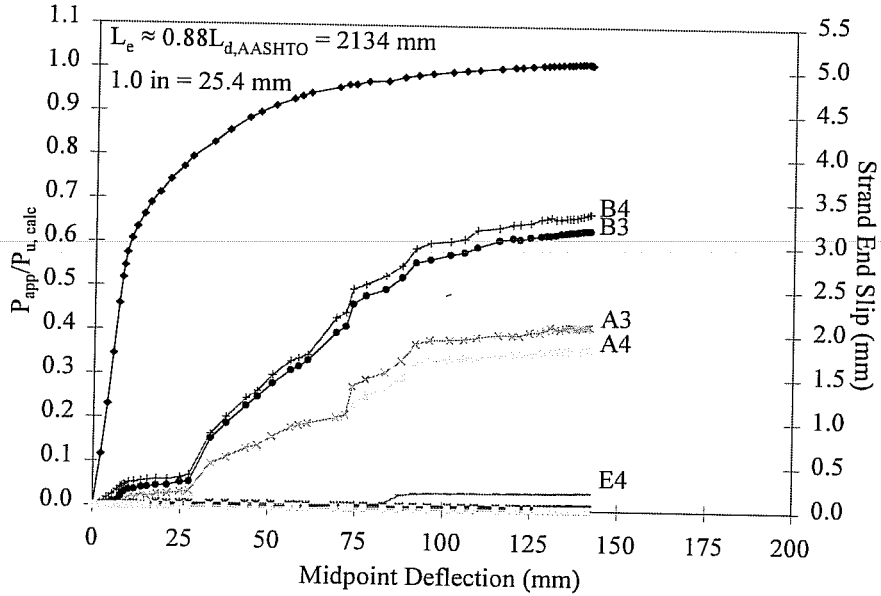


**Figure G.4: Normalized Load and Strand Slip vs Beam Displacement for Specimen L6B-4**

111
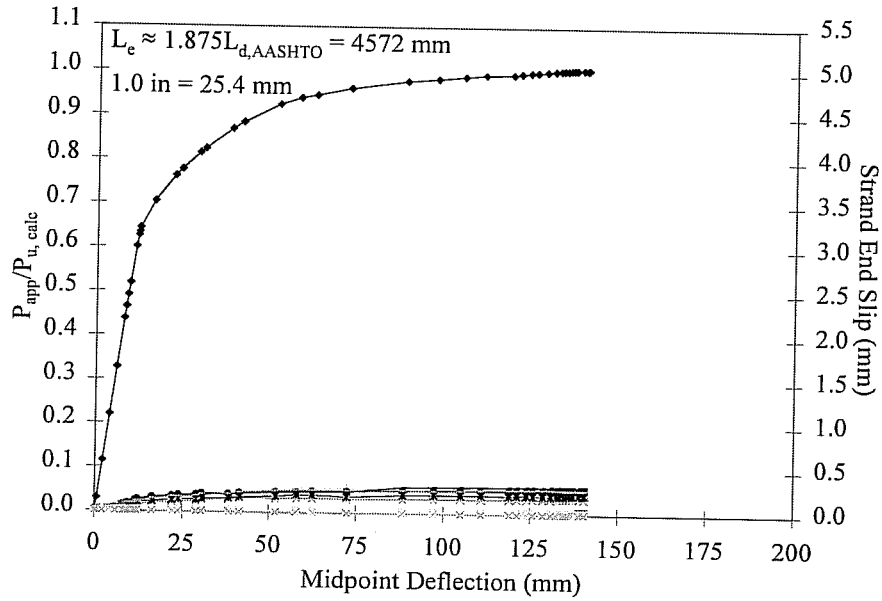
**Figure G.5: Normalized Load and Strand Slip vs Beam Displacement for Specimen M9B-1**
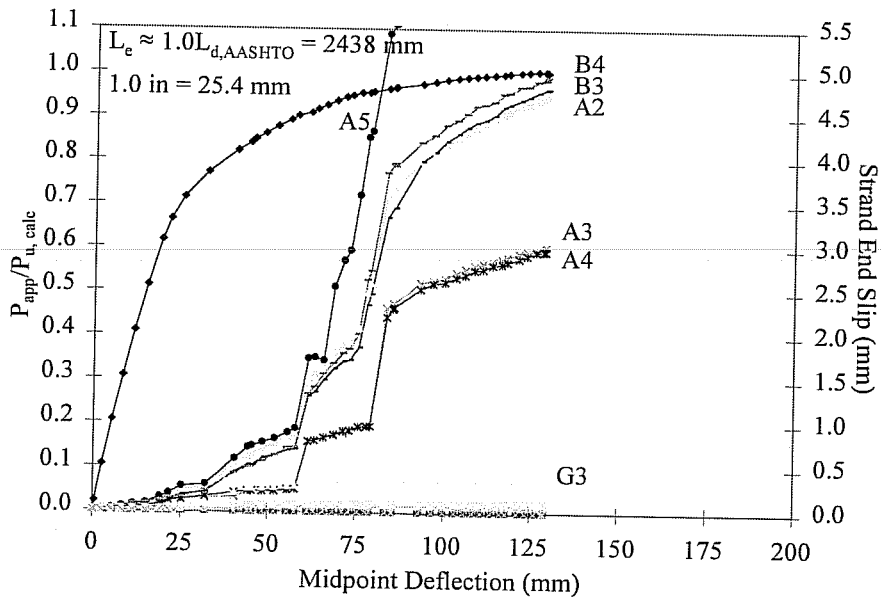


**Figure G.6: Normalized Load and Strand Slip vs Beam Displacement for Specimen M9B-2**

112
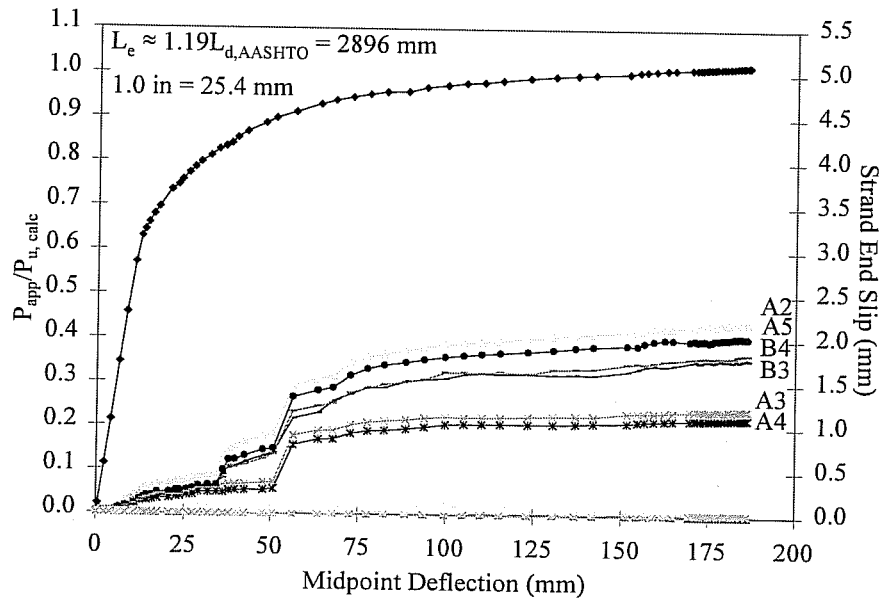
**Figure G.7: Normalized Load and Strand Slip vs Beam Displacement for Specimen M9B-3**
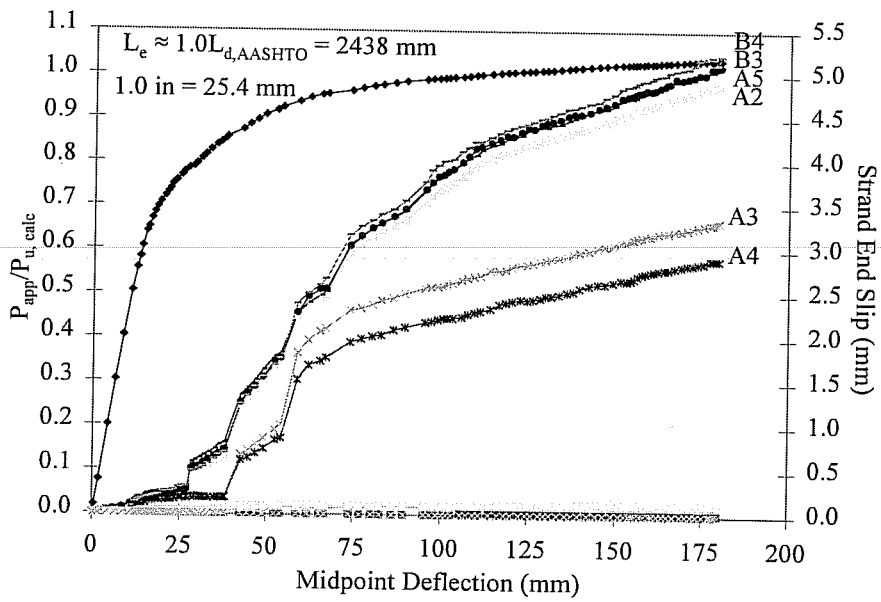


**Figure G.8: Normalized Load and Strand Slip vs Beam Displacement for Specimen M9B-4**

113
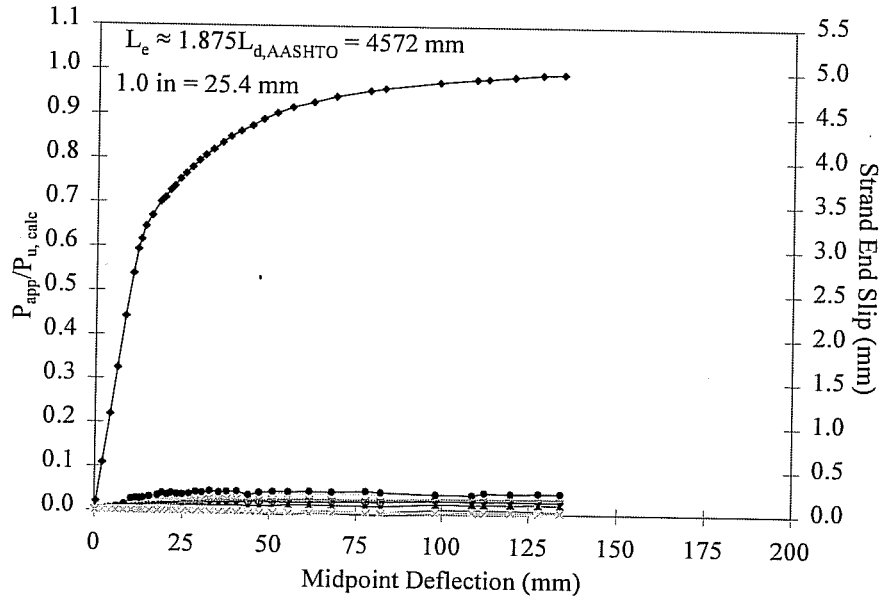
**Figure G.9: Normalized Load and Strand Slip vs Beam Displacement for Specimen H9B-1**
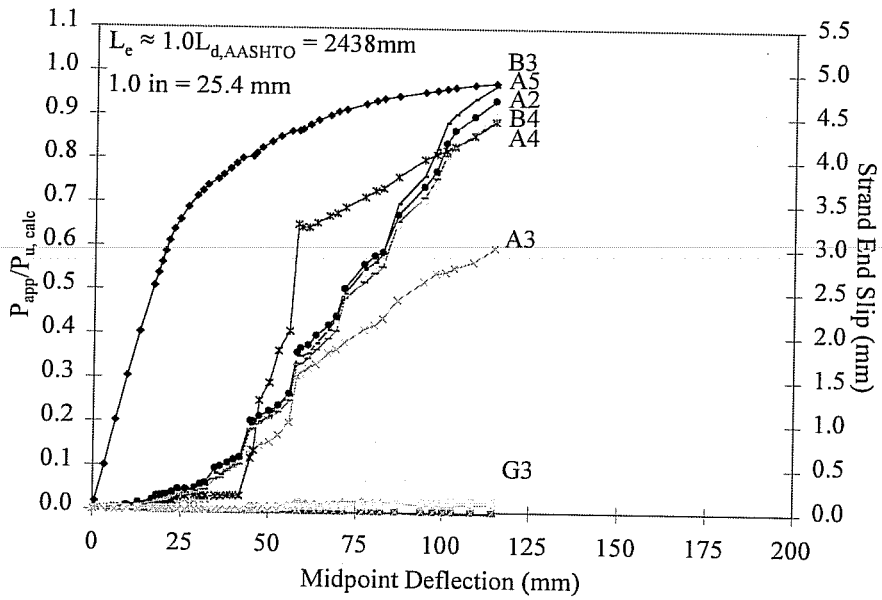


**Figure G.10: Normalized Load and Strand Slip vs Beam Displacement for Specimen H9B-2**

114
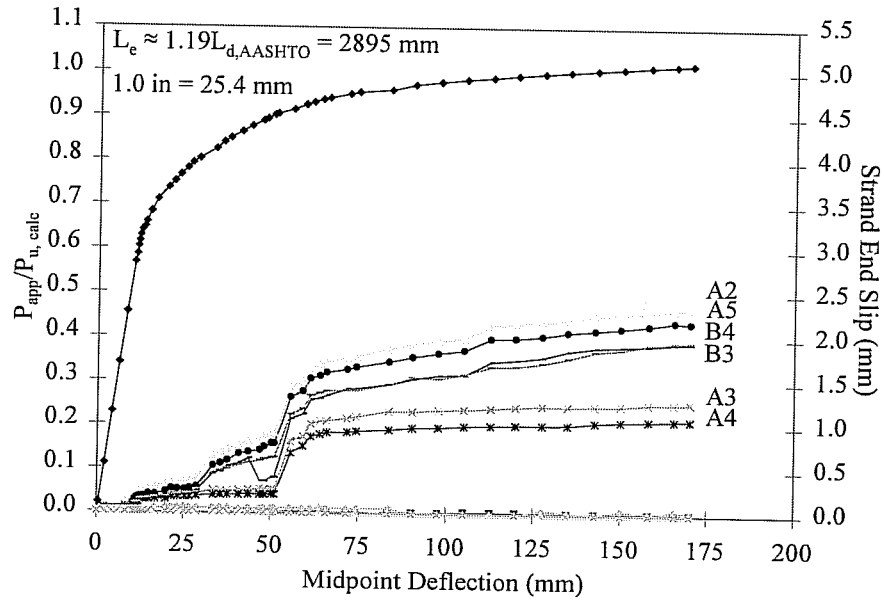
**Figure G.11:** Normalized Load and Strand Slip vs Beam Displacement for Specimen H9B-3
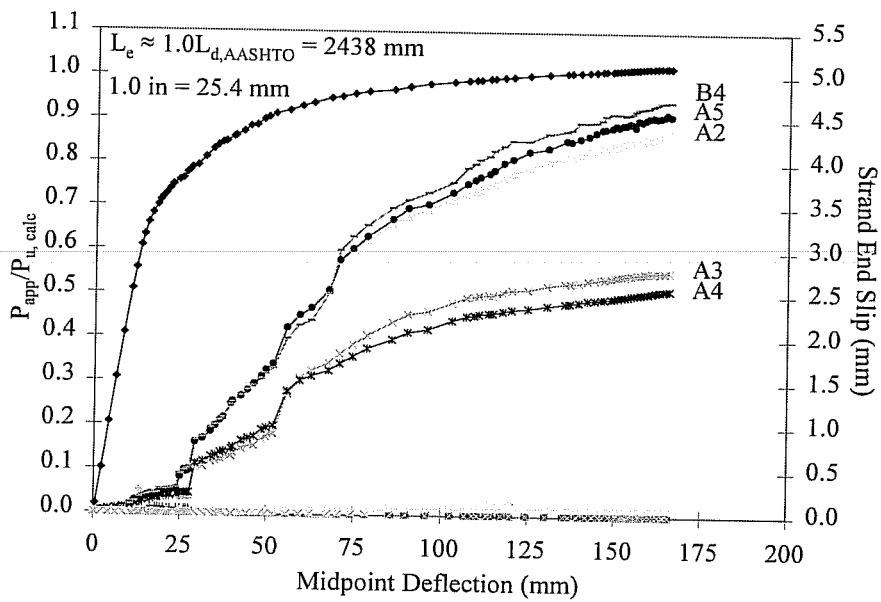


**Figure G.12:** Normalized Load and Strand Slip vs Beam Displacement for Specimen H9B-4

115

# APPENDIX H

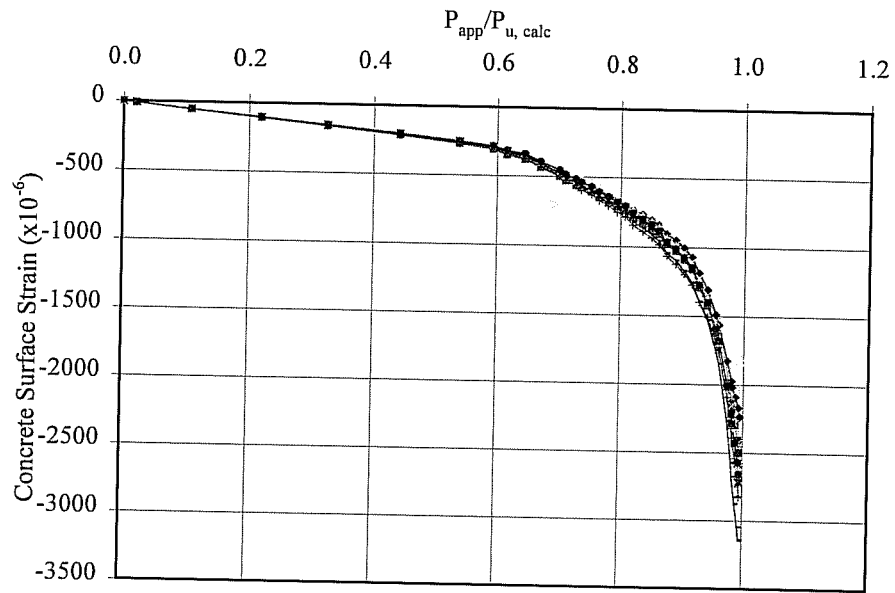## Deck Slab Concrete Strains vs Normalized Load Plots
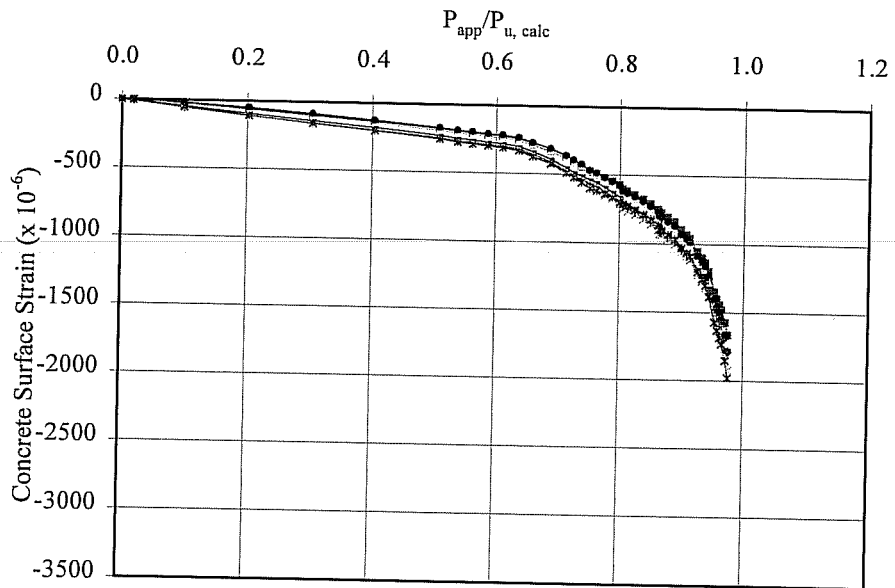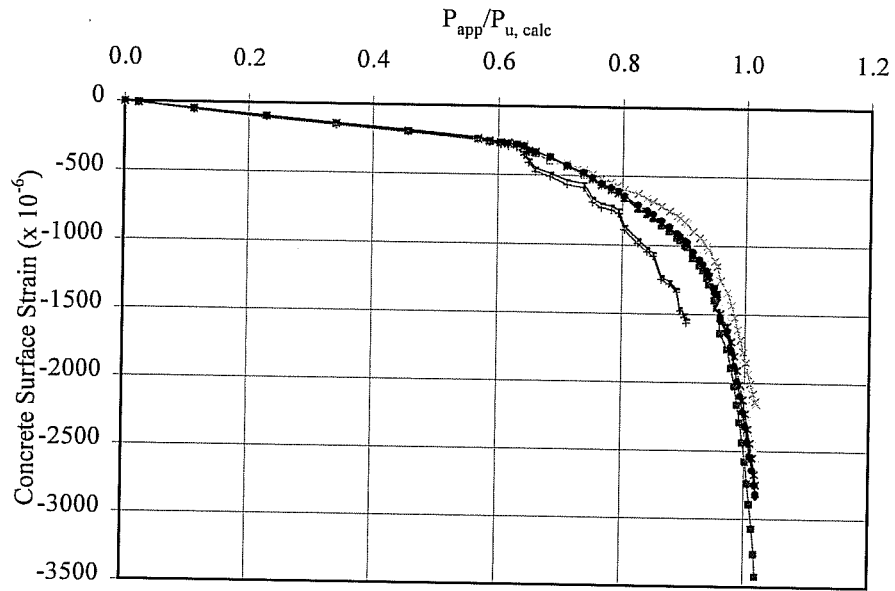
116
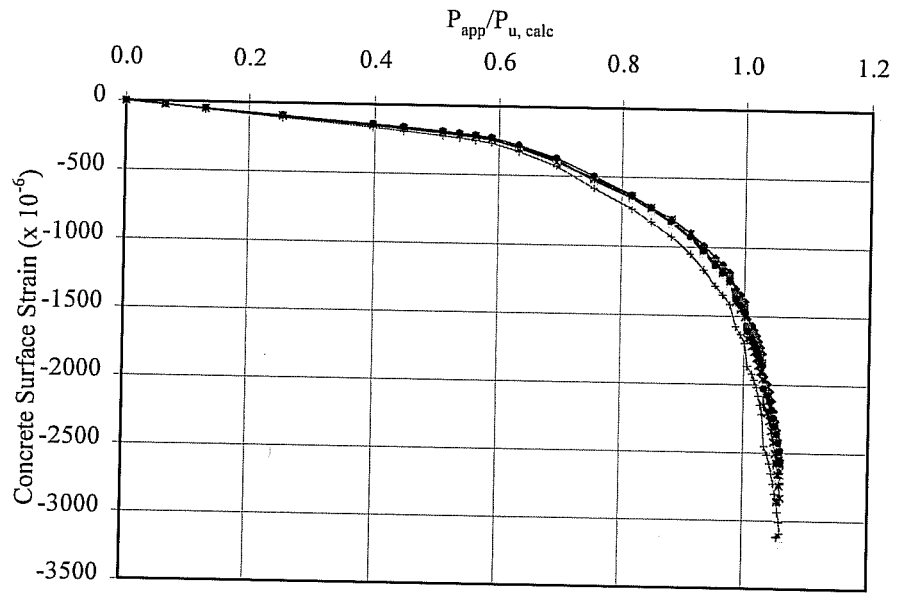
**Figure H.1: Deck Slab Concrete Strains vs Normalized Load for Specimen L6B-1**
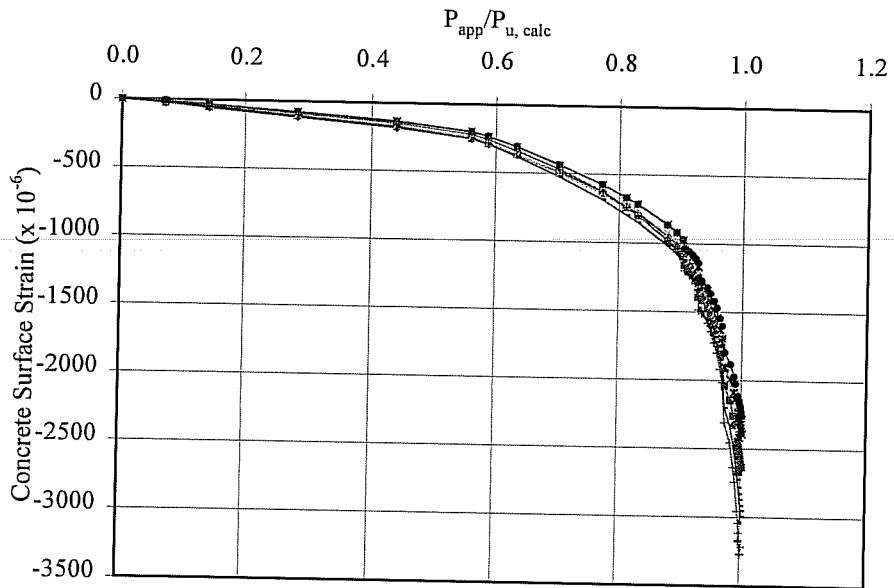


**Figure H.2: Deck Slab Concrete Strains vs Normalized Load for Specimen L6B-2**

117
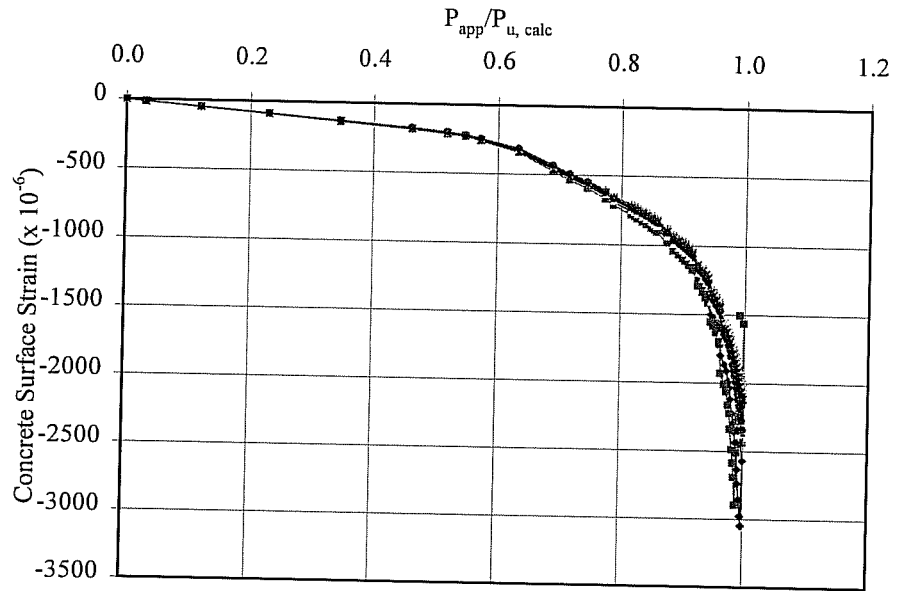
**Figure H.3: Deck Slab Concrete Strains vs Normalized Load for Specimen L6B-3**
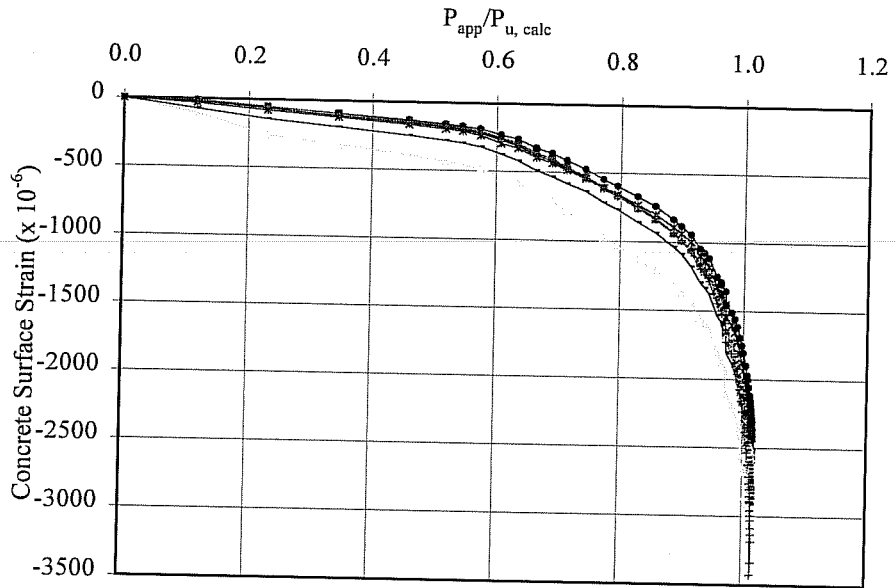


**Figure H.4: Deck Slab Concrete Strains vs Normalized Load for Specimen L6B-4**
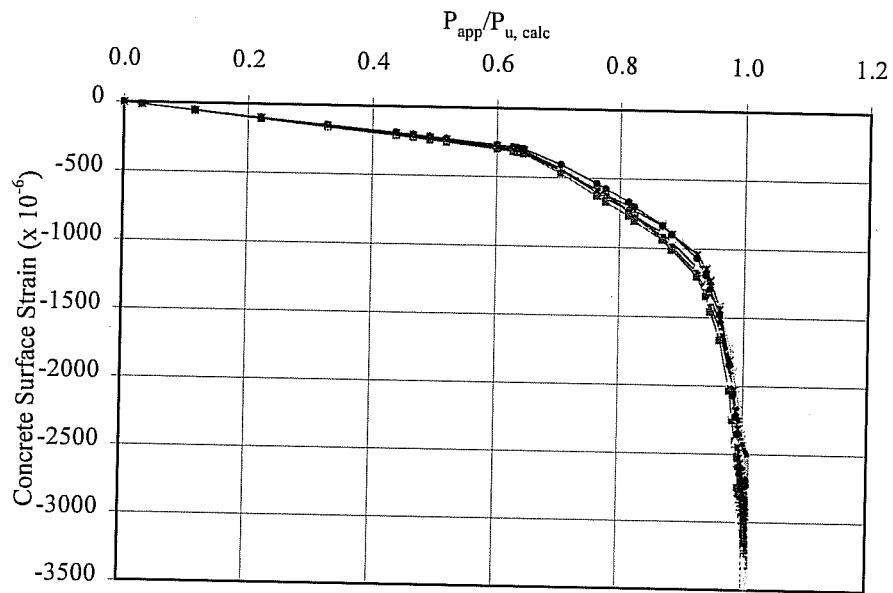
**Figure H.5:  Deck Slab Concrete Strains vs Normalized Load for Specimen M9B-1**
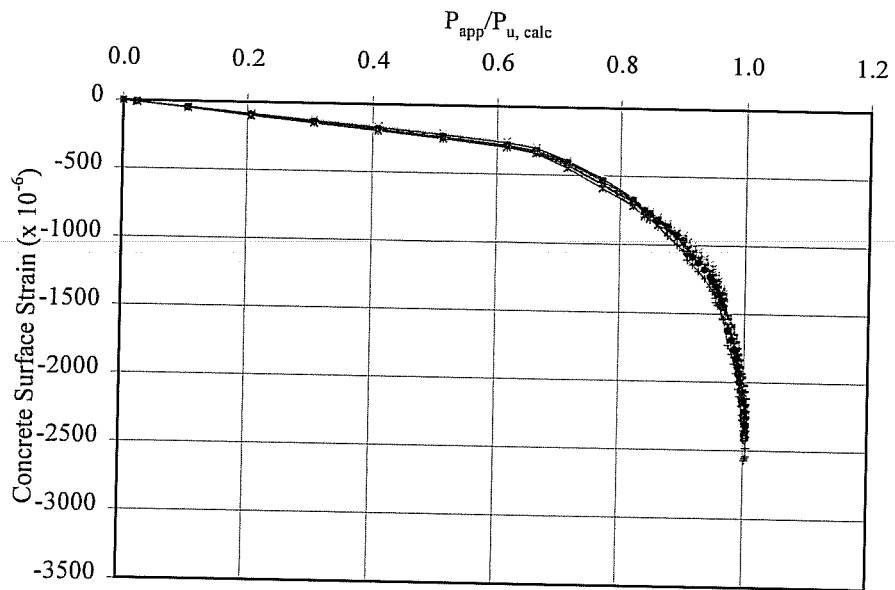


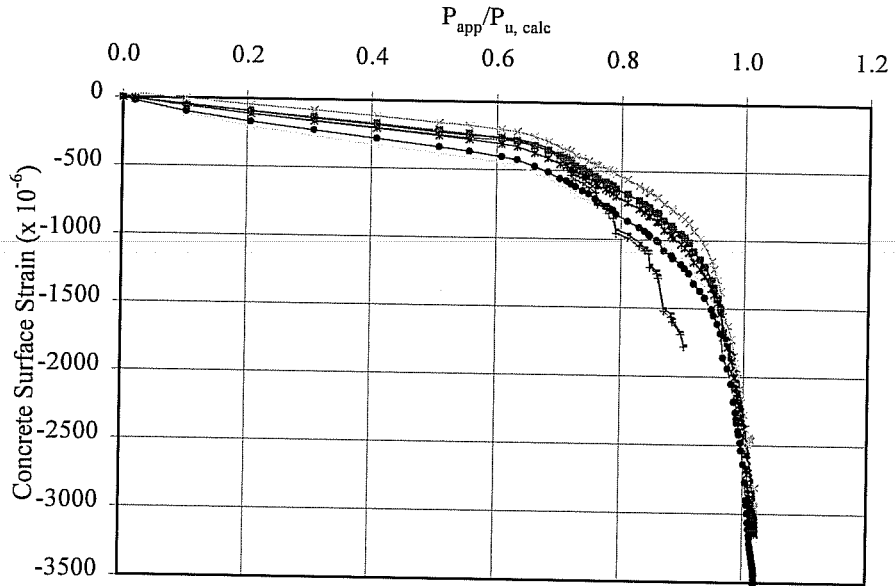**Figure H.6:  Deck Slab Concrete Strains vs Normalized Load for Specimen M9B-2**
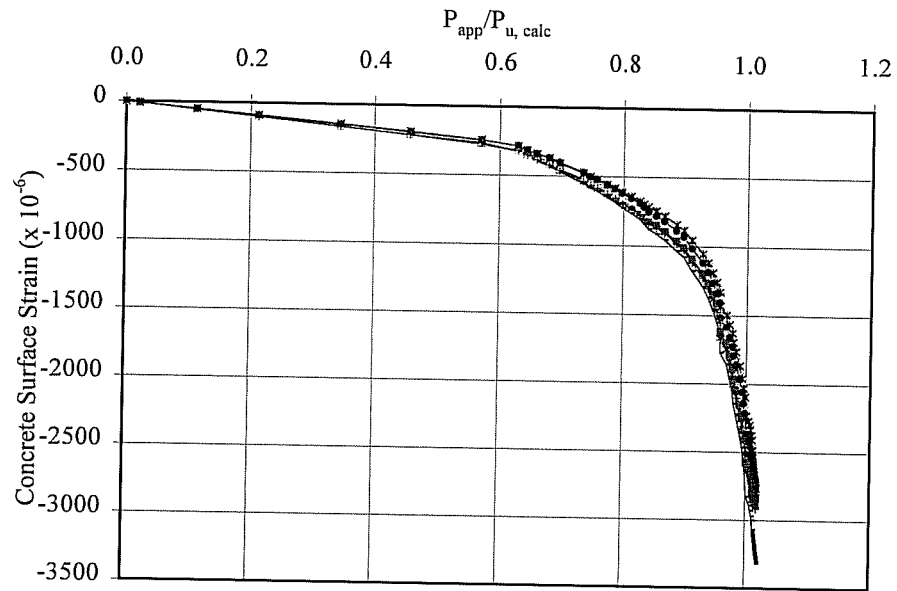
**Figure H.7:** Deck Slab Concrete Strains vs Normalized Load for Specimen M9B-3
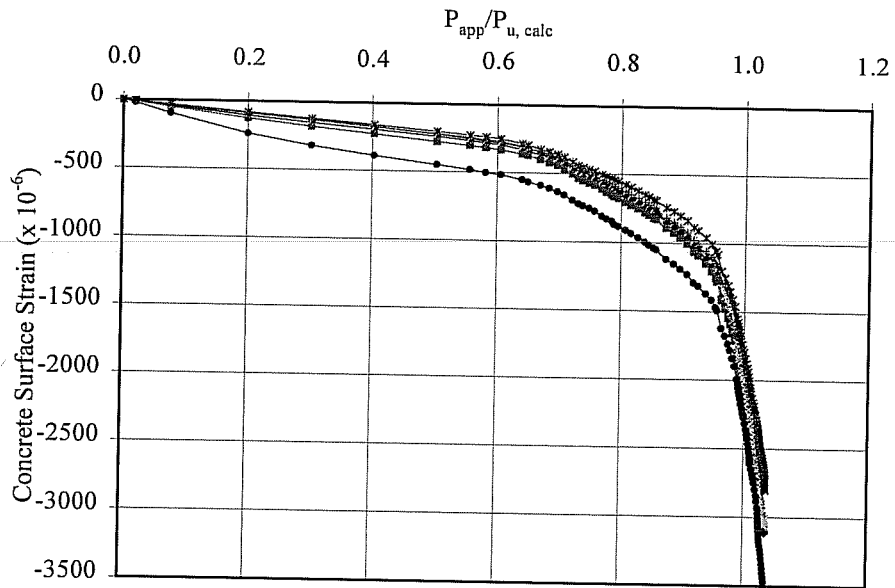


**Figure H.8:** Deck Slab Concrete Strains vs Normalized Load for Specimen M9B-4

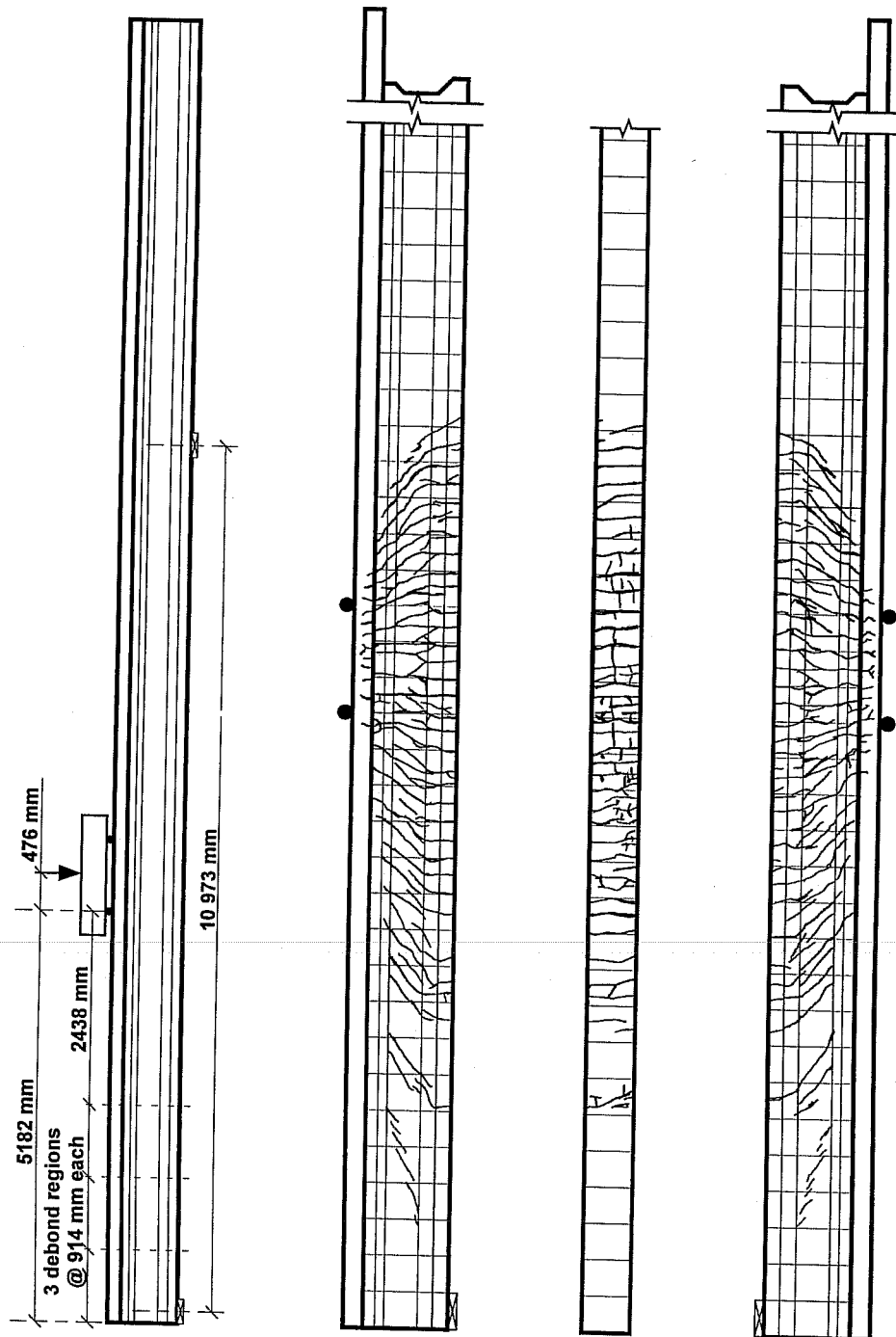**Figure H.9: Deck Slab Concrete Strains vs Normalized Load for Specimen H9B-1**



**Figure H.10: Deck Slab Concrete Strains vs Normalized Load for Specimen H9B-2**

121

**Figure H.11: Deck Slab Concrete Strains vs Normalized Load for Specimen H9B-3**



**Figure H.12: Deck Slab Concrete Strains vs Normalized Load for Specimen H9B-4**

122

# APPENDIX I

## Crack Patterns

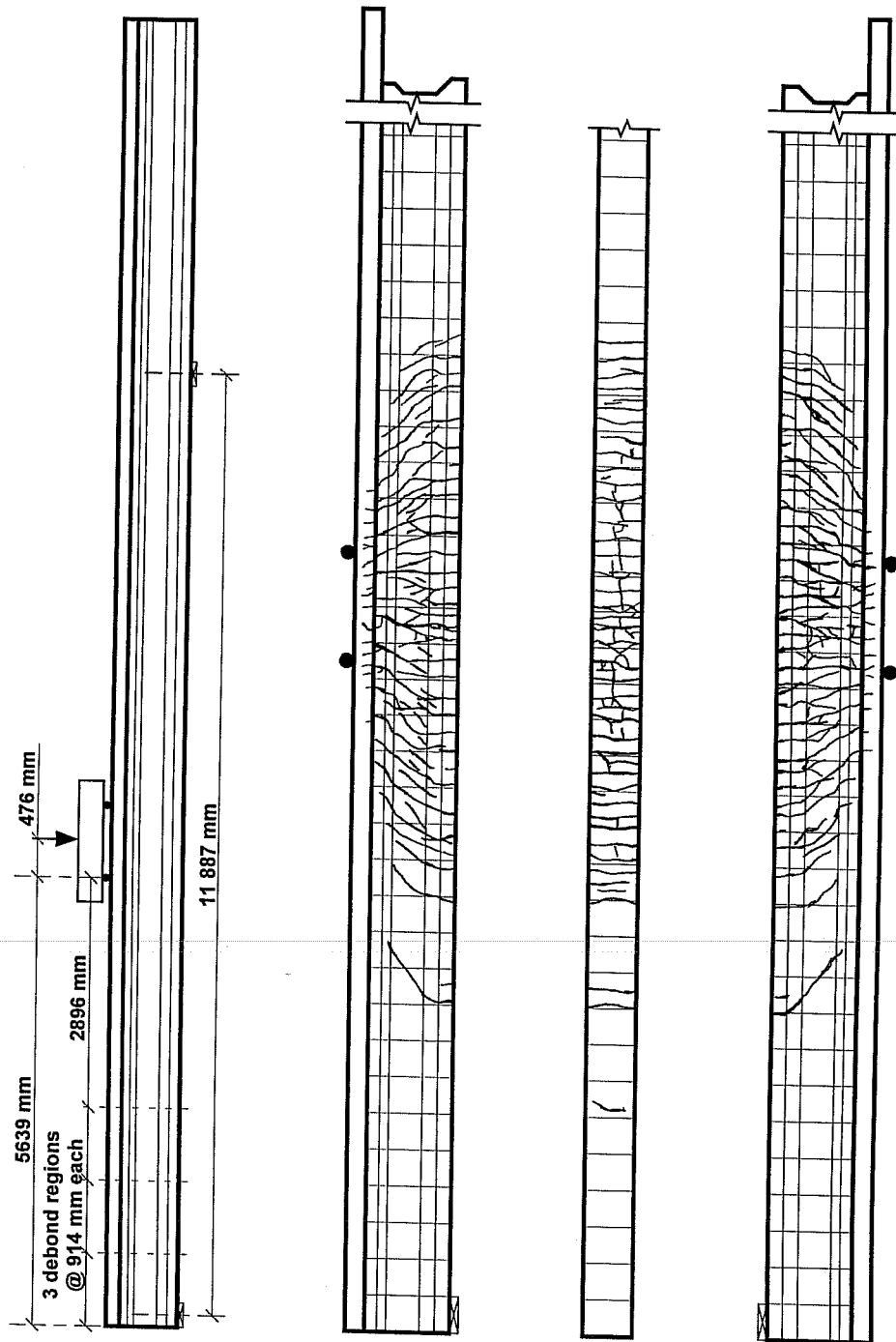Figure I.1: Crack Pattern for Specimen L6B-1
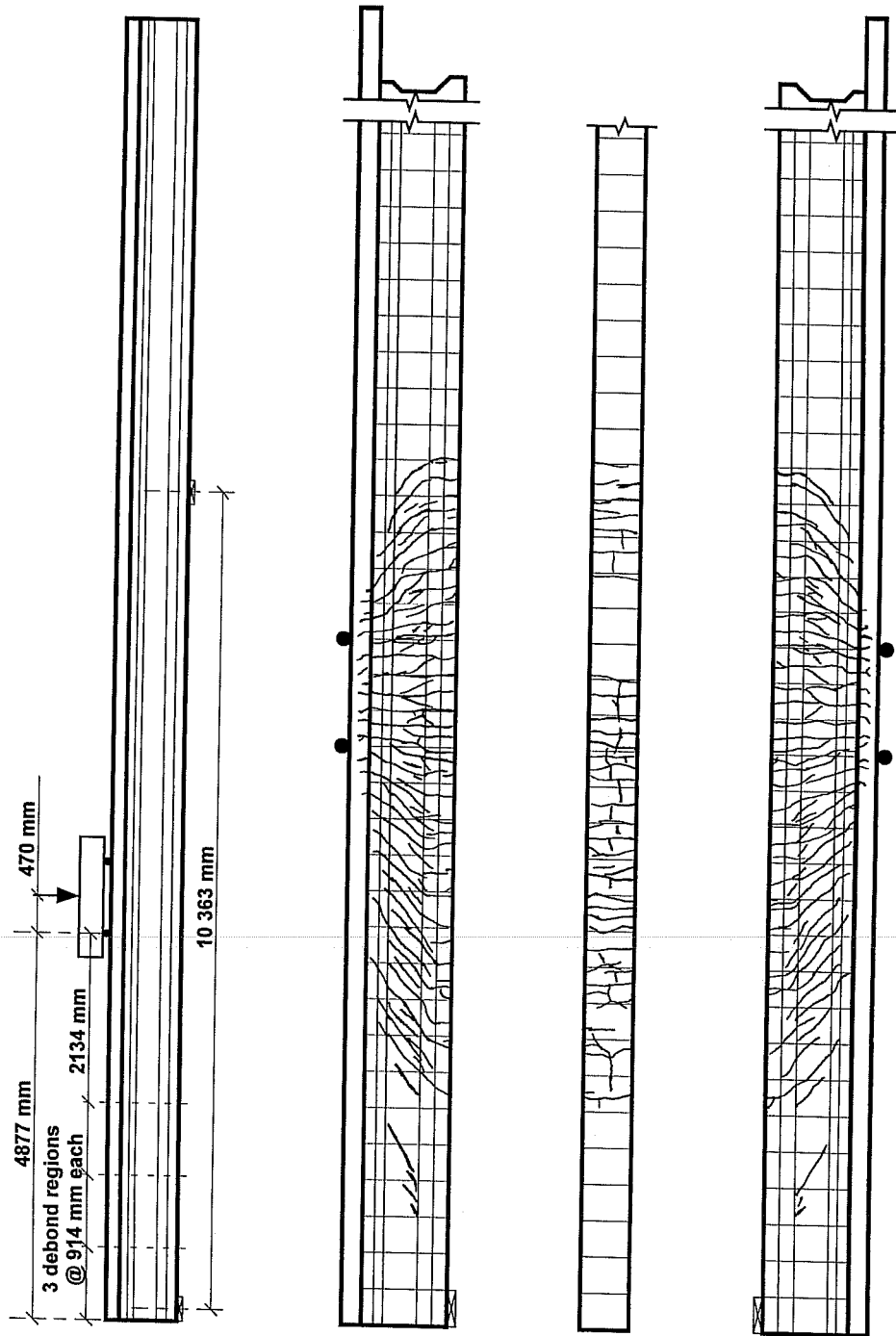
124

Figure I.2: Crack Patterns for Specimen L6B-2
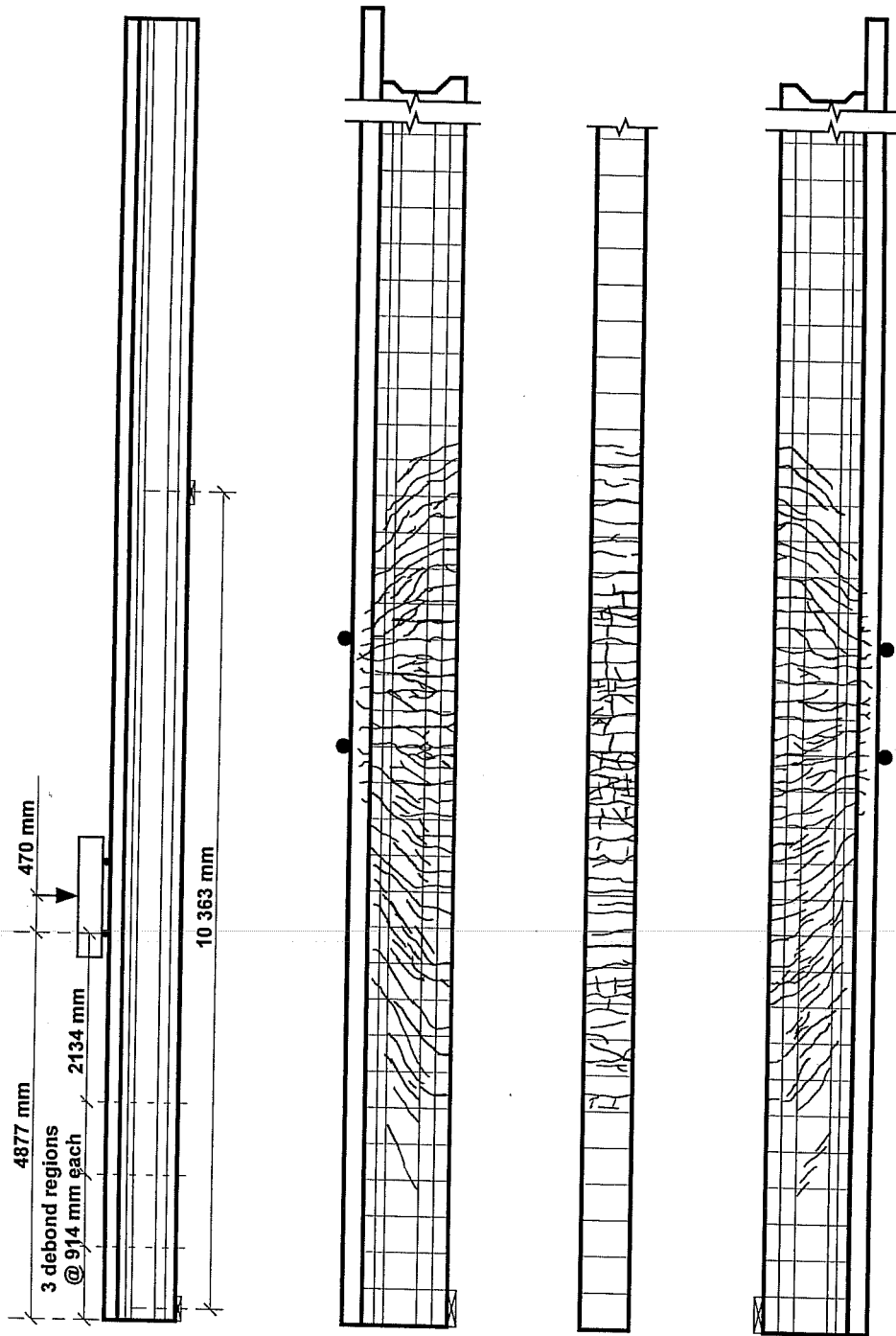
125

**Figure I.3: Crack Patterns for Specimen L6B-3**

126

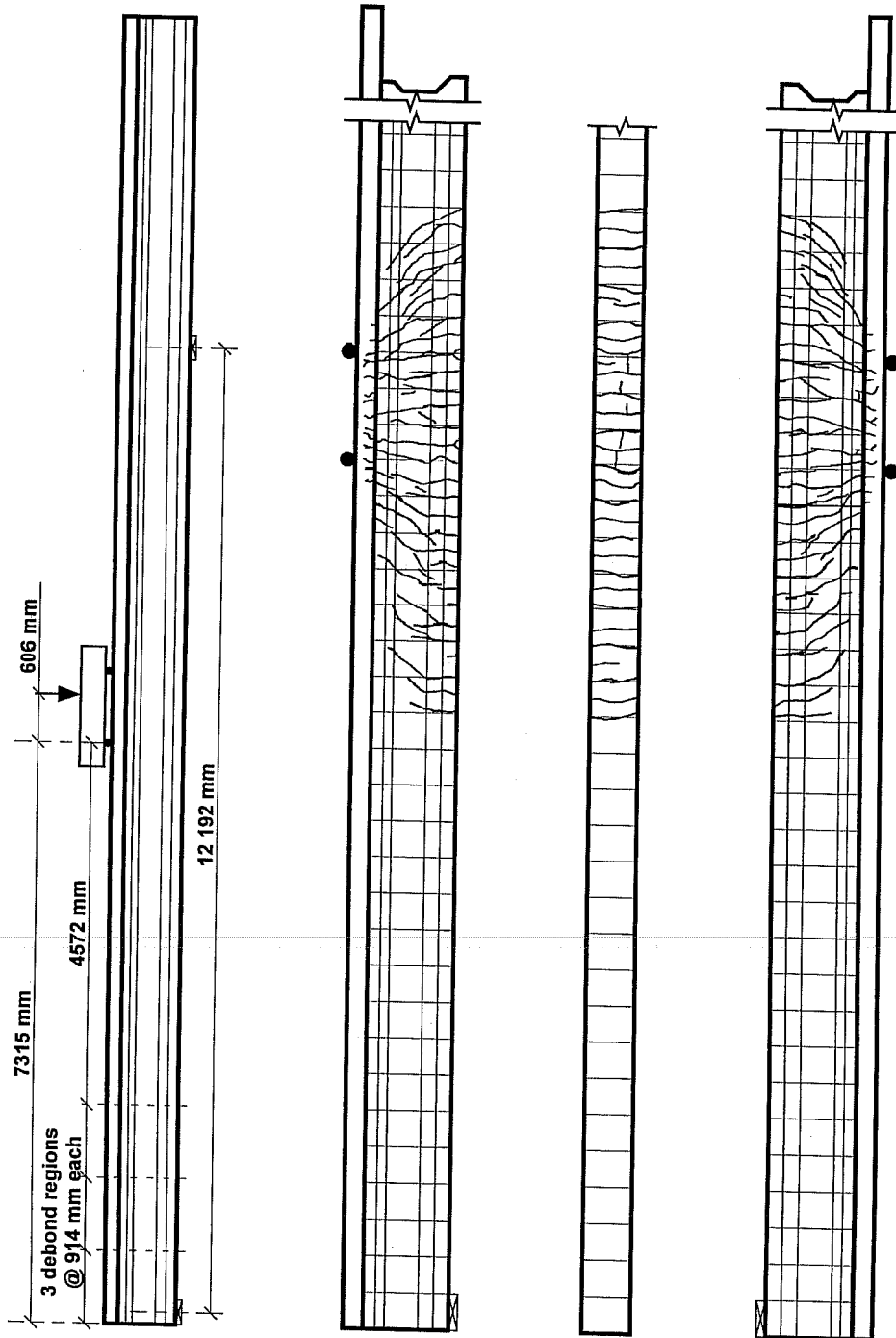**Figure I.4: Crack Patterns for Specimen L6B-4**

127

**Figure I.5: Crack Patterns for Specimen M9B-1**

**Figure I.6: Crack Patterns for Specimen M9B-2**

129

**Figure I.7: Crack Patterns for Specimen M9B-3**

130

**Figure I.8: Crack Patterns for Specimen M9B-4**
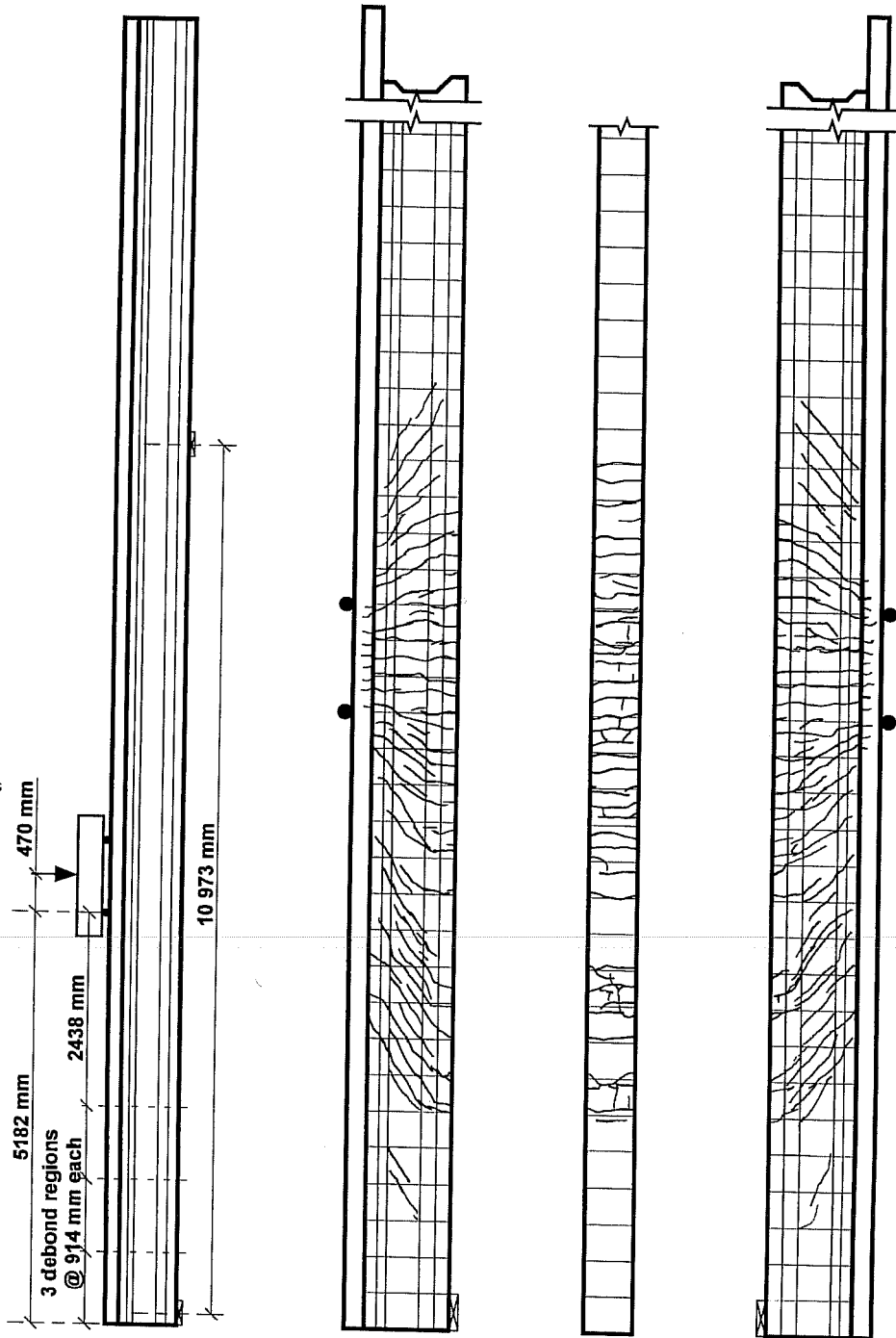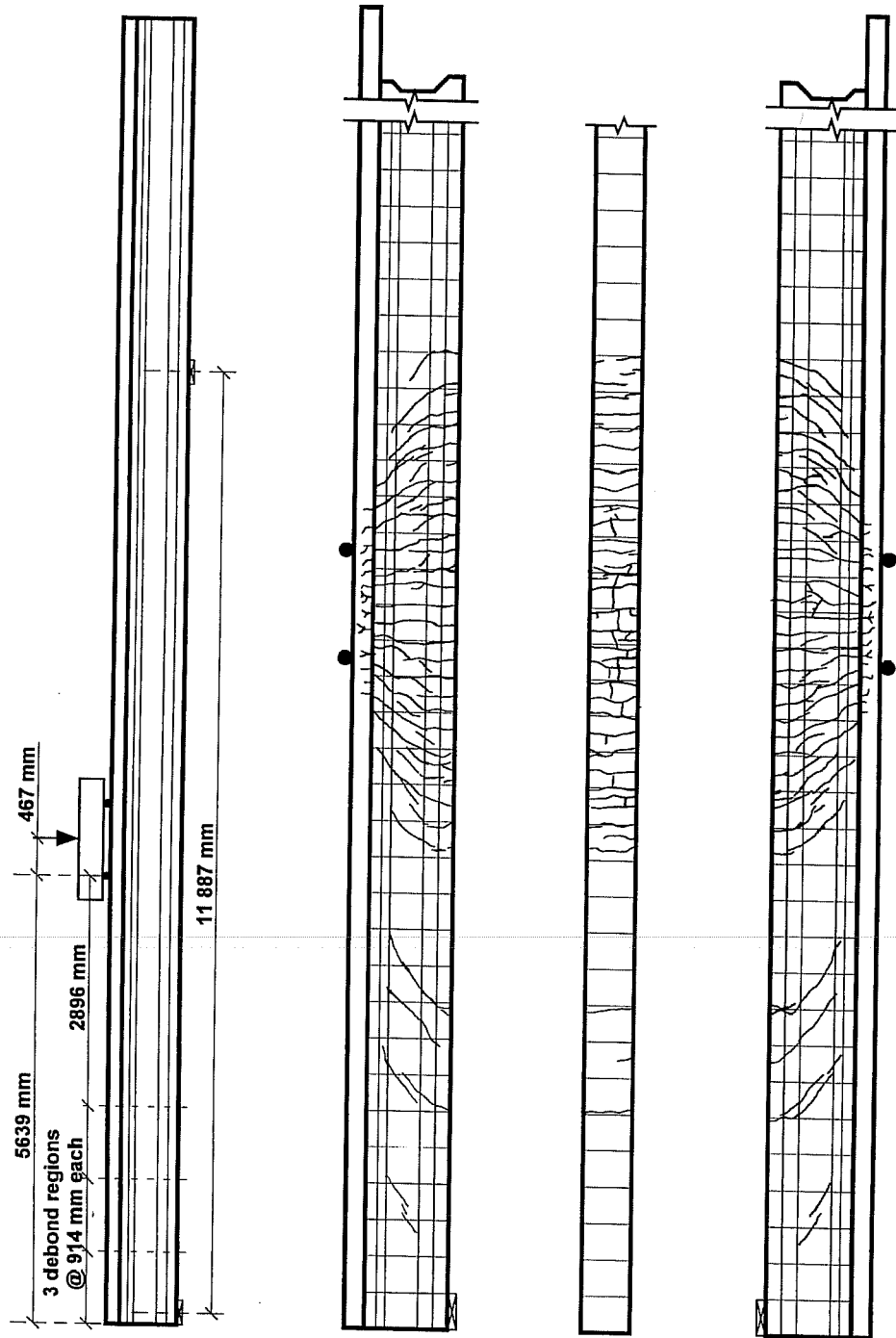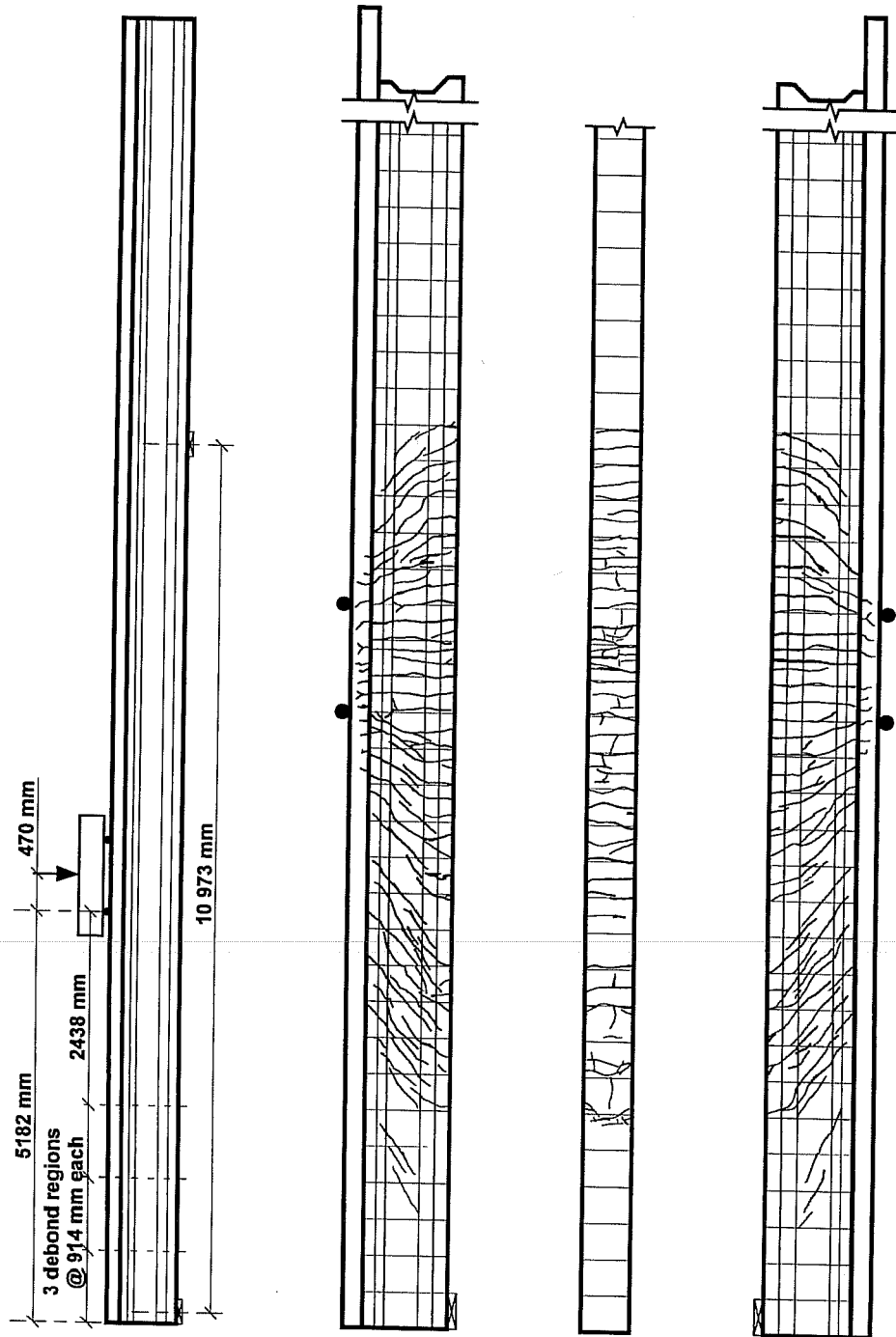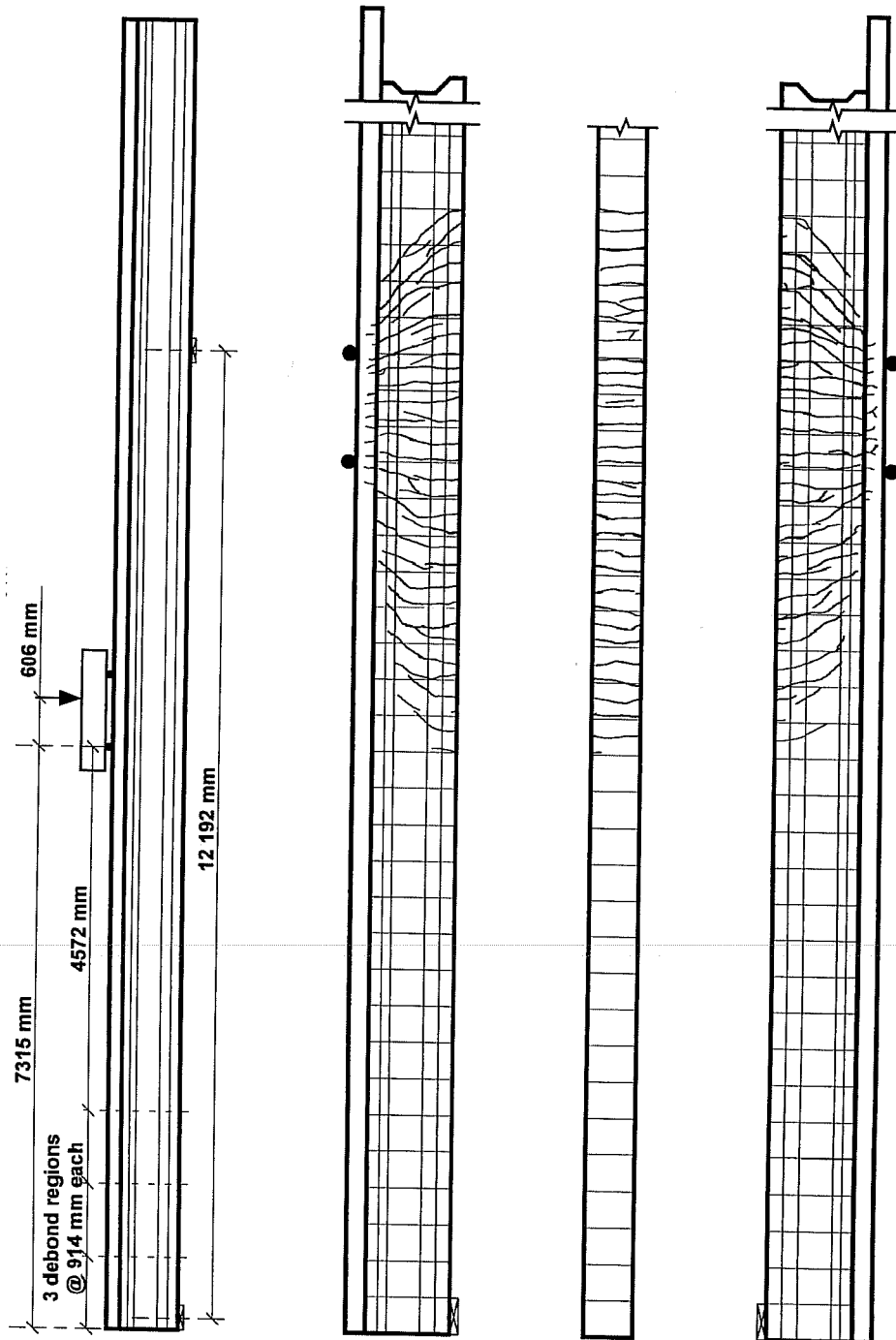
131

**Figure I.9: Crack Patterns for Specimen H9B-1**
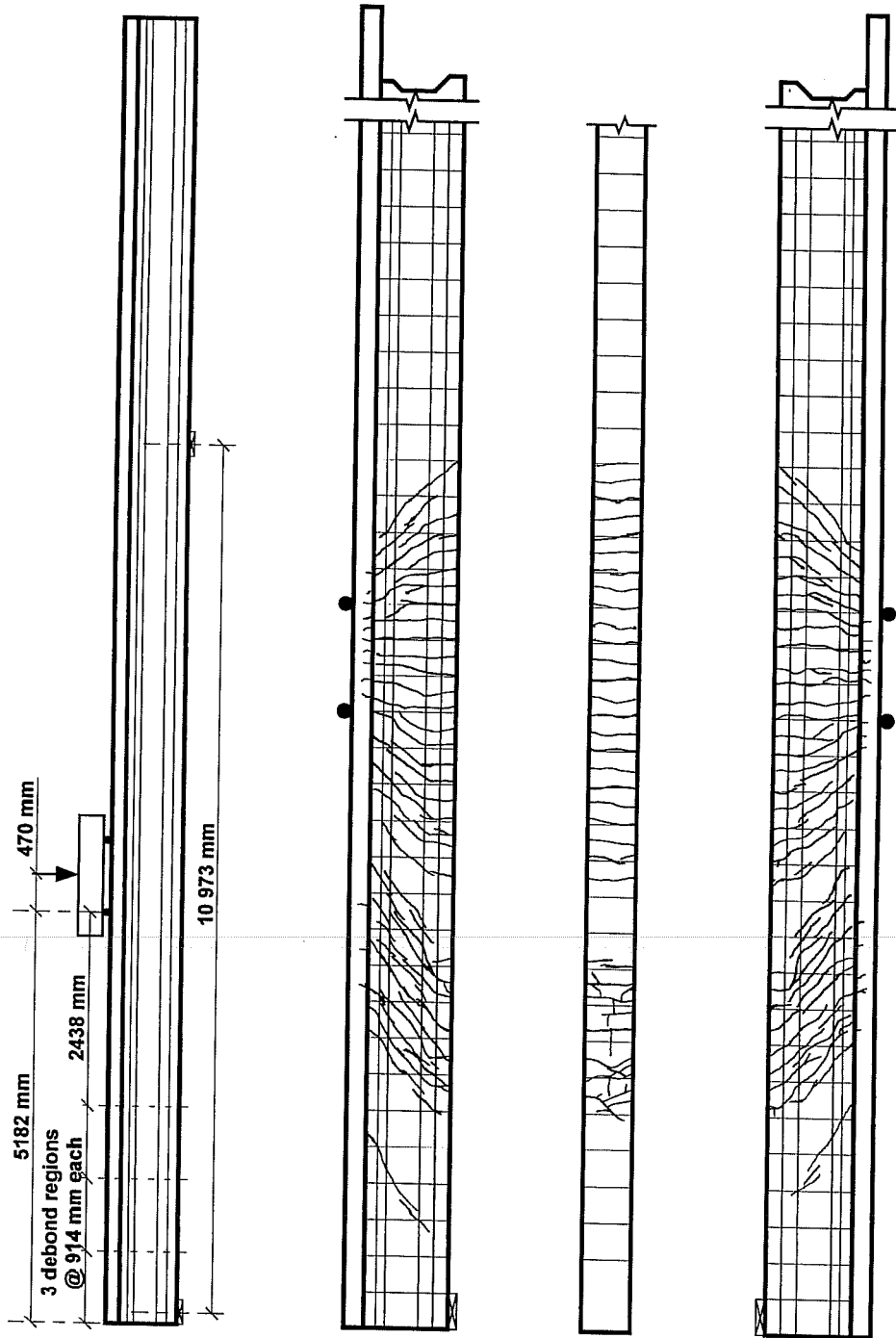
132

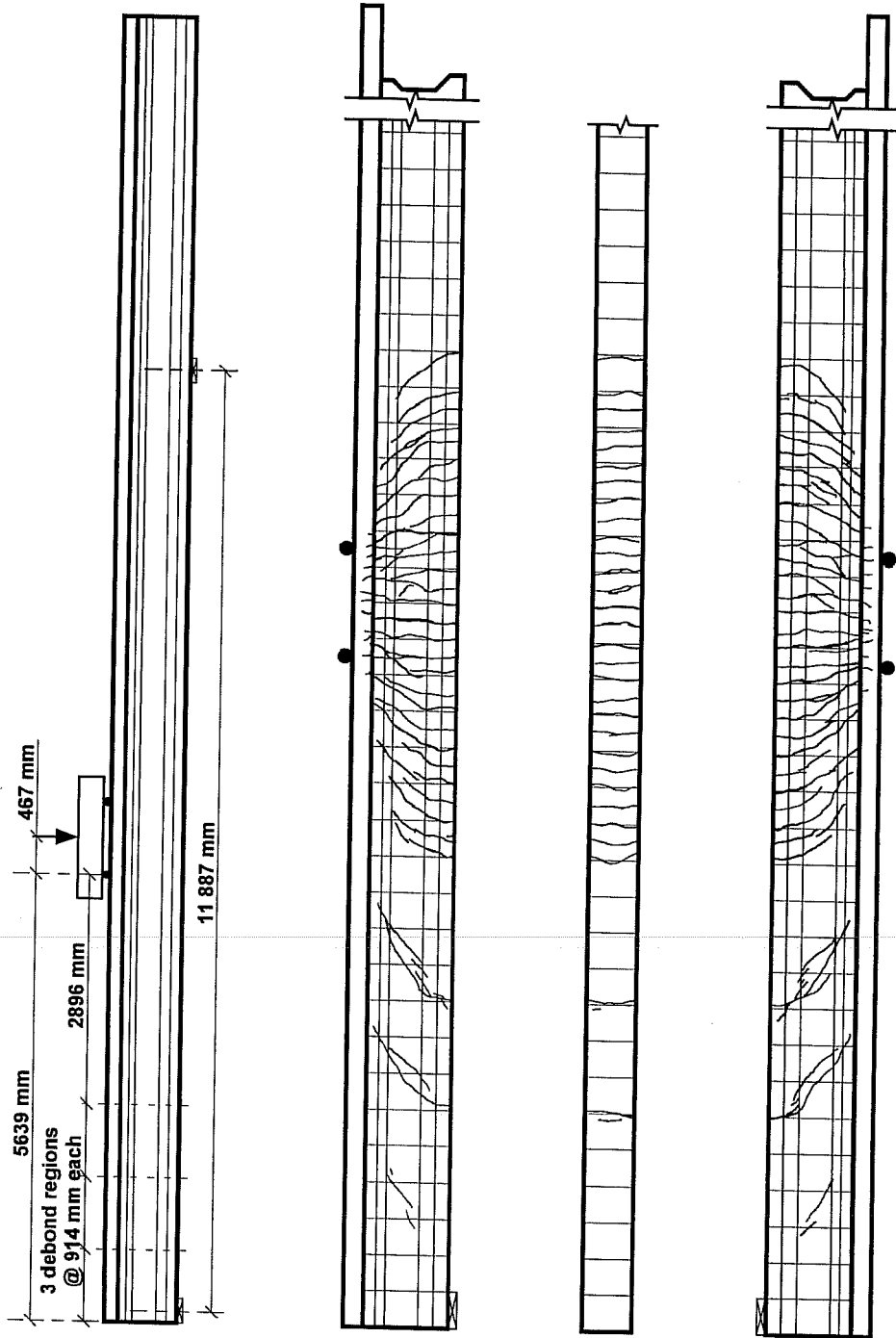Figure I.10:  Crack Patterns for Specimen H9B-2

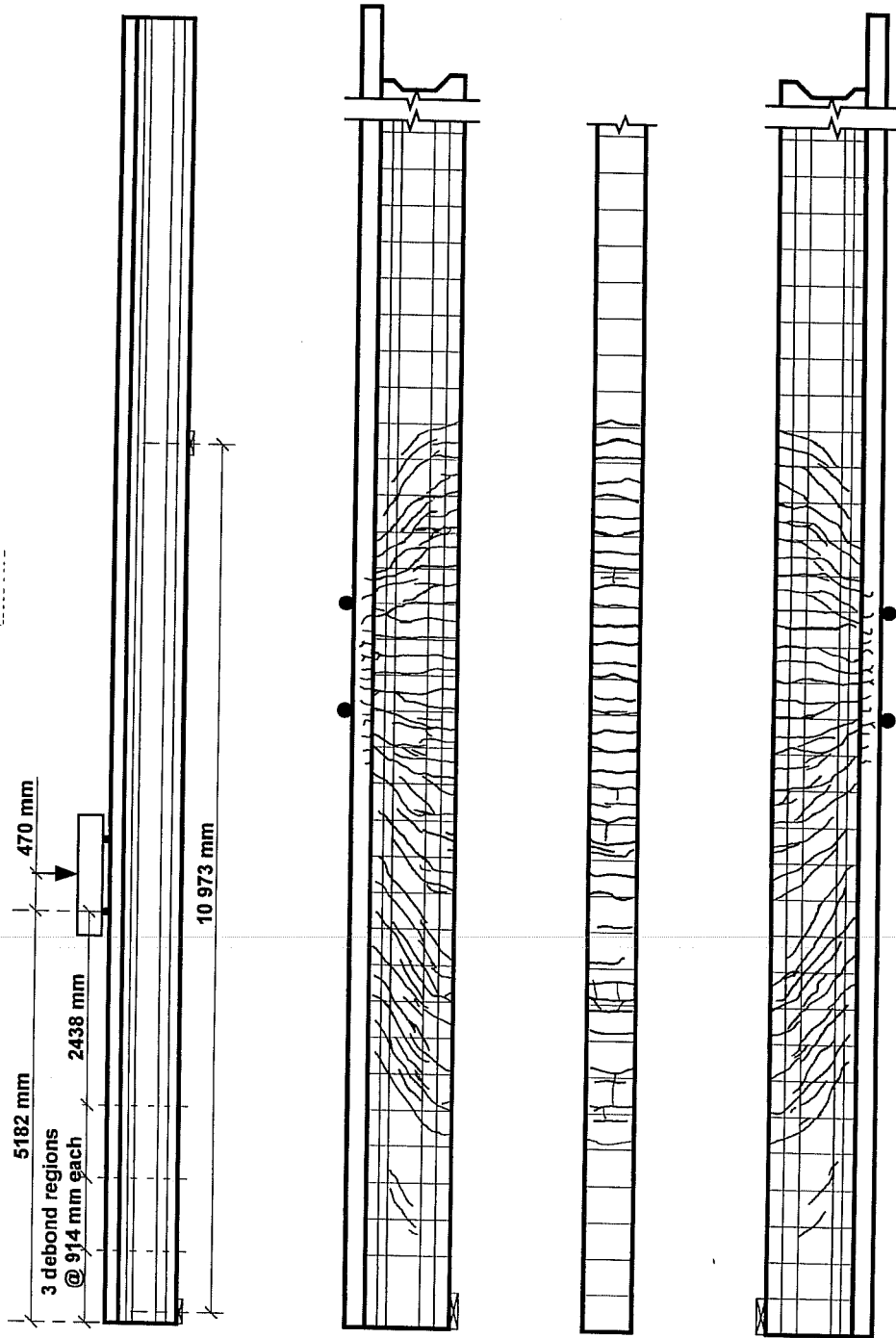**Figure I.11: Crack Patterns for Specimen H9B-3**

134

**Figure I.12: Crack Patterns for Specimen H9B-4**

135

# REFERENCES

1. Castrodale, R.W., Kreger, M.E., and Burns, N.H. "A Study of Pretensioned High Strength Concrete Girders in Composite Highway Bridges — Laboratory Tests." Research Report 381-3. Center for Transportation Research, The University of Texas at Austin, January 1988.

2. Hanson, Norman W., and Kaar, Paul H. "Flexural Bond Tests of Pretensioned Prestressed Beams." *ACI Journal*. Proceedings V. 55, No. 7, January 1959, pp.783–802.

3. Cousins, Thomas E., Johnston, David W., and Zia, Paul. "Transfer and Development Length of Epoxy Coated and Uncoated Prestressing Strand." *PCI Journal*. V. 35, No. 4, July-August 1990, pp. 92–103.

4. Federal Highway Administration. "Prestressing Strand for Pretension Applications — Development Length Revisited." Memorandum. Chief, Bridge Division, Federal Highway Administration, Washington, D.C., October 26, 1988.

5. American Association of State Highway and Transportation Officials (AASHTO). *Standard Specifications for Highway Bridges*. Sixteenth Edition. AASHTO, Washington, D.C., 1996.

6. American Association of State Highway and Transportation Officials (AASHTO). *AASHTO LRFD Bridge Specifications: Customary U.S. Units*. First Edition. AASHTO, Washington, D.C., 1994.

7. Federal Highway Administration. "Prestressing Strand for Pretension Applications Revisited." Memorandum. Chief, Bridge Division, Federal Highway Administration, Washington, D.C., May 8, 1996.

8. ACI Committee 318. *Building Code Requirements for Reinforced Concrete Structures (ACI 318-95)*. American Concrete Institute, Detroit, Michigan, 1995.

9. Janney, Jack R. "Nature of Bond in Pre-tensioned Prestressed Concrete." *ACI Journal*. Proceedings V. 50, No. 9, May 1954, pp. 717–736.

10. Russell, B.W., and Burns, N.H. "Design Guidelines for Transfer, Development and Debonding of Large Diameter Seven Wire Strands in Pretensioned Concrete Girders." Research Report 1210-5F. Center for Transportation Research, The University of Texas at Austin, January 1993.

11. Hoyer, E., and Friedrich, E., "Beitrag zur Frage der Haftspannung in Eisenbetonbauteilen," *Beton und Eisen*, V. 38, March 20, 1939.

12. Kaar, P.H., and Magura, D.D. "Effect of Strand Blanketing on Performance of Pretensioned Girders," *PCI Journal*. V. 10, No. 6, December 1965, pp. 20–34.

13. Dane, J., III, and Bruce, R.N., Jr. "Elimination of Draped Strands in Prestressed Concrete Girders (Final Report)," Department of Civil Engineering, Tulane University, New Orleans. Submitted to the Louisiana Department of Highways, State Project No. 736-01-65, Technical Report No. 107, 1975.

14. Rabbat, B.G., Kaar, P.H., Russell, H.G, and Bruce, R.N., Jr. "Fatigue Tests of Pretensioned Girders with Blanketed and Draped Strands," *PCI Journal.* V. 24, No. 4, July-August 1979, pp. 88-112.

15. Martin, Leslie D., and Scott, Norman L. "Development of Prestressing Strand in Pretensioned Members." *ACI Journal*, Proceedings. V. 73, No. 8, August, 1976, pp. 453–456.

16. Zia, P., and Mostafa, T. "Development Length of Prestressing Strands." *PCI Journal.* V. 22, No. 5, September-October 1977, pp. 54–65.

17. Mitchell, Denis, Cook, William D., Kahn, Arshad A., and Tham, Thomas. "Influence of High-Strength Concrete on Transfer and Development Length of Pretensioning Strand." *PCI Journal.* V. 38, No. 3, May-June 1993, pp. 52–66.

18. Deatherage, J.H., Burdette, E.G., and Chew, C.K. "Development Length and Lateral Spacing Requirements of Prestressing Strand for Prestressed Concrete Bridge Girders." *PCI Journal.* V. 39, No. 1, January-February, 1994, pp. 70–83.

19. Buckner, C. Dale. "An Analysis of Transfer and Development Lengths for Pretensioned Concrete Structures." Publication No. FHWA-RD-94-049. Turner-Fairbank Highway Research Center, Federal Highway Administration, McLean, Virginia, December 1994.

20. Collins, Michael P., and Mitchell, Denis. *Prestressed Concrete Structures.* Prentice-Hall, Englewood Cliffs, New Jersey, 1991.

21. Lin, T.Y., and Burns, Ned H. *Design of Prestressed Concrete Structures.* Third Edition. John Wiley & Sons, New York, New York, 1981.

22. American Society for Testing and Materials (ASTM), *Test Method for Compressive Strength of Cylindrical Concrete Specimens (C39)*, ASTM, Philadelphia, 1993.

23. American Society for Testing and Materials (ASTM), *Standard Test Method for Static Modulus of Elasticity and Poisson's Ratio of Concrete in Compression (C469-94)*, ASTM, Philadelphia, July, 1994.

24. Gross, S.P., and Burns, N.H. "Transfer and Development Length of 15.2 mm (0.6 in) Diameter Prestressing Strand in High Performance Concrete: Results of the Hoblitzell-Buckner Beam Tests." Research Report 580-2. Center for Transportation Research, The University of Texas at Austin, June 1995.

25. Thorsen, Niels, "Use of Large Tendons in Pre-tensioned Concrete," *ACI Journal, Proceedings*, V. 52, February 1956, pp. 649-659.

26. Moustafa, Saad, "Pull-Out Strength of Strand and Lifting Loops," *Concrete Technology Associates Technical Bulletin*, 74-B5, May 1974.

27. Logan, D.R., "Acceptance Criteria for Bond Quality of Strand for Pretensioned Prestressed Concrete Applications," *PCI Journal*, V. 42, No. 2, March-April 1997, pp.52-90.

28. Kaar, Paul H., LaFraugh, Robert W., and Mass, Mark A. "Influence of Concrete Strength on Strand Transfer Length." *PCI Journal*. V. 8, No. 5, October 1963, pp.47–67.

# VITA

John William Grove was born May 14, 1969, in Camp Hill, Pennsylvania. He is the eldest son of William L. Grove and Shirley M. Grove (nee Lewis). After graduating from Palmyra Area High School in June, 1987, he served in the United States Army from September, 1987 to September, 1990. He attended Drexel University in Philadelphia, Pennsylvania, where he graduated summa cum laude, receiving Bachelor of Science Degrees in Architectural Engineering and Civil Engineering in June, 1996. In September, 1996, he entered the Graduate School of Civil Engineering at The University of Texas at Austin to begin work on a Master of Science Degree in Engineering.

John participated in several engineering internships while an undergraduate. He worked with the Hershey Foods Corporation, and Mid-State Construction, Incorporated both of Hershey, Pennsylvania, as well as Modjeski and Masters Engineering in Mechanicsburg, Pennsylvania. He passed the Engineer-in-Training exam in June, 1995. Upon completion of his thesis, John will be employed by T.Y. Lin, International in Alexandria, Virginia as a bridge design engineer.

Permanent address:      227 South Locust Street
                                    Palmyra, PA 17078

This thesis was typed by the author.